The University of Jordan
Authorization Form

I, Khansaa Al. Essa authorize the University of Jordan to supply copies of my Thesis/Dissertation to libraries or establishments or individuals on request.

Signature: خنساء العيسى

Date: ٢٠١١/٧/٢٤

الجامعة الأردنيـــة
كلية الدراسات العليا

التاريـــخ: / /

نموذج رقم (16)
اقرار والتزام بالمعايير الأخلاقية والأمانة العلمية وقوانين الجامعة الأردنية وأنظمتها وتعليماتها لطلبة الدكتوراة

أنا الطالب: خنساء محمد سلامه العيسى الرقم الجامعي: (9060406)

تخصص: كيمياء الكليـــــة: العلوم

عنوان الاطروحة: Adsorption of heavy metal ions on modified Jordanian kaolin clay by humic acid

....

....

....

اعلن بأنني قد التزمت بقوانين الجامعة الأردنية وأنظمتها وتعليماتها وقراراتها السارية المفعول المتعلقة باعداد اطروحات الدكتوراه عندما قمت شخصيا" باعداد اطروحتي وذلك بما ينسجم مع الأمانة العلمية وكافة المعايير الأخلاقية المتعارف عليها في كتابة الأطروحات العلمية. كما أنني أعلن بأن اطروحتي هذه غير منقولة أو مستلة من أطاريح أو كتب أو أبحاث أو أي منشورات علمية تم نشرها أو تخزينها في أي وسيلة اعلامية، وتأسيسا" على ما تقدم فانني أتحمل المسؤولية بأنواعها كافة فيما لو تبين غير ذلك بما فيه حق مجلس العمداء في الجامعة الأردنية بالغاء قرار منحي الدرجة العلمية التي حصلت عليها وسحب شهادة التخرج مني بعد صدورها دون أن يكون لي أي حق في التظلم أو الاعتراض أو الطعن بأي صورة كانت في القرار الصادر عن مجلس العمداء بهذا الصدد.

توقيع الطالب:.................................. التاريخ:21 / 7 /2011

ADSORPTION OF HEAVY METAL IONS ON MODIFIED JORDANIAN KAOLIN CLAY BY HUMIC ACID

By
Khansa'a Mohammad Al–Essa

Supervisor
Dr. Fawwaz Khalili, Prof.

This Dissertation was submitted in Partial Fulfillment of the Requirements for the Doctor of Philosophy Degree in Chemistry.

Faculty of Graduate Studies
University of Jordan

July, 2011

COMMITTEE DECISION

This Thesis/Dissertation (Adsorption of Heavy Metal Ions on Modified Jordanian Kaolin Clay by Humic Acid) was Successfully Defended and Approved on

Examination Committee | **Signature**

Dr. Fawwaz Khalili, (supervisor)
Prof. of Inorganic and Nuclear Chemistry

Dr. Afif Seyam
Prof. of Inorganic Chemistry

Dr. Ammar Al–Dujaili
Prof. of Polymer Chemistry

Dr. Abeer Al–Bawab
Prof. of Physical Chemistry

Dr. Akl Awwad
Prof. of Environmental Chemistry
Royal Scientific Society

Dedication

To whom love me and guide
My parents,

To whom support me and help
My brothers and sisters.

Acknowledgment

First of all, this work would not be succeeded without the care of Allah; Allah provides me with strength and patience to complete this wok and Allah deserve thanks in all cases.

I would like to express my deepest appreciation for Prof. Dr. Fawwaz Khalili for his guidance and consultations during the research period. Dr Fawwaz Khalili showed patience and his fruitful suggestions enhanced the scientific value of my thesis.

Special thanks to the members of committee: Dr. Afif Seyam, Dr. Ammar Al–Dujaili, Dr. Abeer Al–Bawab and Dr. Akl Awwad for their useful discussion and suggestions.

My deepest thanks and grateful for Dr. Imad Hamadneh for his help in XRD analysis.

Special thanks to all my friends, especially Dr. Safa'a AL–Momani for her concern and help, Heba, Sanabel, Aseel and Noor for help.

Special thank for Dr. Muhammad Dweri for his help in XRD measurement.

Special thanks to Ruba Zallom, Samar Hazboun, Zahra Faori and Mr Waddah for their help and technical measurements.

My special thanks and deepest gratitude for all my family; my parents, my brothers specially Eng. Aows, Dr. Harith, Dr. Musab, my sisters specially Dr. Arwa, Dr. Khuzama and sedeqa, for their great efforts, patience and motivation. Nothing could be done without their support, thank you all.

List of contents

List of Tables

List of Figures

List of Schemes

List of Abbreviations

Symbol	Meaning
AAS	Atomic absorption spectrometer.
a_m	The area of the adsorbate effectively occupied by an adsorbed molecule.
A_s	Surface area of the adsorbent (m^2/g).
C_e	The residual concentration of the metal ion in solution at equilibrium in (ppm).
CEC	Cation exchange capacity.
C_o	Initial concentration (ppm).
D	Pore diameter (µm).
D–R	Dubinin–Radushkevich.
E	Adsorption free energy (kJ/mol).
EDS	Energy dispersive spectrum.
FHA– kaolin clay	Modified kaolin clay by humic acid from Fluka Company.
FTIR	Fourier Transform Infrared.
HA	Humic acid.
FHA	Humic acid from Fluka company.
HSAB	Hard and Soft Acids and Bases theory.

KTD	King Talal Dam.
KTD– kaolin clay	Modified kaolin clay by humic acid from KTD region.
K_d	Distribution coefficient.
K_F	Freundlich constant relates to adsorption capacity (L g^{-1}).
K_L	Langmuir constant (L mg^{-1}).
k_2	Second order reaction constant (g mg^{-1} min^{-1}).
L	Maximum adsorption capacity (expressed in mol/g of adsorbent).
m	Mass (g).
n	Freundlich constant relates to adsorption intensity (g/L).
N_{av}	Avogadro’s number.
P	Applied pressure (PSI).
ppm	Parts per million.
q	Metal ion uptake by kaolin clay in (mg metal ion (II)/ g kaolin clay).
q_e	The amount of solute adsorbed per unit weight of adsorbent (mgg^{-1}).
q_m	Monolayer adsorption capacity.
q_t	amount of heavy metal adsorbed at time t.
R	The ideal gas constant, (8.3145 $J.mol^{-1}.K^{-1}$).
R^2	Correlation coefficient.
S	Surface of kaolinite.
SEM	Scanning Electron Microscope.
SO	Surface of unmodified kaolinite.
SOH	Surface of modified kaolinite by HA.
T	The absolute temperature (Kelvin).
TGA	Thermal gravimetric analysis.
UV–VIS	Ultraviolet–visible spectroscopy.

V	Volume of solution (L).
V_B	Bulk volume.
V_T	Total volume.
V_V	Void volume.
ϕ	Porosity.
γ	Surface tension of the mercury (480 dyne cm^{-1}).
θ	The contact angle between mercury and the pore wall, usually taken as 140° in mercury porosimeters.
XRD	X–Ray Diffraction.
β	The activity coefficient constant related to mean sorption energy ($mol^2.kJ^{-2}$).
ΔG°	Change in standard Gibbs free energy (kJ/mol).
ΔH°	Change in standard enthalpy of adsorption (kJ/mol).
ΔS°	Change in standard entropy of adsorption (J/mol.K).
ε	The Polanyi potential.

ADSORPTION OF HEAVY METAL IONS ON MODIFIED JORDANIAN KAOLIN CLAY BY HUMIC ACID

By:
Khansa'a Mohammad Al–Essa

Supervisor:
Dr. Fawwaz I. Khalili, Prof

ABSTRACT

The modification of kaolin clay from azraq area was done by adsorption humic acid (HA), adsorption isotherm was studied at different pH (3.00, 4.00, 5.00 and 6.00) and temperatures (25, 35, 45 °C). The maximum percentage (%) uptake of HA adsorbed by kaolin clay was at pH =3.00, 45 °C and at low concentration of HA.

Adsorption of Pb(II), Cd(II) and Zn(II) on modified kaolin clay was studied using batch technique at different temperatures (25, 35 and 45°C) and different pH (4.00, 5.00 and 6.00). The effects of contact time, adsorbent dose, and initial metal ions concentration were studied.

The kinetic studies were done, and showed that the uptake increases with time until it reaches equilibrium in less than 2 hrs. These experiments fitted pseudo second–order model for both modified kaolin clay.

The isothermal behaviors of the metal ions uptake onto the surface of both modified kaolin clay were also investigated, and we found that the shape of isotherm for Pb(II) adsorption on both modified kaolin clay is L–curve, while the shape of isotherm for Cd(II) and Zn(II) adsorption on both modified kaolin clay is C–curve.

The metal ions uptake properties on both modified kaolin clay fit Langmuir, Freundlich and Dubinin–Radushkevich adsorption isotherms. But the best model that represents our data is Langmuir. The adsorption process was on both homogeneous and heterogeneous surfaces.

Both modified kaolin clay showed higher metal ion uptake capacity toward Pb(II). The uptake at low concentration reaches above 90% for Pb(II). The q_m trend is as follows: Pb(II) > Cd(II) > Zn(II) for both modified kaolin clay. Kaolin clay modified by Fluka (HA) shows higher uptake for all metal ions than kaolin clay modified by KTD–(HA). From the Langmuir isotherms calculations, the diminsionless constant (R_L) values were in the range (0–1), and from Freundlich parameter (n>1) indicating the favorability of metal adsorption on both modified kaolin clay. The energy of adsorption process was calculated and it was found that the adsorption is physical process.

The negative value of ΔG indicates the degree of favorability of the adsorption process, while ΔH values indicated that this process is endothermic. On the other hand, the process has positive entropy which means that the adsorption process increases the disorder of the system.

Column experiment was used effectively for the determination of metal ion loading capacity. The uptake percentage with the metal ions in column technique fall in the same order; Pb(II) > Cd(II) > Zn(II) for both modified kaolin clay. Desorption studies were done using column experiments where (0.1M) HNO_3 and (1M) EDTA were efficiently used for elution and in order to regenerate the modified kaolin clay.

1. Introduction

1.1. Clays in the Environment

Clays are hydrous aluminosilicates broadly defined as those minerals that make up the colloid fraction (<2 μ) of soils, sediments, rocks and water, and may be composed of mixtures of fine grained clay minerals and clay–sized crystals of other minerals such as quartz, carbonate and metal oxides. Usually the term clay is used for materials that become plastic when mixed with a small amount of water. Clays play an important role in the environment by acting as a natural scavenger of pollutants by taking up cations and anions either through ion exchange or adsorption or both. Thus, clays invariably contain exchangeable cations and anions held to the surface. The prominent cations and anions found on clay surface are Ca^{2+}, Mg^{2+}, H^+, K^+, NH_4^+, Na^+, and SO_4^{2-}, Cl^-, PO_4^{3-}, and NO_3^-. These ions can be exchanged with other ions relatively easily without affecting the clay mineral structure.

Large specific surface area, chemical and mechanical stability, layered structure, high cation exchange capacity (CEC), etc., have made the clays excellent adsorbent materials (Bhattacharyya and Gupta, 2008).

1.2. Kaolin clay

Kaolinite is the most common two–sheet type clay mineral. It has favorable properties such as fine particle size, non–abrasiveness, chemical stability, low viscosity at high solids content in many systems, and can be produced with a controlled particle size distribution. Some of the important physical constants of kaolinite are: specific gravity, 2.60; index of refraction, 1.56; hardness (Mohs scale), 2; fusion temperature, 1850 ^oC (Murray, 1961).

The largest single user of kaolinite is the paper industry, also as filler in many rubber goods, in ceramic products and insulators, and in paint because it is chemically inert and insoluble in the paint system. The addition of kaolinite to thermosetting and thermoplastic mixes gives smoother surfaces, a more attractive finish, good dimensional stability, and high resistance to chemical attack (Murray, 1961).

Kaolinite has a 1:1 layer structure, first suggested by Pauling (Pauling, 1930); with the basic unit consisting of a tetrahedral sheet of SiO_4 and an octahedral sheet with Al^{3+} as the octahedral cation. The repeating layers of the mineral are hydrogen bonded together (Trevino and Coles, 2003; Srivastava, et al., 2005). Both sheets combine to form a common layer such that the tips of the silica tetrahedral point towards the octahedral layer. The tetrahedral layer is inverted over the octahedral layer with the apical 'O' atoms being shared by the two layers (Figure 1.2). The Al–atoms are placed in such a manner that any two Al–atoms are separated by two hydroxyl groups —one above and one below; making a hexagonal distribution in a single plane in the centre of the octahedral sheet. The hydroxyl groups are placed directly against the centers of oxygen–hexagons of the basal plane of the tetrahedral layer (Bhattacharyya and Gupta, 2008).

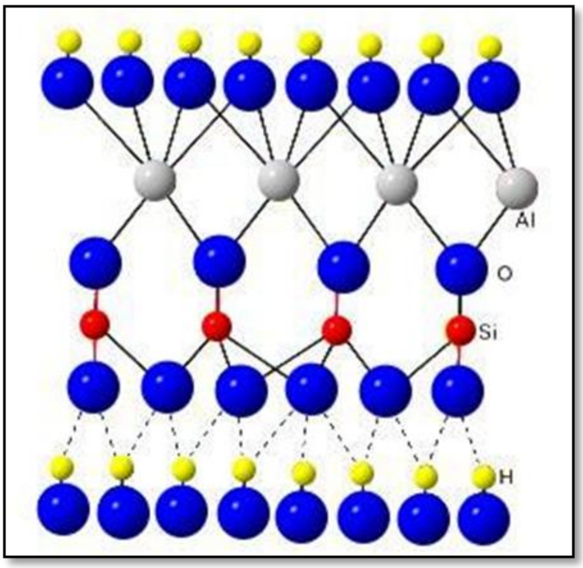


Figure 1.1: Structure of kaolinite (Varga, 2007).

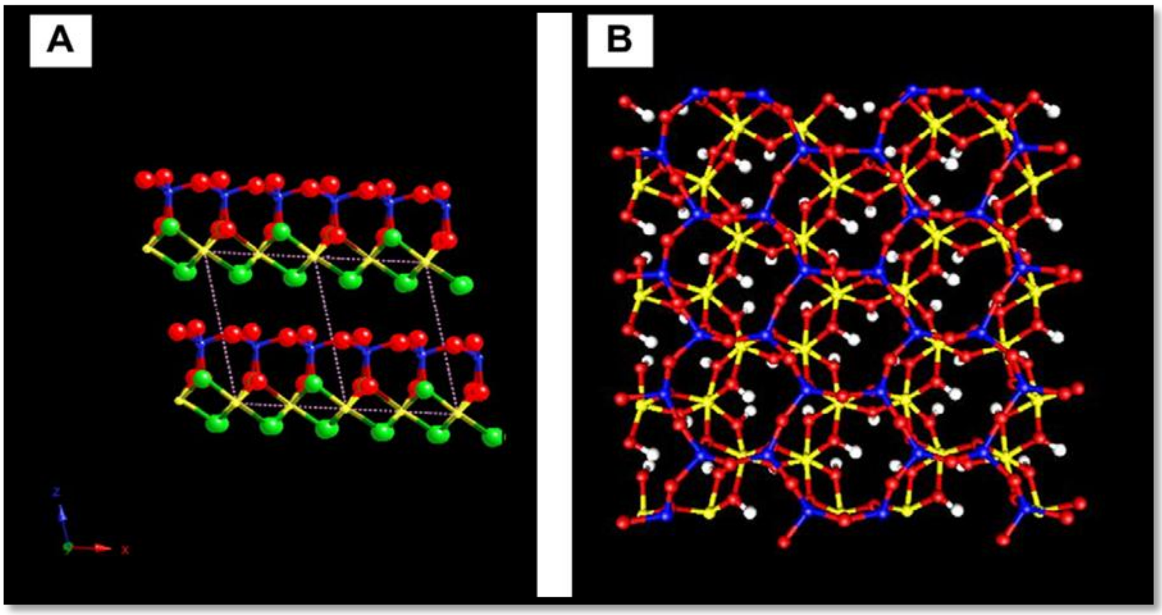


Figure 1.2: Side view (A) and top view (B) of kaolinite (0 0 1) surface structure. The silica tetrahedral (red: oxygen, blue: silicon) and alumina octahedral (yellow: aluminum, green: hydroxyl) bilayers thought to be bound together via hydrogen bonding are illustrated in (A) (Gupta and Miller, 2010).

Kaolinite, $(Si^{IV})_4$ $(Al^{III})_4$ $O_{10}(OH)_8$, has the theoretical composition of SiO_2 46.54%, Al_2O_3 39.50%, H_2O 13.96% expressed in terms of the oxides. The formula indicates that there is no substitution of Si^{4+} with Al^{3+} in the tetrahedral layer and no

substitution of Al^{3+} with other ions (e.g., Mg^{2+}, Zn^{2+}, Fe^{2+}, Ca^{2+}, Na^{+} or K^{+}) in the octahedral layer. Thus, the net layer charge of kaolinite is: [4 (+4)]+[4 (+3)]+[10 (−2)]+[8 (−1)]=0, but in nature, kaolinite has a small net negative charge arising from broken edges on the clay crystals. This negative charge, although small, is responsible for the surface not being completely inert; it allows electrostatic interaction with positively charged ions.

Though kaolinite is the least reactive clay, its high pH dependency enhances or inhibits the adsorption of metal ions according to the pH of the environment. A pH–dependent variable charge caused by protonation and deprotonation of surface hydroxyl (SOH) groups (Hizal and Apak, 2006b), and they can become SOH_2^{+} and SO^{-} at low and high pH, respectively (Angove et al., 1997).

The layer edges where exposed OH groups will exhibit acid–base behavior are primarily responsible for interaction of kaolinite with environmental contaminant metal ions (Bhattacharyya and Gupta, 2008).

Adsorption may also take place on the flat exposed planes of the silica and the alumina sheets. Cation adsorption mainly occurs on proton–bearing surface functional groups such as silanols and aluminols via covalent binding (Hizal and Apak, 2006b).

The tetrahedral sheet of kaolinite carries a small permanent negative charge due to isomorphous substitution of Si^{4+} by Al^{3+}. (Hizal and Apak, 2006b) or of trivalent metal ions (such as Al^{3+}) by divalent ions (such as Fe^{2+} and Mg^{2+}) in the alumina octahedral sheet, leaving a single negative charge for each substitution (Srivastava et al., 2005).

Hence, the kaolinite surface is expected to have two kinds of binding sites that could interact with metal ions via ion exchange and adsorption mechanisms.

Natural clays as adsorbent with low cost have received much attention on heavy metal ions sorption from contaminated water (Jiang, et al., 2010). Typically, kaolinite has a relative low cation–exchange capacity (CEC) [3–15 meq/100 g of clay] and smaller surface area ranged from 10 to 20 m^2/g (Adebowale, et al., 2006). So it is often modified from its natural state by physical or chemical treatments to enhance the properties of the material, and to improve its sorption capacity. Kaolinite, like most of the clay minerals, can intercalate various molecules in their interlayer space. Strong polar molecules can expand the basal spacing, which eventually leads to the rupture of the interlayer hydrogen bonds, or by either impregnation or grafting of organic/inorganic molecules on its surface (Unuabonah, et al., 2007).

Kaolinite in such sediments may show a higher selectivity for transition heavy metal ions due to the presence of pH dependent adsorption sites. Moreover, (Davis, 1982) has shown that the reactive edge sites of kaolinite may be coated with adsorbed organic matter, further enhancing metal ion adsorption capacity. Inorganic particles (e.g., kaolinite) coated with humic substances play an important role in the environmental behavior of various ions (Hizal and Apak, 2006a).

Jordanian kaolin clay has a high percentage (%) of iron as iron dioxide, which made its color to be pink. It presents in Azraq region in east of Jordan, Baten El-Ghoul region, which is located about 75 km south east of Ma'an city in south Jordan (Khoury, and El-Sakka 1986).

1.3. Humic Acids

Humic acids are complex aggregates of dark–colored amorphous high molecular weight substances extracted from the natural degradation products of plant and animal residues.

Humic acid (HA), being a component of natural soil, has an organic material content of about 60–80%. The percentage of carbon is about (52–62), hydrogen is (3.0–5.5), oxygen is (30–33) and nitrogen is (3.5–5.5).

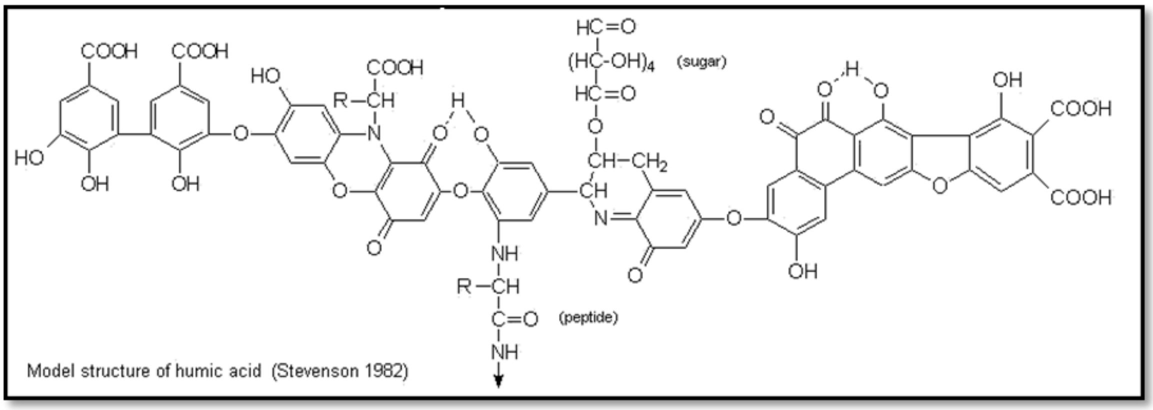


Figure 1.3: Model structure of humic acid.

Although considerable work about humic acid exists, only a few of them have dealt with humic acid adsorption on clay minerals. Humic acid is completely soluble only in strongly basic solution. Its solubility increases with increasing pH.

Humic acids are chemically heterogeneous compounds having different types of functional groups at different proportions and configurations. It contains carboxyl (–COOH), amine (–NH_2), hydroxyl (–OH), and phenol (Ar –OH) functional groups, and has negative charge in weakly acidic–to–basic media because of deprotonation.

Humic acids may both enhance or diminish heavy metal ion adsorption depending on the relative stabilities of metal ion–humate and metal ion– humate–surface complexes as a function of pH. Humic acid forms negatively charged complexes with heavy metal ions (especially Fe(III)) as a result of phenolate and carboxylate ligands (Hizal and Apak, 2006a).

In accord with (Hard and Soft Acids and Bases) HSAB theory, Cu(II) and Pb(II) ions react with humic acid via O and N donor atoms and form stable complexes. Most heavy metal ions are known to bind as inner–sphere complexes to the same type

of sites in humic substances such as the carboxylate and phenolate groups irrespective of the type of metal and humic acid. The acidity constants (pKa) of a particular humic acid were reported as 3.94 for pKa_1 (due to carboxylic acid groups), 5.49 for pKa_2 (due to amine groups), and 8.29 for pKa_3 (due to phenol groups) (Westall, 1982). For Azraq humic acid pKa_1 equal to 3.82 and pKa_3 equal to 9.74 (Khalili, 1988).

Organic mineral interactions over geological periods such as condensation/adsorption of organic compounds on the surface of kaolinite–type minerals have been exemplified by the interaction of serine with silica (Hizal and Apak, 2006b).

Several mechanisms are involved in the adsorption of humic substances by clay minerals, the main ones being: Van der Waals forces, bonding by cation bridging, and H – bonding. The Al–OH tetrahedral in the clay mineral phase may interact via H bonds with Ar–OH, –COOH, and alcohol groups in humic acids, resulting in the surface binding or occlusion of organic C within the clay matrix, and adsorption on interlamellar spaces of clay minerals. (http://www.humintech.com/pdf/humicfulvicacids.pdf, 2010).

Organic matter additions to soils immobilize heavy metal ions and decrease their uptake by plants. The adsorption capacity of xonotlite for HA is (2.43 mg/g or 0.044 mg/m^2) (Araujoa, et al., 2007; Katsumata, et al., 2003).

1.4. Heavy Metal Ions Removal by Adsorption

The metals of major environmental concern today are arsenic, cadmium, chromium, cobalt, copper, lead, manganese, mercury, nickel and zinc. Because of their toxicity and non biodegradable nature, metals are of special significance (Alkan, et al., 2008).

Heavy metals such Cd, Pb, and Zn occur commonly at elevated concentrations in contaminated soils. Metal such as Zn is known to be essential to plants, humans, and animals, but they can also have adverse effects if their availability in soils exceeds certain threshold values. Other heavy metals, such as Cd and Pb, which are not essential to plants or animals, are known to be hazardous to health, even at low concentrations.

Among the important heavy metals, Pb is reportedly the least mobile. Whereas, Zn and Cd are considerably more mobile and have a greater tendency to dissociate from insoluble inorganic and organic complexes. They form soluble ionic species that remain stable at neutral or slightly alkaline pH (Srivastava, et al., 2005).

1.4.1. Lead

As one of the important pollutants in wastewater, heavy metal becomes a severe public health problem because of its non biodegradable and persistent nature. Lead is an important metal from the viewpoint of environmental toxicology as the metal finds its way into air and water from a multitude of sources like lead smelter, battery manufacturer, paper and pulp industry, boat and ship fuel and ammunition industry (Jiang, et al., 2009). Acute lead poisoning has been known to affect gastrointestinal track, or nervous system and sometimes both **(**Unuabonah, et al., 2007).

1.4.2. Cadmium

Industrial emissions, plating and mining activities contributes largely to the presence of these metal ions in water either as direct discharge into water bodies or as atmospheric discharge, which are then deposited on water surfaces **(**Unuabonah, et al., 2007).

Cadmium ions cause serious cases of acute toxicity and diseases such as lung cancer and kidney failure. As cadmium is a highly toxic element for living organisms (Hizal and Apak, 2006a).

1.4.3. Zinc

Zinc is found throughout the environment in air, soil, and water. It can be released by human activities, especially in areas where ores are mined, processed, and smelted for zinc. Zinc can be released to the atmosphere during the production of steel and burning of coal or waste. Surface water can be impacted by discharges of metal manufacturing and chemical industry wastes.

Zinc is an essential element in our diet, but too little or too much can be harmful. Taking large amounts of zinc can cause stomach cramps, nausea, and vomiting, while taking it in large amounts over an extended period can cause anemia, damage the pancreas, and lower the levels of high–density lipoprotein cholesterol (the good form of cholesterol).

Breathing dust or fumes containing large amounts of zinc can cause a short–term disease called metal fume fever. This disease is an immune response affecting the lungs and body temperature (Human Health Fact Sheet, 2005).

There is a range of effects that signal zinc deficiency such as retardation of growth in children, male reproduction, low blood sugar, poor bone growth, brain disorders, high blood cholesterol, poor circulation, eating disorders, problems with female reproduction, poor skin, nails and hair conditions and poor sense of taste and smell (Hambidge, 2000).

1.5. Adsorption

The presence of heavy metals in wastewater and surface water is becoming a severe environmental and public health problem. A few familiar methods in practice for removal of these and other metals are chemical precipitation, ion exchange, solvent extraction, reverse osmosis, adsorption, etc. Reverse osmosis, although very effective, is a cost–prohibitive process as the membranes get easily spoiled requiring frequent replacement. Chemical precipitation is not very suitable when the pollutants are present in trace amounts and also a large amount of sludge is produced. Ion exchange is expensive and sophisticated. Solvent extraction or electrolytic processes are also available but they are considered to be cost–effective only for more concentrated solutions. The process of adsorption has become one of the preferred methods for removal of toxic contaminants from water as it has been found to be very effective, economical, versatile and simple. Adsorption has the additional advantages of applicability at very low concentrations, suitability for using batch and continuous processes, ease of operation, little sludge generation, possibility of regeneration and reuse, and low capital cost. The processes have acquired global importance for minimization of the problem of contamination of water and air, and these processes have become a significant addition to Green Chemistry endeavours (Bhattacharyya and Gupta, 2008).

1.5.1. Adsorption Isotherm

The adsorption phenomenon at the solid/liquid interface involves the change in concentration of the solution. Adsorption isotherm is constructed by measuring the concentration of the adsorbate in the medium before and after adsorption, at a fixed

temperature. This is generally used to study the interaction between the adsorbate and the surface of the adsorbent and to know about the structure of the adsorbed layer (Parida et al., 2006).

The shape of isotherm provides qualitative information on the nature of solute–surface interaction (Figure 1.4).

Giles (1960) divided the isotherms into four major classes (S, L, H, C) depending on their initial sections plotted when the solution is very dilute. These classes include subclasses (1, 2, 3, 4, and 5) depending on the increase in the solute concentration. He interpreted the shapes as follows:

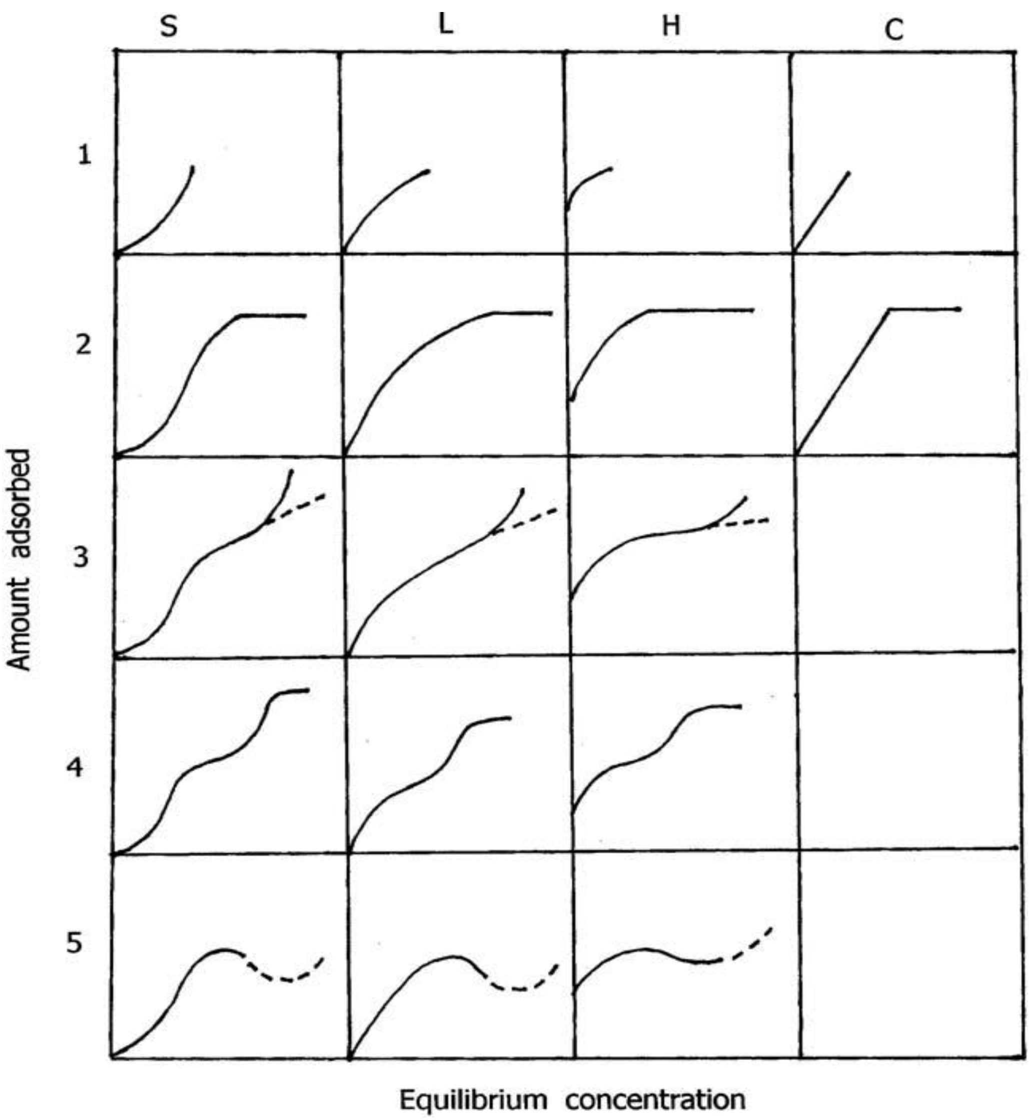


Figure 1.4: Classification of isotherm shapes.

(a) S–curves are indicative of vertical orientation of adsorbed molecules. In the initial part of an S–curve, the more solute that is already adsorbed, the easier it is for additional amounts to become fixed.

(b) L–curves, normal Langmuir isotherms are indicative of molecule adsorbed flat on the surface. The more solute that is adsorbed, the harder it is for the additional amounts to become fixed.

(c) H–curves are attained when there is a high adsorption affinity as in the case of high molecular weight compounds like proteins and polymers; this isotherm can be observed even if the solution is very dilute.

(d) C–curve, constant–partition linear curves are given by substances which penetrate into the adsorbent more readily than does the solvent.

1.5.2. Type of Adsorption Isotherm (Isotherm Models)

1.5.2.1. Langmuir Isotherm

Adsorption characteristics can be depicted by an adsorption isotherm. An adsorption isotherm is the presentation of the amount of solute adsorbed per unit weight of adsorbent as a function of the equilibrium concentration in the bulk solution at constant temperature. Langmuir and Freundlich adsorption isotherms are commonly used for the description of adsorption data (Chantawong, et al., 2003).

The Langmuir isotherm is a valid monolayer adsorption on completely homogeneous surfaces containing a finite number of binding sites. It assumes uniform energies of adsorption on the surface and no transmigration of adsorbate in the plane of the surface, with negligible interaction between adsorbed molecules (Srivastava and Singh, 2010).

The Langmuir equation is expressed as: (Langmuir, 1918):

$$q_e = \frac{q_m K_L C_e}{1 + K_L C_e} \quad (1)$$

where q_e is the amount of solute adsorbed per unit weight of adsorbent (mgg^{-1}), C_e is the equilibrium concentration of solute (ppm), q_m is the adsorption capacity (mg g^{-1}), or monolayer capacity, and K_L is the Langmuir equilibrium constant related to the affinity of binding sites and energy of adsorption (L mg^{-1}) (Tashauoei et al., 2010).

The linear forms of the Langmuir equation are written as follows:

$$\frac{C_e}{q_e} = \frac{1}{K_L q_m} + \frac{C_e}{q_m} \qquad \text{(Form I)} \qquad (2)$$

$$\frac{1}{q_e} = (\frac{1}{K_L q_m})\frac{1}{C_e} + \frac{1}{q_m} \qquad \text{(Form II)} \qquad (3)$$

$$\frac{q_e}{C_e} = K_L q_m - K_L q_e \qquad \text{(Form III)} \qquad (4)$$

The values of q_m and K_L can be evaluated from the slope and the intercept of the linear plot of experimental data of C_e/q_e versus C_e, equation 2, or from the intercept and the slope of the linear plot of experimental data of $1/q_e$ versus $1/C_e$, equation 3.

One of the essential characteristics of the Langmuir isotherm model can be explained in terms of the dimensionless constant called equilibrium parameter R_L which is defined as (Juang et al., 1997):

$$R_L = \frac{1}{1 + K_L C_o} \quad (5)$$

Where C_o is the highest initial concentration (ppm). The value of R_L indicates the shape of the isotherm to be either unfavorable adsorption ($R_L > 1$), linear adsorption ($R_L = 1$), favorable adsorption ($0 < R_L < 1$) or irreversible adsorption ($R_L = 0$) (Anirudhan and Suchithra, 2010; Unuabonaha et al., 2007).

1.5.2.2. Freundlich Adsorption Isotherm

The Freundlich isotherm theory says that the ratio of the amount of solute adsorbed onto a given mass of sorbent to the concentration of the solute in the solution is not constant at different concentrations (Adebowale et al., 2006).

The Freundlich isotherm can be used for non ideal adsorption that involves heterogeneous adsorption surface and active sites with different energies (Manohar, et al., 2006).

It can be defined according to the following formula (Freundlich, 1906, 1932):

$$q_e = K_F C_e^{1/n} \quad (6)$$

Where q_e is the amount adsorbed per unit weight of adsorbent (mgg^{-1}), C_e is the equilibrium concentration of the adsorbate (ppm); K_F is the Freundlich constant ($L\ g^{-1}$) indicating the adsorption capacity and n (g/L) is the adsorption intensity (Jiang et al., 2009).

The logarithmic linear form of the Freundlich equation is given as:

$$\log q_e = \log K_F + \frac{1}{n} \log C_e \quad (7)$$

When $\log q_e$ was plotted against $\log C_e$, a straight line was obtained, then n and K_F can be calculated from the slope and the intercept respectively.

Both K_F and n are empirical constants; where K_F indicates the adsorbate priority for adsorption (Baraka et al., 2007; Qinyan et al., 2009). On the other hand, greater

values of K_F indicate higher capacity for the adsorption than smaller values (Donat, et al., 2005).

Theoretically, the Freundlich equation represents a situation in which the quantity of solute adsorbed increases indefinitely with increasing concentration. This will occur when multilayer is formed and heterogeneous adsorption sites are implied (Stevenson, 1982).

1.5.2.3. Dubinin–Radushkevich (D–R) Adsorption Isotherm

This model seems to be used more and more widely during the recent years, especially in the adsorption removal of metal ions, dyes and other organic contaminates onto solids from aqueous solutions.

The D–R equation is an adaptation of the earlier Polanyi potential theory of adsorption (Polanyi 1963), which is for the volume filling of microspores. The idea that the mechanism for adsorption of gas molecules in microspores is that of pore filling rather than a layer–by–layer formation of a film on the walls of the pores (Holm and Zhu, 1994).

The D–R isotherm model is valid at low concentration ranges and can be used to describe adsorption on both homogeneous and heterogeneous surfaces (Wanga et al., 2009).

The commonly used equation forms are shown by Dubbin et al. (1947):

$$q = q_{max} \exp(-\beta \varepsilon^2) \quad (8)$$

Where β: is the activity coefficient constant related to mean sorption energy ($mol^2.kJ^{-2}$)

ε: the Polanyi potential (Polanyi, 1963).

The linear form has the following expression:

$$\ln q = \ln q_{max} - \beta\, \varepsilon^2 \qquad (9)$$

Where

$$\varepsilon = R\, T \ln (1+1/C_{eq}) \qquad (10)$$

Where: R is the ideal gas constant (8.3145 $J.mol^{-1}.K^{-1}$) and T is the absolute temperature (Kelvin).

According to the linear form of Equation (9), the slope of the plot of ln q_e versus ε^2 gives β and that of the intercept yields the adsorption capacity q_m.

The D–R adsorption isotherm is applied on the adsorption data in order to distinguish between chemical and physical adsorption. The adsorption mean free energy (E) is the energy required to transfer one mole of the adsorbate from infinity in solution to the surface of solid.

This energy is calculated as following:

$$E = 1/\,(2\beta)^{-0.5} \qquad (11)$$

The magnitude of adsorption mean free energy E (kJ/mol) is widely used for estimating the type of adsorption (Xu, et al., 2007).

1.6. Method of operation

The principle techniques of contacting solutions with an ion exchanger are known as the batch operation or the continuous column operation.

1.6.1. Batch operation

The batch is far easier to use than any other method. The solid is shaken in the solution until the adsorption or desorption equilibrium is reached. Then, the remaining solute concentration is measured. The disadvantages are numerous. The solid/ solution ratio is often either too high compared with the natural conditions in rivers, lakes or seas, or too low compared with the natural conditions of porous media. Moreover, the hydrodynamic conditions of natural porous media are not met. A long–term experiment with continuous shaking can lead to side reactions such as the destruction of particles, which prevents the study of very slow reaction (Limousin, et al., 2007).

1.6.2. Column operation

Column operation may be considered to consist of a large number of batch operations that take place in series. Although the extent to which the exchange takes place in each of these small batches is limited by the appropriate selectivity coefficient. The overall efficiency of column operation may be much more favorable than the batch process (Benefield and Weand, 1982). In the majority of the ion exchange plant operations, a vertical cylinder (a column) is filled with an ion exchanger. The solution containing the desired metal ion is passed down through the exchanger (down–flow operation), or up through the exchanger (up–flow operation) (Eckenfelder, 1980).

In batch technique, the displaced competitive substances remain in solution, and thus may interact with the solid. In contrast, the open–flow methods supplies the system with a constant solution and the displaced substances are flushed out and thus do not compete for adsorption. Many studies show that the adsorption is higher in batch than in open flow column. The reasons for this paradoxical behavior are mainly, (i) The

presence of immobile water in the column, which acts as a kinetic barrier, (ii) The difference of solid/solution ratio between batch and column, (iii) The unachievement of chemical equilibrium in column if the mean residence time is significantly lower than the mean reaction time (Limousin, et al., 2007).

1.7. Kinetics of Adsorption

Adsorption kinetics is used in order to explain the adsorption mechanism and adsorption characteristics. Two kinetic models; Lagergreen (pseudo-first-order) and pseudo-second-order reaction were used to test experimental data to predict the adsorption kinetic.

1.7.1. Pseudo-first-order reaction kinetic

The adsorption rate constant was first proposed by Lagergreen in 1898. The first order reaction kinetic equation is shown below (Wen et al., 2006):

$$\frac{dq_t}{dt} = k_1 (q_e - q_t) \qquad (12)$$

Where $k_1(min^{-1})$ is the Pseudo-first-order adsorption rate constant for the first order adsorption, q_e and q_t (mg g^{-1}) are the amount of metal ions adsorbed per unit mass at equilibrium and at any time t, respectively, and is the amount of metal ions adsorbed at (mg g^{-1}).

After definite integration by applying the conditions q_t =0 at t = 0 and $q_t = q_t$ at t = t, equation (12) becomes the following

$$\ln (q_e - q_t) = \ln q_e - k_1 t \qquad (13)$$

The values of k_1 can be obtained from the slopes of the linear plots of $\ln(q_e - q_t)$ versus t. The validity of the first-order kinetics and hence the Lagergren equation could be tested by comparing q_e values obtained from the intercepts of the plots with those obtained. If the validity is weak, the kinetics can be tested for following second-order mechanism (Gupta and Bhattacharyya, 2008).

1.7.2. Pseudo–second–order Reaction Kinetic

The pseudo–second–order reaction assumes that the rate limiting step may be chemical adsorption (Wang et al., 2010).

Adsorption data was evaluated according to the pseudo–second–order reaction kinetic proposed by Ho and McKay (1998):

$$\frac{dq_t}{dt} = k_2 (q_e - q_t)^2 \qquad (14)$$

Where k_2 is the second order reaction constant (g mg^{-1} min^{-1}). For the boundary conditions, t = 0 to t = t and q_t = 0 to $q_t = q_e$, the integrated linear form of the equation is written as:

$$\frac{t}{q_t} = \frac{1}{k_2 q_e^2} + \frac{t}{q_e} \qquad (15)$$

The plot of t / q_t vs. t gives a linear relationship, allowing for computation of q_e and k_2.

The validity of this model can be tested by comparing values of the experimental q_e values (when q_e reach's plateau) with the calculated (1/ slope) of the pseudo–second–order kinetic plots as obtained from equation (15) (Gupta and Bhattacharyya, 2008).

1.8. Metal ions uptake

The metal ion uptake by the kaolin clay (q) was obtained using the following equation:

$$q = \frac{(C_i - C_e)}{m} V \qquad (16)$$

Where;

q: Metal ion uptake by kaolin clay in (mg metal ion (II)/ g kaolinite).

C_i : Initial metal ion concentration (ppm) in the solution.

C_e: The residual concentration of the metal ion in solution at equilibrium in (ppm).

V: volume of solution (L).

m: mass of kaolin clay (g).

The percentage of metal ion loading by the kaolin clay expressed as % uptake where

$$\%\ \text{Metal uptake} = \frac{(C_i - C_e)}{C_i} \times 100$$ (Samal et al., 2002) (17)

1.9. Thermodynamics of Adsorption

Thermodynamic parameters include Gibbs free energy changes ΔG°, enthalpy changes ΔH° and entropy changes ΔS°. The following equations were used for calculation:–

$$\Delta G° = -RT \ln K \qquad (18)$$

Where R is the gas constant (8.3145 $J.mol^{-1}.K^{-1}$), T is the temperature in Kelvin and K is the equilibrium constant which equal to:

$$K = \frac{q_e}{C_e} \tag{19}$$

The K value was obtained from the intercept of the plot of $Ln(q_e/C_e)$ versus q_e.

The values of enthalpy (ΔH°) and entropy (ΔS°) are calculated using the following equation:–

$$\ln K = \frac{\Delta S^o}{R} - \frac{\Delta H^o}{RT} \tag{20}$$

The plot of ln K against 1/T gives a linear relationship, then we can obtain (ΔH°) and (ΔS°) from the slope and intercept of this plot, respectively.

The decrease in the negative value of ΔG° with an increase in temperature indicates that the adsorption process becomes more favorable at higher temperatures, then a spontaneous nature of adsorption. The increase in the ΔG^o with the increase in temperature indicates that the adsorption process becomes energetically less favorable because the free energy becomes more positive at higher temperature (Al–Omari, 2007).

If the adsorption capability increases with temperature, positive value of ΔH° indicates that the adsorption reaction is endothermic. The negative value of ΔH^o shows that the adsorption process is exothermic and less favorable at higher temperatures.

Entropy has been defined as the degree of chaos of a system. The positive value of ΔS° shows the increased randomness after the adsorption. Suggests that some structural changes occur on the adsorbent and randomness at the solid/liquid interface in the adsorption system increases during the adsorption process (Jing et al., 2010; Ramesh et al., 2005). Due to the exchange of the metal ions with more mobile ions present on the exchanger, which would cause increase in the entropy during the adsorption process

(Unlu and Ersoz., 2006). Whereas the negative value of ΔS^o indicates that the adsorption involves a stable arrangement of metal ions on the surface (Xu et al., 2007).

1.10. Literature Survey

A number of studies concerning kaolinite clay used to remove heavy metal ions from aqueous solution. Angove, et al., (1997) used three types of experiment to study the adsorption of Cd(II) onto two kaolinite samples at 25 °C.

(1) Adsorption edges were characterized by a plateau around pH 5–6 separating an initial adsorption stage beginning about pH 4, and a second stage in the pH range 7–9. The plateau was higher for the sample with greater face area.

(2) Adsorption isotherms at constant pH could be fitted closely by a simple Langmuir model at pH 5.50.

(3) Potentiometric titrations of kaolinite suspensions in the presence and absence of Cd^{2+} could be modeled very closely by a surface complexation model assuming constant capacitance. Parameters from this model were used in turn to predict the adsorption edges with remarkable precision.

The results from all the experiments are consistent with the view that Cd^{2+} adsorbs to kaolinite by two distinct processes: ion–exchange at the permanently–charged sites on the silanol faces, and complexation to aluminol and perhaps silanol groups, which occur in particular at the crystal edges.

Holm and Zhu (1994) studied the adsorption of Cd^{2+}, Pb^{2+} and Cu^{2+} on kaolinite from landfill leachate–contaminated groundwater, artificial groundwater (same major–ion concentrations as groundwater) and $NaNO_3$(same ionic strength as the groundwater) was studied. Complexation of Cu^{2+} and Cd^{2+} by dissolved organic matter in the groundwater was also studied. There was less adsorption of all three metals from

groundwater than from $NaNO_3$ for large pH ranges. Adsorption of Cd^{2+} and Pb^{2+} seemed to be due to a combination of ion exchange and surface complexation. This hypothesis was supported by agreement between an ion exchange/surface complexation model and the adsorption data.

Bhattacharyya and Gupta (2006) investigated the removal of Cu^{2+} ions from an aqueous solution by kaolinite, montmorillonite, and their poly(oxozirconium) (ZrO) and tetrabutylammonium (TBA) derivatives.

The entry of ZrO and TBA into the layers of both kaolinite and montmorillonite was confirmed by XRD measurement. The specific surface areas and the cation exchange capacity of kaolinite, ZrO–kaolinite, TBA–kaolinite, montmorillonite, ZrO–montmorillonite, TBA–montmorillonite were measured. Adsorption increased with pH till Cu^{2+} ions became insoluble in alkaline medium. The kinetics of the interactions suggests that the interactions could be best represented by a mechanism based on second order kinetics. The adsorption followed Langmuir isotherm model with monolayer adsorption capacity of 3.0–28.8 mg g^{-1}. The process was endothermic accompanied by increase in entropy and decrease in Gibbs energy. The results have shown that kaolinite, montmorillonite and their poly (oxozirconium) and tetrabutyl–ammonium derivatives could be used as adsorbents for separation of Cu^{2+} from aqueous solution.

Srivastava and Singh (2010) studied the effect of ionic strength on cadmium adsorption onto kaolinite in single– and multi–element systems at three ionic strengths (I) 0.01, 0.1 and 0.5 using $NaNO_3$ as a background electrolyte and at an equilibrium pH 6. Applied concentration of Cd^{2+} ranged from 16.7 to 950.0 μM in the single–element system, whereas, applied concentration of Cd^{2+} and other metals (Cu^{2+}, Pb^{2+} and Zn^{2+}) ranged from 4.2 to 237.5 μM each in the multi–element system. Cd^{2+} adsorption

increased with increase in equilibrium concentration at any ionic strength and decreased with increase in ionic strength at any given equilibrium concentration in both single– and multi–element systems.

Another study concerned in removal of Cu^{2+} from synthetic waste water using kaolinite clay–sequencing both batch and fixed bed reactor system systems. Batch studies revealed that the initial uptake of copper ion on kaolinite clay was rapid and equilibrium was established about in 1 hr. The adsorption isotherm studies clearly indicated that the adsorptive behavior of metal ions on kaolinite clay not only the Langmuir assumptions but also the Freundlich ion exchange and surface adsorption might be involved in the adsorption process of copper on kaolinite clay.

In fixed bed column modeling, adsorption of copper on kaolinite clay at three different flow rates was investigated. They used a column having a diameter of 2 cm with different bed depths such as 10, 20 and 30 cm. The experimental results demonstrated that kaolinite clay can be used as an effective adsorbent for removing Cu(II) from aqueous solutions (El–Said, 2010).

Clay can be modified to improve its sorption capacity. Intercalation, pillaring, and other chemical modifications are the common techniques. An alternative technique, chemically modified clay minerals represent a new class of adsorbents for water purification and industrial wastewater treatment. A study was done to remove Pb(II) from aqueous solution using modified kaolinite clay with 25% (w/w) aluminium sulphate and unmodified kaolinite as adsorbents. The results show that amount of Pb(II) adsorbed onto modified kaolinite (20 mg/g) was more than 4.5–fold than that adsorbed onto unmodified kaolinite (4.2 mg/g) under the optimized condition. In addition, the linear Langmuir and Freundlich models were used to describe equilibrium isotherm. It is observed that the data from both adsorbents fitted well to the Langmuir

isotherm. The kinetic adsorption of modified and unmodified kaolinite clay fitted well to the pseudo–second–order model (Jiang, et al., 2009).

Unuabonah and others (2007) studied the adsorption of lead and cadmium ions from aqueous solutions by tripolyphosphate–impregnated kaolinite clay and they found that the pretreatment of kaolinite clay with tripolyphosphate (TPP) increased the cation exchange capacity of kaolinite clay. The equilibrium adsorption capacity of TPP–kaolinite clay for Pb^{2+} and Cd^{2+} was 126.58 mg/g and 113.64 mg/g, respectively. Binary mixtures of Pb^{2+} and Cd^{2+} in various concentrations caused a decrease in the adsorption capacity of TPP–Kaolinite for either metal ion. However, this may have caused the adsorption of Cd^{2+} onto high energy sites on the surface of the TPP–kaolinite clay. Langmuir– Freundlich, Freundlich, Toth and Temkin isotherms reveal that the adsorption of Pb^{2+} and Cd^{2+} by TPP–kaolinite clay were best described by the Toth and Freundlich isotherms, respectively.

Kinetic and thermodynamic aspects of the adsorption of Pb^{2+} and Cd^{2+} ions on tripolyphosphate–modified kaolinite clay was studied, kaolinite clay was modified with tripolyphosphate reagent to obtain TPP–modified kaolinite clay. The kinetics and thermodynamics of the adsorption of Pb^{2+} and Cd^{2+} by TPP–kaolinite clay were studied. Increasing temperature and initial metal ion concentration increased the adsorption capacity of the adsorbent. The rates of adsorption of both Pb^{2+} and Cd^{2+} increased with increasing temperature but decreased with increasing initial metal ion concentration and time. The adsorption of both metal ions was endothermic and spontaneous for Pb^{2+} and Cd^{2+}. Activation energy values obtained were between +8 kJ mol^{-1} and +22 kJ mol^{-1}. These values suggest that the rate–controlling step in the adsorption of Pb^{2+} and Cd^{2+} by TPP–kaolinite clay was diffusion–controlled. The adsorption capacity of TPP–kaolinite

clay for both metal ions was decreased by simultaneous presence of both metal ions (Adebowale, et al., 2008).

Equilibrium and thermodynamic studies for the adsorption of Pb^{2+} and Cd^{2+} from aqueous solutions onto sodium tetraborate–modified kaolinite clay (NTB–modified kaolinite) were done. Modification with sodium tetraborate reagent increased the adsorption capacity of kaolinite clay for Pb^{2+} and Cd^{2+} at 298 K, because its specific surface area was increased. Increasing temperature was found to increase the adsorption of both metals onto both adsorbents suggesting an endothermic adsorption reaction.

The thermodynamic calculations for the modified kaolinite clay sample indicated an endothermic nature of adsorption for Pb^{2+} and Cd^{2+} and an increase in entropy as a result of adsorption of Pb^{2+} and Cd^{2+}. The small positive values of free energy change (ΔG mean) indicated that the adsorption of Pb^{2+} and Cd^{2+} onto the modified adsorbent may require some small amount of energy to make it more feasible.

Modeling equilibrium adsorption data obtained suggested that NTB–modified adsorbent sample has homogeneous adsorption sites and fit very well with Langmuir adsorption model (Unuabonah, et al., 2008).

Amer, et al., (2010) determine the potential of application of sodium polyphosphate–modified kaolinite clay as an adsorbent for the removal of lead(II), zinc(II) and cadmium(II) ions from aqueous solutions. The adsorbent dosage, pH, temperature and contact time were investigated. The adsorption isotherms of all three metal ions followed well Langmuir equation. Modified sodium polyphosphate–kaolinite clay was found to remove heavy metal ions efficiently from aqueous solutions with selectivity in the order of $Pb^{2+} > Zn^{2+} > Cd^{2+}$. The maximum heavy metal ions adsorbed by modified kaolinite clay was found to be 92.10, 74.26 and 55.12% and the adsorption capacity for Pb^{2+} was 40.00 mg/g, for Zn^{2+} 27.78 mg/g, and for Cd^{2+} 13.23 mg/g. The

thermodynamic parameters, standard Gibb's free energy (ΔG^o), standard enthalpy (ΔH^o) and standard entropy (ΔS^o) calculated using the Langmuir constants for metal ions adsorption on the sodium polyphosphate–kaolinite clay showed that the adsorption process is spontaneous and endothermic in nature. The results of this study showed that the sodium polyphosphate–kaolinite clay powder can be efficiently used as a low–cost adsorbent for the removal of divalent lead, zinc and cadmium from aqueous solution.

Some studies concern at the role of humic acid in adsorption of heavy metals on kaolinite, for example:–

Hizal and Apak (2006b) explain how clay minerals adsorb heavy metals individually and in the presence of humic acid, and model heavy metal adsorption specifically based on surface–metal binary and surface–metal–ligand ternary complexation. Copper(II) showed a higher adsorption capacity and higher binding constants, while lead(II), being a softer cation preferred the softer basic sites with aluminol–phenol functional groups. Metal adsorption onto clay at low pH increased in the presence of humic acid, and the metal adsorption vs. pH curves of metal–kaolinite–humic acid suspensions were much steeper (and distinctly S shaped).

Saada, et al., (2003) investigated the influence of organic matter on arsenic retention, they used batch experiments at pH 7 to determine the adsorption of As(V) on three different solids: a crude, purified, Ca–exchanged kaolinite and two kaolinite coated with humic acids (HAs) having different nitrogen contents. They first examined the adsorption of each HA onto kaolinite, and then used the HA–kaolinite complexes to study As(V) adsorption. The results clearly show an influence of the HA coating on As(V) adsorption.

Comparison of adsorption behavior of multiple inorganic ions on kaolinite and silica in the presence of humic acid using the multitracer technique was studied.

This technique provided the solid–aqueous distributions of 32 elements, namely, Be, Na, Sc, V, Cr, Mn, Fe, Co, Zn, Ga, As, Se, Rb, Sr, Y, Zr, Tc, Ru, Rh, Ag, Te, Ba, Ce, Pm, Eu, Gd, Tm, Yb, Lu, Hf, Re, and Pt, in the absence and presence of humic acid. Speciation calculations under experimental conditions were also conducted for 19 elements among them. Comparison of the pH dependences of each element and humic acid dissolved in the aqueous phase enabled to evaluate the interaction between them. We discussed the predominant species that would control the environmental behavior of each ion. Among the elements studied, it was suggested that humate formation greatly affects the behavior of rare earth elements, which would indicate that the environmental behavior of these ions is influenced by humic substances. For alkaline earth metals (Be, Sr, Ba), divalent transition metals (Mn, Co, Zn), trivalent transition metals (Cr, Fe), and Ag, the influence of the formation of humate complexes on their distribution behavior was observed. It was estimated that the organic–inorganic complex made up of inorganic particles (e.g., kaolinite and silica in this study) coated with humic substances, plays an important role in the behavior of various ions in the environment. Based on the present results and an equilibrium model expressed by stability constants of hydroxides and carbonates or oxalates, the environmental behaviors of various cations are compared. For the oxoanions found in this study, such as As, Se, Tc, and Re, humate formation also was not important. The inhibiting effect, on the adsorption of ions onto the solid surface, of the humic acid coating on the surface was observed for the distributions of As, Se, Zr, Ru, Rh, Hf, and Pt. These results show that the adsorption of humic substances alters the nature of inorganic particles in adsorbing metal ions (Takahashi, et al., 1999).

The effect of humic acid on the adsorption of the rare earth elements (REEs) on kaolinite and its controlling factors were studied, adsorption experiments were

performed at pH range of from 3 to 10 with kaolinite (1500 mg/L) in a matrix of various concentration of $NaNO_3$ and about 20µg/L of the total REEs as well as various amounts of humic acid (HA). The adsorption of HA onto the kaolinite occurred over a wide pH range and decreases with increasing pH and with increasing HA concentration. The results show that humic acid has ability to either increase or decrease the adsorption of the REEs onto kaolinite, depending on pH, which may be related to their speciation distribution, interaction of HA with the mineral surface. Furthermore, the light REEs are more adsorbed onto kaolinite in presence of higher concentration of HA, presumably because the increase in HA concentration in the solution enhance stronger complexing of HA with heavy REEs as compare to light REEs. The ionic strength has strong effect on the adsorption of HA and REEs onto the kaolinite but little on the REEs fractionation. The results presented here indicate that mineral/water adsorption may generate the enrichment of the dissolved heavy REEs in the presence of a significant amount of humic acid, which is consistent with the fractionation of REEs in the most of natural waters (Wan and Liu, 2006).

Another isotherms of adsorption of humic acid (HA) onto bentonite were studied at different pH (3.0–6.0) and temperature values. The Langmuir monolayer adsorption capacity was found to be 53 mg HA/g raw bentonite at pH=3.0 and 25 °C, ΔH°=54.8 kJ/mol, ΔS°=220 J/mol.K. In the case of bentonite, the q_m and Langmuir constant (K_L) values are significantly greater than those reported for zeolite. These results indicate the importance of sheet structure of bentonite in the adsorption process. Treatment of raw bentonite with NaCl, CH_3COOH and HCOOH does not affect adsorptivity (q_m and K_L) of HA on bentonite, while treatment with HCl causes great decrease in adsorptivity. The adsorptivity of HA on bentonite was found to be inversely

proportional to the increase in pH because of the increase in repulsion between HA and bentonite (Salman et al., 2007).

1.11. Aims of the Current Work

The main aim of this work is to use modified Jordanian kaolin clay which is rich of iron dioxide, as adsorbent for some heavy metal ions from aqueous solution. The modification of kaolin clay from Azraq area will be done by humic acid (HA) in order to increase the ability of kaolin clay to adsorb heavy metal ions.

Adsorption isotherm of two types of HA; one isolated from sediment of King Talal Dam (KTD) and the other purchased from Fluka Company, on kaolin clay will be studied at different (pH) and temperatures using UV–Vis spectroscopy.

The modified kaolin clay will be characterized by XRD, IR, SEM and TGA to understand its nature, structure, behavior and properties.

Adsorption of heavy metal ions (Pb(II), Cd(II) and Zn(II)) onto the modified kaolin clay at different pH, temperatures and constant ionic strength will be studied using batch technique. The desorption process after adsorption will be also studied using column technique. Concentrations of the metal ions were determined using atomic absorption spectrometer (AAS). All this will shed the light on the role of kaolin clay in the Jordanian environment and to understand the fate of heavy metal ions on the modified Jordanian kaolin clay.

Modeling of adsorption data using Langmuir, Freundlich and Dubinin–Radushkevich (D–R) models will be the final goal in this study to understand and explain the adsorption behaviors. The kinetic and thermodynamic parameters of adsorption will be calculated. This is expected to be of great benefit because all these processes are interrelated; especially no previous studies on Jordanian kaolin clay in took all these processes into consideration.

Comparing the results obtained from adsorption and desorption of heavy metal ions (II) by FHA– kaolin clay with the other from KTD– kaolin clay.

It is hoped that this modest effort may substitute the deficiency in the literature on the spectroscopic, XRD, thermal, SEM, surface area and porosity characterization, adsorption mechanism and adsorption characteristics of clay minerals in Jordan.

2. Experimental

2.1. Materials

All chemicals were obtained from commercial sources as either analytical reagent grade or chemically pure grade and were used as received. The chemicals were purchased from the corresponding companies: sodium perchlorate ($NaClO_4$) (Acros), lead(II) nitrate; $Pb(NO_3)_2$ (PRS Paureac), cadmium(II) nitrate. tetrahydrate; $Cd(NO_3)_2.4H_2O$ (BDH), zinc nitrate. hexahydrate; $Zn(NO_3)_2.6H_2O$ (BDH), sodium hydroxide NaOH (LOBA), hydrochloric acid; HCl 37% (TEDIA), potassium chloride; KCl (Puriss), and ethylenediaminetetraacetate–disodium salt ($EDTANa_2$), silver nitrate; $AgNO_3$ (Puriss). Two types of humic acid; one from Fluka company and the other extracted from King Talal Dam sediments (Khalili, 1987), kaolin clay from the Azraq region in east of Jordan.

2.2. Instrumentation

Concentrations of the metal ions were determined using (Varian Spectra AA–250 pulse) atomic absorption spectrometer (AAS). Concentrations of humic acid were determined using UV–VIS Spectrophotometer (Varian cary100). Drying of modified kaolin clay by freeze–dryer (ALPHA 1–4). Shaking of samples was done using Clifton Shaker equipped with thermostat and pH was measured using METROHM 605 pH–meter.

2.2.1. Fourier transform infrared (FT–IR)

FT–IR spectra were recorded using Thermo Nicolet NEXUS 670 FT–IR Spectrophotometer. Powder of KBr was dried at 200 °C for 24 h, and then KBr was homogenized with kaolin clay (1:100) in ball grinder. The disc (diameter 1 cm,

thickness 0.1 cm) was prepared using hydraulic press. The disc was mounted in the sample holder of the FT–IR. The infrared spectrum was recorded in the wavelength range 400 – 4000 cm^{-1}.

2.2.2. X–ray diffraction (XRD)

XRD of kaolin clay samples were recorded using Philips X pert pro, operated at 30 KV and 30 mA, scatter slit: 1 deg, receiving slit: 0.3 mm, drive axis: 2 theta, scan speed: 2 deg/min and sampling pitch: 0.02 deg. The samples were dried and grounded into fine powder prior to their characterization. Then, X–rays are generated by impinging copper metal target with high–energy electrons in a vacuum.

2.2.3. Elemental analysis

Elemental analyses of the two humic acid samples were done by using Euro Vector 3000 Elemental Analyzer.

2.2.4. Thermal gravimetric analysis

The thermal gravimetric analysis (TGA) of the kaolin clay samples was studied using NETZCH STA 409 PG/PC Thermal Analyzer in the temperature range (0–1000)^{o}C, at a heating rate of 20 ^{o}C/min.

2.2.5. Scanning electron microscope

The scanning electron microscopy technique was used to obtain information about the surface of unmodified and modified kaolin clay with humic acids and loaded modified kaolin clay with lead ions. The FEI inspect F50 scanning electron microscope was used to record micrographs of the particles after coating with platinum then the energy dispersion spectrum (EDS) was used to determine the elements present.

2.2.6. Surface area

Surface area of unmodified and both modified kaolin clay were measured using (Gemini VII) instrument from micromeritics according to Langmuir surface area method which is based on the isothermal adsorption of nitrogen.

2.2.7. Porosity

Porosity of unmodified and both modified kaolin clay were measured using Mercury Porosimetry Analyzer instrument (Model: PM–60–13) from Quantachrome Instruments.

2.3. Part (I): Adsorption of humic acid by kaolin clay

2.3.1. Batch adsorption

A 1000 ppm of HA was prepared by dissolving 1.0g ± 0.1 mg of HA in 1.0 L of 0.01M NaOH solution. The stock solution was diluted with 0.01M of NaOH solution for the preparation of more diluted solutions keeping pH=11.00.

Batch adsorption was carried out using pyrex glass vessels. An accurate mass (0.04g ± 0.1 mg) of kaolin clay measured to the nearest 0.0001g was shaken with 20.0 mL of (10, 30, 50, 70, 90, 110, 130 and 150 ppm) solutions of HA for 24 hr at 25, 35 and 45^{o}C, and pH=3.00 , 4.00, 5.00 and 6.00.

Aliquot of solution was then filtered using 0.45µm micro filter and analyzed by UV–VIS spectrophotometer at λ=320 nm for FHA and λ=215 nm for KTD humic acid to measure the concentration of free HA.

Calibration curve was determined using standard samples prepared from both HA's at each pH.

2.4. Part (II): Adsorption of heavy metal ions by modified kaolin clay

2.4.1. Humic acid– kaolin clay complex preparation

The kaolin clay was brought from Azraq region in the east of Jordan. The >250μm clay fractions were obtained by wet sedimentation and subsequently exchanged with K^+ by washing the clay fractions with 0.5 M KCl solution four times. The excess KCl was removed by repeatedly washing with deionized water until negative Cl^- was determined by $AgNO_3$ solution. The clay suspensions were quickly frozen, freeze–dried, and stored in closed containers prior to use (Li, et al., 2003).

The humic acid–clay complexes were prepared by dissolving Fluka humic acid (FHA) or King Talal Dam humic acid (KTD) 1.0 g ± 0.1 mg in 1.0 L of 0.5 M KCl solution, followed by mixing with 10 g ± 0.1 mg of the corresponding K^+ – clay for 1 week. The humic acid–clay complexes were obtained by centrifugation, then mixed with 0.5M KCl solution (three times) to saturate the cation–exchange sites in humic acid, dialyzed against deionized water, and then washed (>20 times) with deionized water until neither light brown–colored humic substances in supernatants nor humic acid particulates accumulating on the top of clay fractions after centrifugation were visualized. The humic acid–clay complexes were quickly frozen and freeze–dried.

2.5. Preparation of stock solutions of metal ions

Stock solutions of 1000 ppm for the metal ions were prepared separately by dissolving specific amount of each metal salt of Pb(II), Cd(II) and Zn(II) nitrate in 0.01M $NaClO_4$ and was adjusted by 0.10M HCl and/or 0.10M NaOH to the desired pH. The stock solutions were used to prepare solutions with different concentrations (10, 20,

30, 40, 50, 60, 80 and 100 ppm). The dilution is achieved by using 0.01M $NaClO_4$ to keep the ionic strength constant.

2.6. Metal ions uptake characteristics by batch techniques

The metal ions uptake characteristics for each metal ion were studied using batch equilibrium technique in the following manner.

2.6.1. The rate of metal ions uptake experiments

Experiments for determination of the equilibrium time of the adsorption process were studied by shaking 0.2 g ± 0.1 mg of the modified kaolin clay with 20.0 mL of 100 ppm metal ion solution at a pH value of 5.00. The contact time was varied from 30 minutes to 24 hrs at 35 ^{o}C. The mixture was filtered and the concentration of the metal ion remaining was determined using AAS. Every measurement was repeated three times to make sure of the accuracy and reproducibility of the results.

2.6.2. Effect of pH on the metal ions uptake experiments

Similar experiments as mentioned previously were also carried out, under different pH values of 4.00, 5.00 and 6.00 at fixed contact time of 4 hrs to determine the effect of pH on the metal ion uptake by kaolin clay.

2.6.3. Adsorption isotherms experiments

The adsorption of Pb(II), Cd(II) and Zn(II), was carried out by taking 0.2 g ± 0.1 mg of the modified kaolin clay with 20.0 mL of solutions of various metal ion concentrations ranging between (10–100) ppm for each metal, at different pH values of 4.00, 5.00 and 6.00 and at different temperatures of 25, 35 and 45^{o}C. Every

measurement was repeated three times to make sure of the accuracy and reproducibility of the results, then average was taken.

2.7. Metal ions uptake using the column technique

The adsorption using the column experiments for Pb(II), Cd(II) and Zn(II) were done using 30 cm length and 20 mm inner diameter glass column. The column was packed with 2.0 g ± 0.1 mg dried modified kaolin clay. A 100.0 mL of 1000 ppm and pH=4.00 of metal ion solutions divided into ten portions (10.0 mL each) was passed through the column at 1.0 mL/min flow rate. The eluent was collected in ten test tubes, and the concentrations of the metal ion in each test tube were determined using AAS. Every measurement was repeated three times to make sure of the accuracy and reproducibility of the results, then average was taken.

2.7.1. Desorption experiments

The desorption of the Pb(II), Cd(II) and Zn(II) ions was carried on column, loaded with each metal ion as described in (section 2.7), then eluted using 0.1 M HNO_3, for Pb(II) and Cd(II), and 1 M EDTA for Zn(II) keeping the flow rate of elution 1.0 mL/min. The concentration of metal ions in eluate collected in four portions (10.0 mL each portion) was then determined using AAS. Every measurement was repeated three times to make sure of the accuracy and reproducibility of the results, then average was taken.

2.7.2. Regeneration experiments

Reusing both modified kaolin clay in repeated cycles of adsorption of metal ions, by reloading the modified kaolin clay with 20.0 mL of 1000 ppm and pH=4.00 of metal ion solutions divided into two portions (10.0 mL to each portion) was

passed through the column at 1.0 mL/min flow rate. The eluent was collected in two test tubes, and the concentrations of the metal ion in each test tube were determined using AAS. Every measurement was repeated three times to make sure of the accuracy and reproducibility of the results, then average was taken.

3. Results and Discussion

3.1. Characterization of modified kaolin clay

Both modified kaolin clay FHA– kaolin clay and KTD– kaolin clay were characterized by Fourier transform infrared (FT–IR) spectroscopy, thermogravimetric analysis (TGA), scanning electron microscopy (SEM), X–ray diffraction (XRD) and elemental analysis of the two kinds of humic acid.

3.1.1. FT–IR

Unmodified and both modified kaolin clay samples were analyzed by FT–IR spectroscopy. Figure (3.1) illustrates the FT–IR spectra over the range 400–4000 cm^{-1}. We have investigated the infrared spectrum of kaolin clay which displays well resolved absorption bands. IR spectroscopy was also extensively used to investigate the hydroxyl groups and H–bonding pattern in kaolinite (Farmer, 1998). The structure of kaolinite–group minerals is formed by a stacking of 1:1 layers (Figure 1.2). Each layer contains a pseudo–hexagonal silica sheet of corner–shared SiO_4 units linked to a dioctahedral sheet of edge sharing $AlO_2(OH)_4$ octahedral. Two kinds of OH groups can be distinguished. The inner–surface OH groups, which are located at the top of the dioctahedral sheet, are hydrogen–bonded with the basal plane of oxygen atoms of the next layer. Other OH groups (inner OH groups) are located inside the layer, between the dioctahedral and tetrahedral sheets, pointing horizontally toward the center of the ditrigonal cavity (Bish, 1993).

Table (3.1) summarizes the FT–IR position (cm^{-1}) for kaolinite as recorded in literature, some of them appear in our results and the others are not.

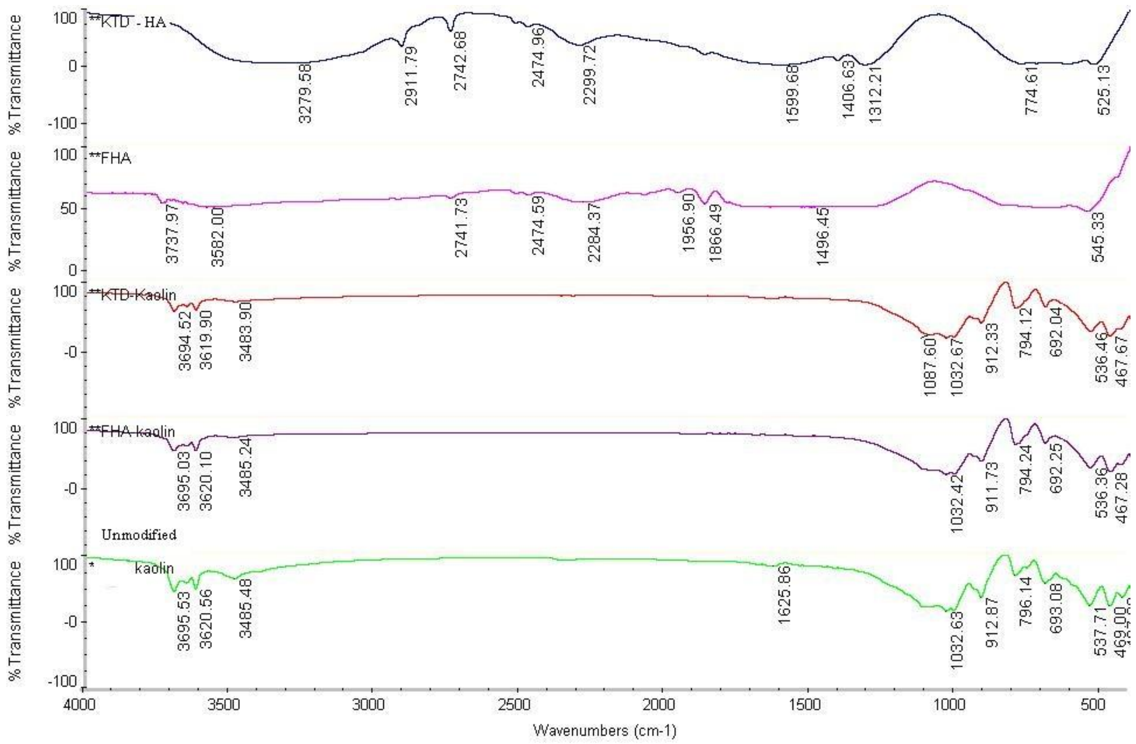


Figure (3.1): FT–IR for unmodified, both modified kaolin clay and two kinds of HAs.

Table (3.1): FT–IR position (cm^{-1}) for kaolinite (Madejova and Komadel, 2001).

Position (cm^{-1})	**Theoretical Assignment**	**Experimental Assignment**
3695	**OH stretching of inner-surface hydroxyl groups**	**Yes**
3669	**OH stretching of inner-surface hydroxyl groups**	**No**
3651	**OH stretching of inner-surface hydroxyl groups**	**No**
3620	**OH stretching of inner hydroxyl groups**	**Yes**
3485	**OH stretching of water**	**Yes**
1625	**OH deformation of water**	**Yes**
1102	**perpendicular Si–O stretching**	**Yes**
1091	**In-plane Si–O stretching**	**Yes**
1002	**In-plane Si–O stretching**	**Yes**
938	**OH deformation of inner-surface hydroxyl group**	**No**
913	**OH deformation of inner hydroxyl groups**	**Yes**
795	**Si–O**	**Yes**
755	**Si–O, perpendicular**	**No**
697	**Si–O, perpendicular**	**Yes**
602	**Si–O**	**No**
507	**Al–O–Si deformation**	**Yes**
469	**Si–O–Si deformation**	**Yes**
428	**Si–O deformation**	**Yes**

According to Figure (3.1), the IR data showed the following characteristic peaks, in the range of the OH stretching vibrations, the band experimentally observed at 3620 cm^{-1}corresponds to the inner OH stretching. The one observed at 3695 cm^{-1} corresponds to the stretching vibration modes of 'inner surface hydroxyls' that are located at the surface of octahedral sheets opposite to the tetrahedral oxygen’s of the adjacent kaolinite layer (Bish, 1993).

The band at 3485 cm^{-1} refers to OH stretching of water, while the bands in the ranges between (1100 to 1000 cm^{-1}) are referred to Si–O stretching vibrations at 1102 and 1091 cm^{-1} while the bands at 1002 cm^{-1} are rather caused by Si–O–Si and Si–O–Al lattice vibrations. The OH bending vibration at 912 cm^{-1} is referred to the ‘inner OH bending'. Further, bands at 794 and 692 cm^{-1} can be largely attributed to different Si–O vibration (Reyes et al., 2010).

The band at 536 cm^{-1} refers to Al–O–Si deformation, but Si–O–Si deformation happened at 469 cm^{-1} , and finally at 428 cm^{-1} there is Si–O deformation.

We can notice that FT–IR is a simple technique that can not differentiate between unmodified and modified kaolin clay, because there is no distinct bands refer to humic acid in the FT–IR spectra.

3.1.2. XRD Analysis

The X–ray diffraction pattern of humic acid extracted from KTD region exhibited very small diffuse peaks with a few intense peaks, implying its non–crystalline nature. This behaviour is consistent with the behaviour observed in the case of humic substances from other sources.

The X–Ray diffraction revealed a 24.99° peak of KTD– HA which was believed to be condensed aromatic carbons (Davies and Ghabbour, 1998; Schnitzer et al., 1991).

All the HAs, showed three peaks at $2\theta = 25°$ or 26°, 40–43°, and 85°, respectively. Since the simultaneous appearance of three bands at these degrees is a typical feature of a graphite–like structure (Ikeya et al., 2011).

The presence of an aromatic structure is supported by the peaks at about 34.511° and 34.102°, which may also indicate the existence of graphite like layers (Khalili and Ajjouri, 1987).

Figure (3.2) shows representative XRD spectra of the unmodified and both modified kaolin clay. The main minerals in the samples were kaolinite with associated some minerals like quartz, illite, feldspar, and hematite. Quartz accounted for the highest proportion, which is a common mineral in all soils.

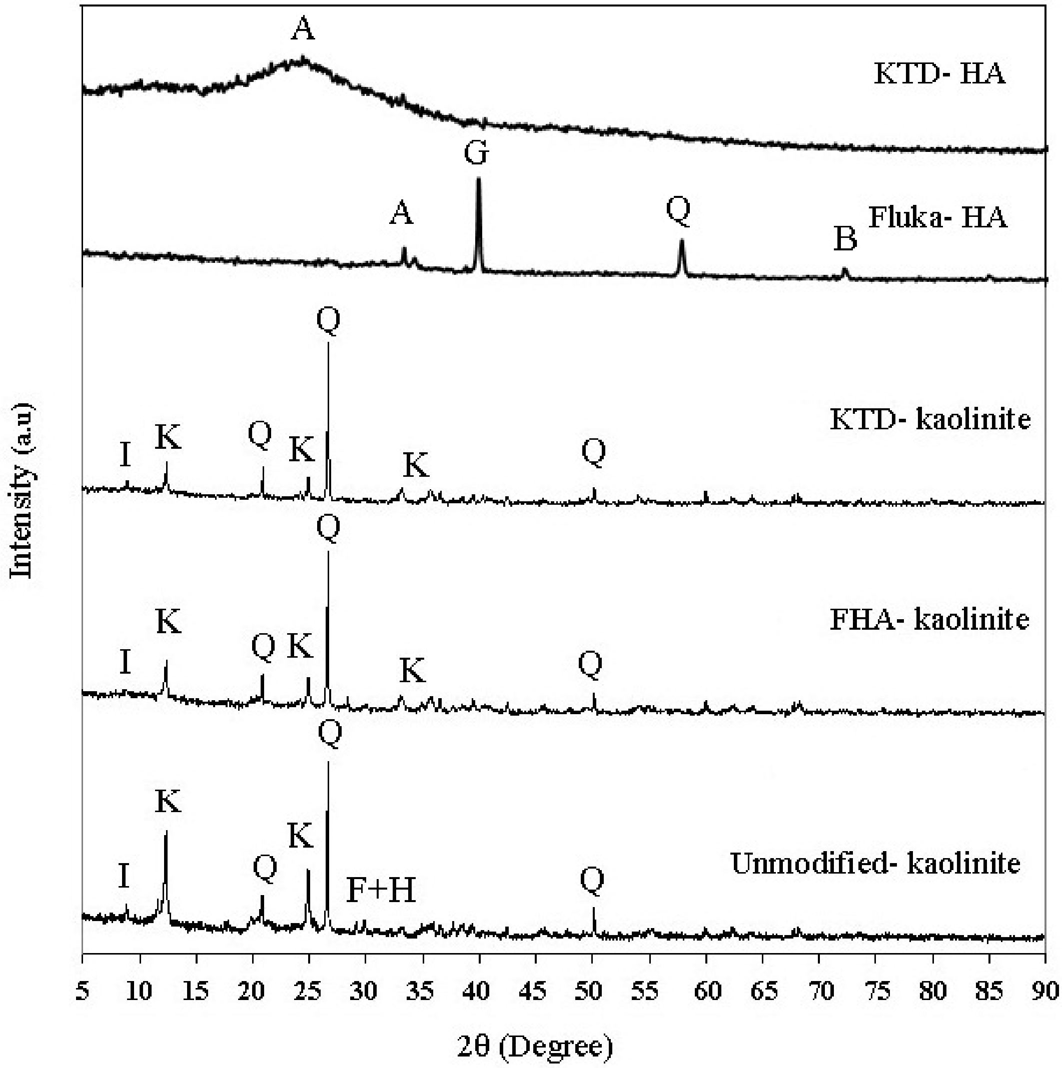


Figure (3.2): XRD pattern of both humic acid, unmodified and both modified kaolin clay. I illite, K kaolinite, Q quartz, F feldspar, H hematite, B bentonite, G graphite like structure and A aromatic structure.

The X–ray diffraction analysis showed (Table 3.2) that the examined unmodified sample was rich in kaolinite mineral. The relative intensities of kaolinite peaks were higher than those in the two modified samples with constant values of other minerals such as quartz (at reference peak 2Θ =26.63). This decrease in relative intensities indicates that the modified ones adsorb humic acid.

On the other hand, there is a decrease in quartz peaks intensities at 2Θ which are equal to 20.86 and 50.14, and another decrease in illite peak intensity in going from the

unmodified kaolin clay to the modified ones, which indicates that the modified ones adsorb humic acid.

Table (3.2): Relative intensity of minerals in XRD data of unmodified and both modified kaolin clay.

Mineral	**2Ө**	**Relative Intensity**		
		Unmodified kaolinite	**FHA-kaolinite**	**KTD-kaolinite**
Kaolinite	**12.37**	**58.91**	**24.97**	**19.71**
	24.89	**37.81**	**18.93**	**13.80**
Quartz	**20.86**	**21.75**	**20.33**	**18.03**
	26.63	**100.00**	**100.00**	**100.00**
	50.14	**18.87**	**11.82**	**10.15**

3.1.3. Elemental Analysis

Elemental analysis were done to show the percentage of each element in FHA and KTD. Table (3.3) shows the percentage of each element in both humic acids.

Table (3.3): Comparison between elemental analysis of FHA and KTD humic acids.

Humic acid	% C	%O	% N	% H
FHA	27.11	70.57	–	2.32
KTD	54.42	31.9	6.50	7.18

Table (3.4): Characterization results of FHA and KTD humic acids.

Humic acid	Atomic H/C ratio	Atomic O/C ratio	Atomic C/N ratio
FHA	0.086	2.603	–
KTD	0.132	0.586	8.372

The exact composition of humic acid varies from one source to another. Our humic acids come from Fluka Company and the other from King Talal Dam. Percentage (%) of oxygen in KTD is less than FHA, while the percentage (%) of nitrogen is higher; it may be due to degradation of dead organic matter in the dam.

3.1.4. Thermal properties

The thermal stability of the kaolin clay was investigated by thermogravimetric analysis (TGA) under dry nitrogen atmosphere.

TGA has been used very widely in the study of thermal reactions of clay minerals. These reactions include dehydration of adsorbed water, dehydroxylation (evolution of water from hydroxyls belonging to the clay skeleton) followed by the transformation of the clay to a meta–phase and recrystallization of the meta–phase into a crystalline phase. As shown in TGA curve in Figure (3.3), in the first step of transformation, kaolinite was transformed to metakaolinite phase with loss of structural hydroxyl groups. In the second step, metakaolinite decomposes and forms spinel phase during the heating.

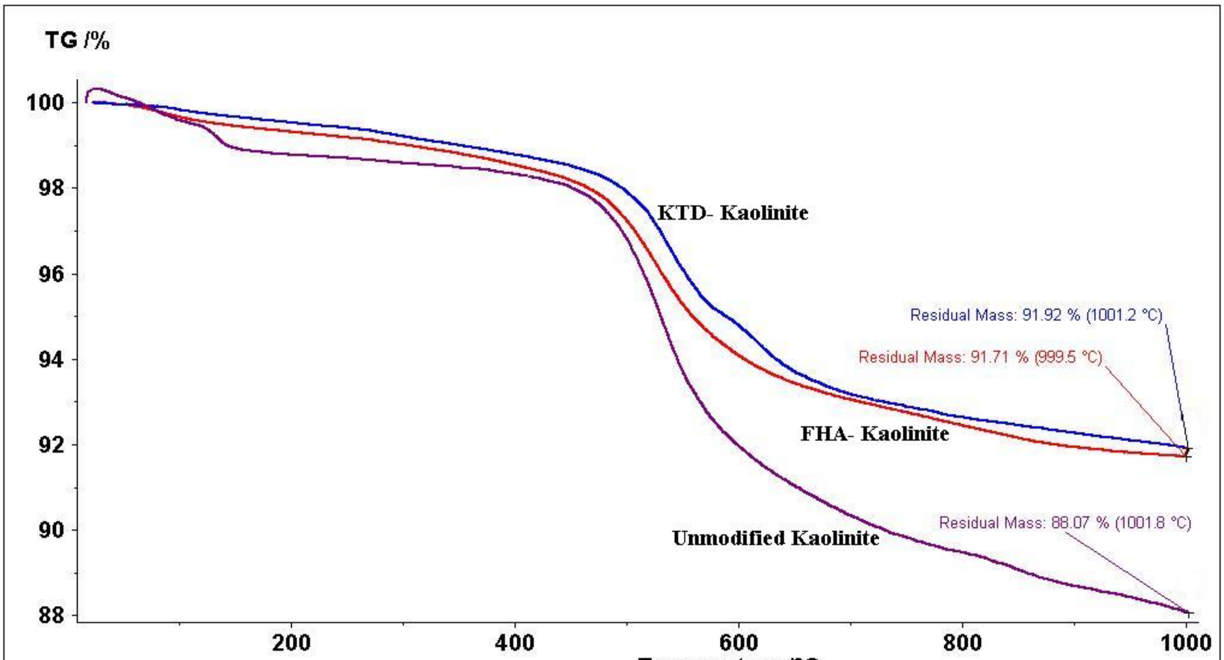


Figure (3.3): TGA thermogram of unmodified and both modified kaolin clay.

When the kaolinite is heated, the adsorbed water is liberated at above 100 °C and the weakest part of the chemical bond is broken or perturbed; then dehydroxylation takes place at 400–600 °C range. The main changes pointed out by TGA, during the heating of the samples are indicated as follows:

(i) T < 100 °C: low temperature released of the absorbed water in pores and on the surfaces.

(ii) 100–400 °C: mass lost that can be correlated with a pre–dehydration process, which takes place as a result of the reorganization in the octahedral layer, first occurring at the OH of the surface.

(iii) 400–650 °C: dehydroxylation of kaolinite and formation of metakaolinite according to the following reaction:

$$2SiO_2 . Al_2O_3 . 2H_2O(s) \rightarrow 2SiO_2 \cdot Al_2O_3 (s) + 2H_2O(l) \qquad (21)$$

(iv) 950 °C: decomposition of metakaolinite was observed according to the following chemical reaction:

$$\underset{\text{(Metakaolinite)}}{2(2SiO_2 \cdot Al_2O_3)(s)} \xrightarrow{950\ °C} \underset{\text{(Al−Si−spinel)}}{Si_3Al_4O_{12}(s)} + \underset{\text{(Amorphous)}}{SiO_2(s)} \qquad (22)$$

The kaolinite structure consists of a single silica tetrahedral sheet and a single alumina octahedral sheet combined to form the kaolinite unit layer. These unit layers are stacked one over the other. During heating, the silicon atoms experience a range of environments of differing distortion due to dehydroxylation.

The aluminium atoms mostly transform from octahedral to tetrahedral geometry. As the calcination temperature increases, the structure becomes more distorted, and finally amorphous silica is liberated. For kaolinite, dehydroxylation might result in the

disturbance of the Al^{3+} octahedral sheets by the outer hydroxyls, but does not much effect on the SiO_4 tetrahedral sheet due to the more stable inner–hydroxyl groups. The outer hydroxyls of octahedral sheets may be more easily removed by heating than inner ones that will maintain a more ordered SiO_4 tetrahedral group in structure during dehydroxylation. After heating at 950 °C, the SiO_4 groups combine with AlO_6 group to form the Al–Si spinel phase that in a short range order structure (Kakali et al., 2001; Alkan et al., 2005).

The thermogram (Figure 3.3) showed sharp drop for unmodified kaolin clay, after about 500 °C, while a less sharp drop for modified kaolin clay, this may indicate there is a slight increase in thermal stability of modified kaolin clay.

The thermogram showed the residual mass percentage at 1000 °C equal to 88.07%, 91.71%, and 91.92%, for unmodified kaolin clay, FHA– kaolin clay and KTD– kaolin clay, respectively. This indicates more thermal stability of modified kaolin clay due to the presence of humic acid, which is estimated to be about 3.64 for FHA– kaolin clay and 3.85 for KTD– kaolin clay.

The thermal analysis data Figure (3.3) showed that the area of the dehydroxylation decreases significantly for unmodified kaolin clay, (in the range of 400–650 °C) because of the dehydroxylation of kaolinite and the formation of metakaolinite. The residual mass percentage is the same for the two modified kaolin clay and higher for unmodified kaolin clay, this may be due to the loss of the crystalline water that decreases with modification, which leads to more thermal stability of the modified kaolin clay due to the presence of humic acid.

The thermogram showed a small drop at T < 150 °C for unmodified kaolin clay, which represent of released of the absorbed water in pores and on the surfaces. While

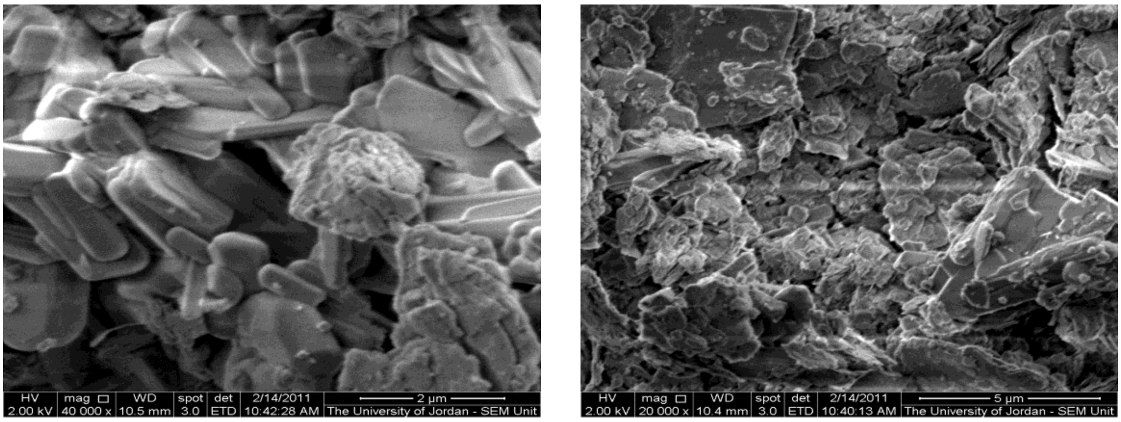
it's absent in both modified kaolin clay, which mean that the modified one adsorbed HA accompanying of water released. This is a good indicator of presence HA on modified kaolin clay.

Even humic acid is an easily thermodegradable molecule, but its adsorption lead to a little increase in the thermal stability of both modified kaolin clay. Humic acid alone is completely degraded at peaks up to 450 °C (Santos et al., 2007; Rosa et al., 2007). Weight losses at 200 °C temperature range are usually due to dehydration, decarboxylation, and dehydroxylation of phenols (Tan, 1998). At a range of 300 °C to 400 °C, humic acid decomposed as OH and COOH groups were completely eliminated. Between 400 °C and 600 °C the weight loss, due mainly to the decomposition of aromatic polycondensates with the lowest oxygen content (Wendlandt, 1974; Tan et al., 1986).

3.1.5. Scanning electron microscope (SEM)

3.1.5.1. Unmodified Azraq kaolin clay

The surface topography of unmodified kaolin clay before adsorption of humic acid was observed by SEM, and the results are shown in Figure (3.4).

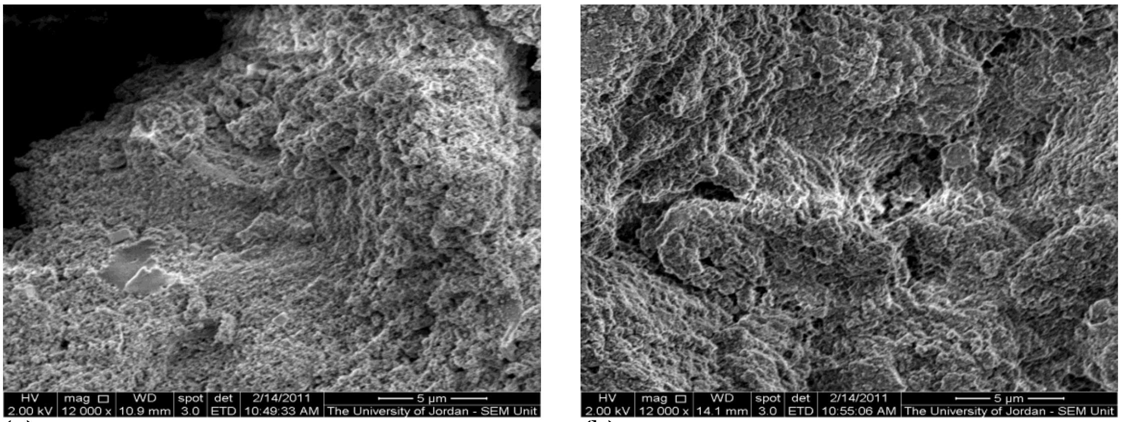


(a) (b)

Figure (3.4): SEM micrographs for unmodified kaolin clay at different magnifications (a) 40000x and (b) 20000x.

The clay fractions that are >250µm of Azraq kaolin clay consists of pseudohexagonal crystals. The crystals typically are thin and flexible plates. As shown there are also distributed pores and a plate–like structure in the photo–micrographs, with high crystallinity and a high degree of ordering.

3.1.5.2. Humic acids



(a) (b)

Figure (3.5): SEM micrographs for FHA and KTD–humic acid (a, b respectively) with same magnifications 12000x.

SEM observations revealed humic acids of different sources (Figure (3.5)) to have polymeric structure, appearing in form of chains, and clusters. Solid humic acids have pores that are too small.

3.1.5.3. Modified Azraq kaolin clay

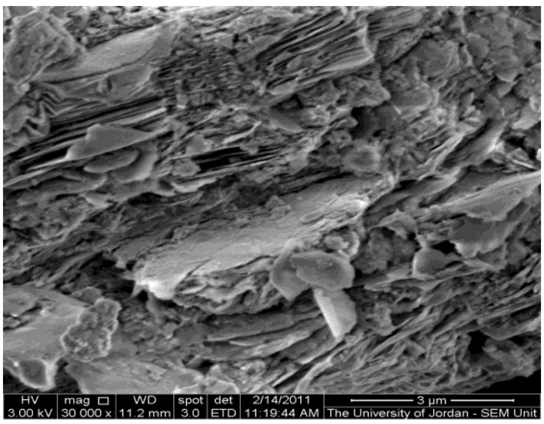
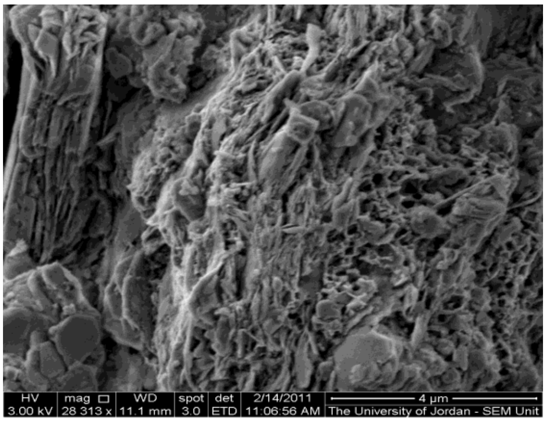
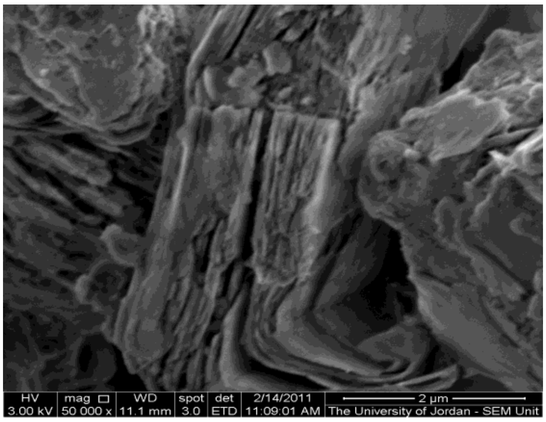


Figure (3.6): SEM micrographs for KTD– kaolin clay with magnification 30000x.



(a)



(b)

Figure (3.7): SEM micrographs for FHA– kaolin clay at different magnifications (a) 28313x, (b) 50000x.

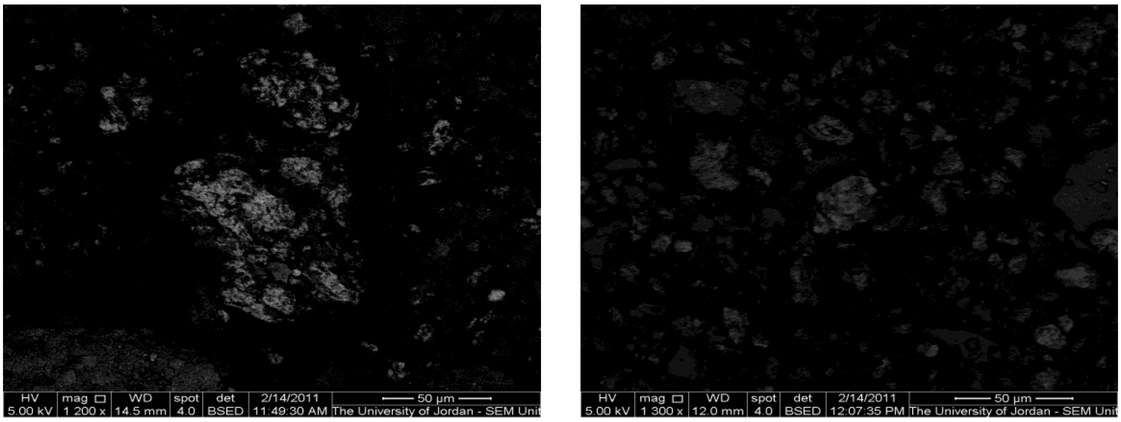
By reference to Figures (3.6) and (3.7), we can observe the changes after the adsorption of the humic acid to the kaolin clay.

SEM shows that aggregation of humic acid particles, which occurred mainly as elongated layers and bundles of fibers, forming a relatively open structure. On the other hand, the fibers tend to mesh into a network to yield a sponge–like and sheet with homogeneous grains distribution.

It has been considered that the adsorption efficiency of humic substances is related to pore size of the adsorbent. According to literature reports 50–200 µm pore size of adsorbent is suitable for the adsorption of humic substances (Summers and Roberts, 1988). The pore size of the kaolin clay used in this study was determined by Mercury Porosimetry Analyzer to be 4.26 µm to 224.23 µm and was effective as an adsorbent for the adsorption of the humic substances.

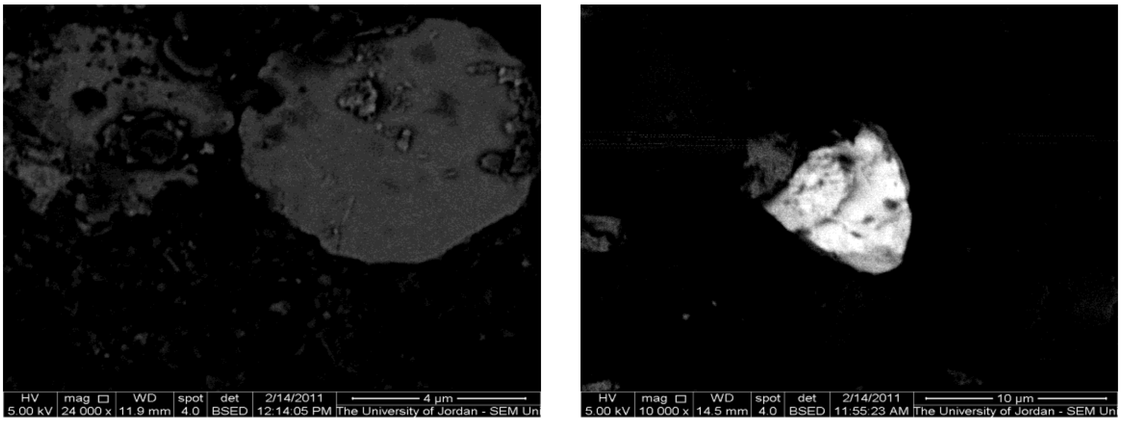
3.1.5.4. Modified kaolin clay loaded with lead

Since the highest uptake of metal ions by modified kaolin clay was for Pb(II). So we studied both modified kaolin clay loaded with lead ions by SEM to observe the changes in surface topography that took place.



(a) (b)

Figure (3.8): SEM micrographs for FHA– kaolin clay and KTD– kaolin clay (a, b respectively) with Pb(II) at different magnifications (a) 1200 x, (b) 1300x.



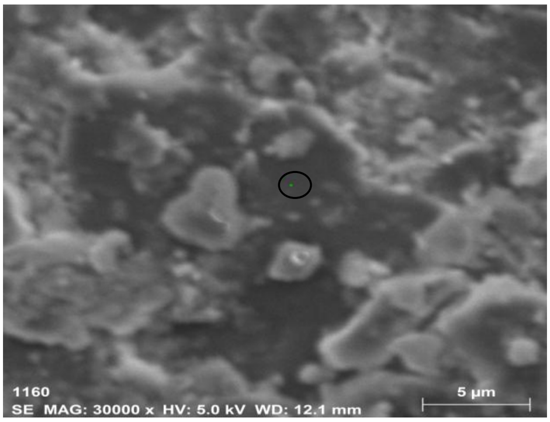
(a) (b)

Figure (3.9): SEM micrographs for FHA– kaolin clay and KTD– kaolin clay (a, b respectively) with Pb(II) at different magnifications (a) 24000x, (b) 10000 x.

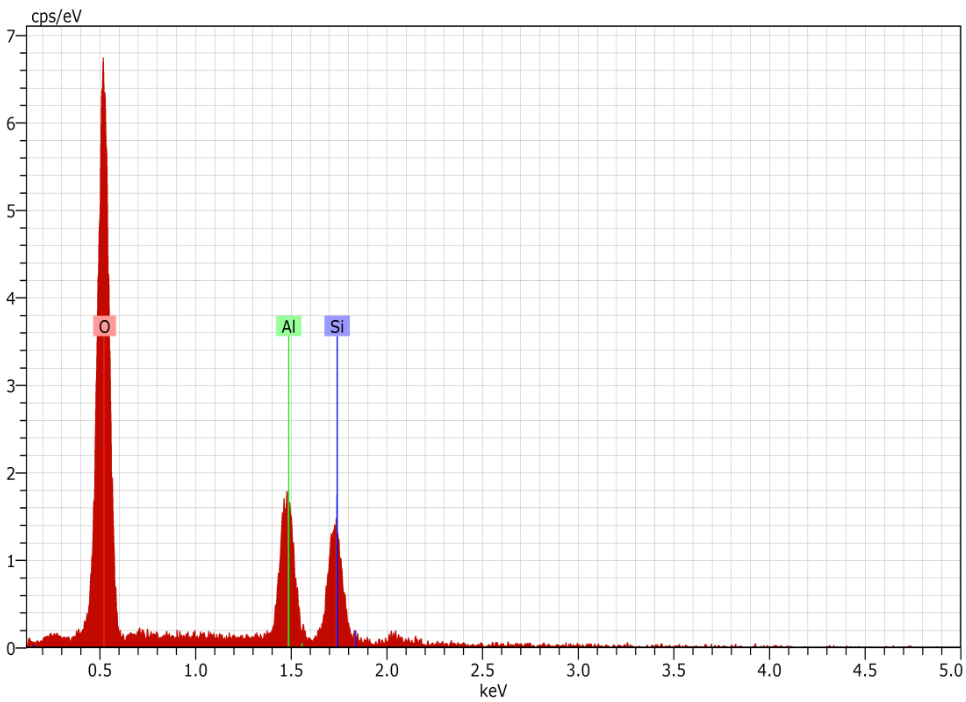
The surface topography of both modified kaolin clay adsorbents gave white particles with irregular structures on the surface of the mineral particles, Figure (3.8) and (3.9), which are likely to be Lead.

3.1.5.5. Energy dispersive X–ray spectroscopy (EDS) of unmodified and both modified kaolin clay

The EDS for unmodified and both modified kaolin clay were done. The EDS results are shown in Figures (3.10) to (3.12). The EDS give the type and weight percent of each element present in the selected point of sample at SEM micrographs. The percentage of each element after normalization is presented in Tables (3.5) to (3.7).



(a)



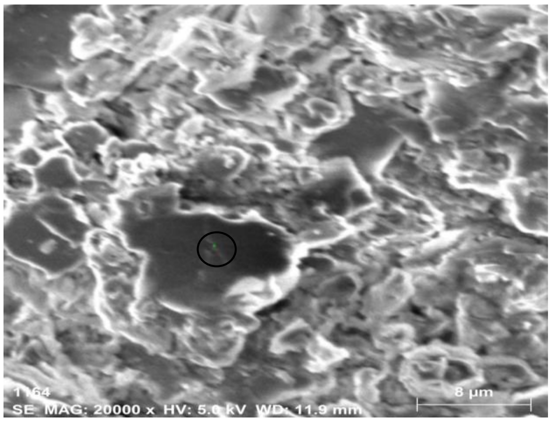
(b)

Figure (3.10): (a) SEM and (b) EDS for unmodified kaolin clay with magnification 30000x.

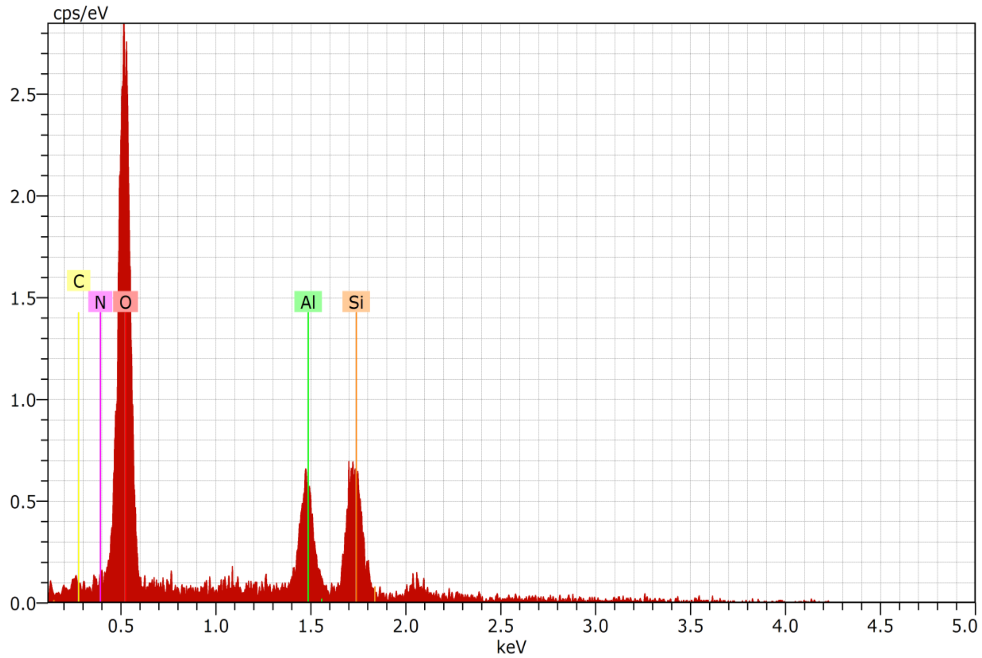
Table (3.5): Normalized % mass of elements in unmodified kaolin clay.

Element	% mass
O	**70.75**
Al	**10.10**
Si	**19.15**

According to the definition of kaolinite, it consists of Si, Al and O. Same results were obtained from EDS analysis.



(a)

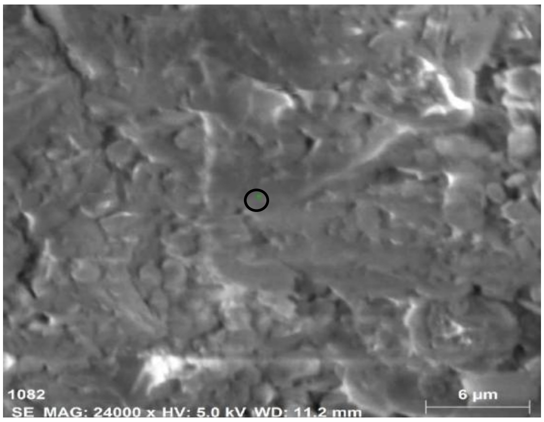


(b)

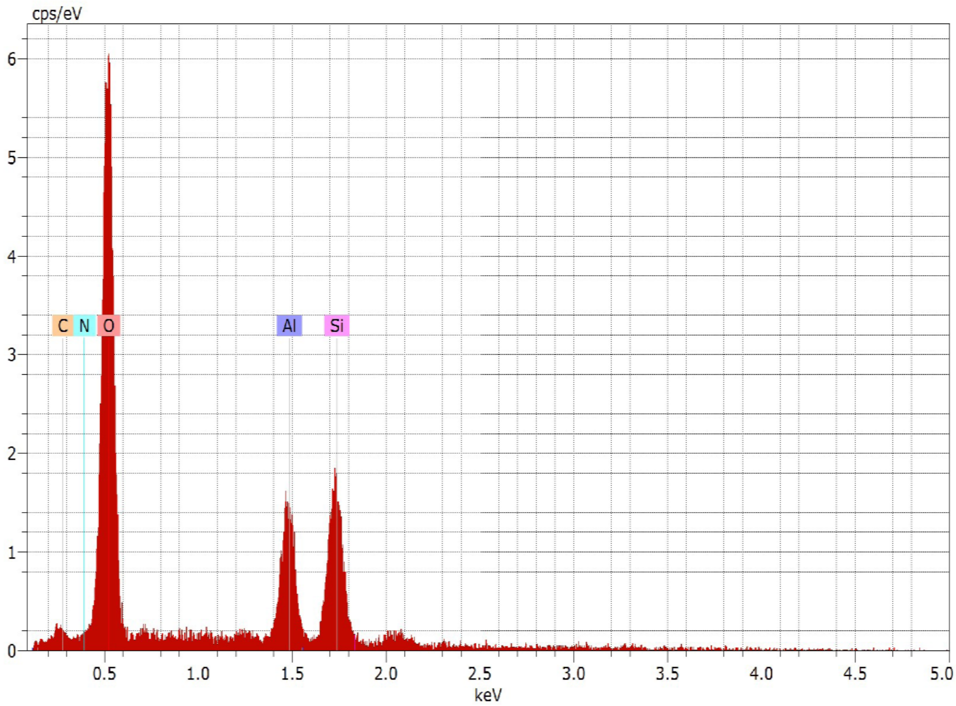
Figure (3.11): (a) SEM and (b) EDS for FHA– kaolin clay with magnification 20000x.

Table (3.6): Normalized % mass of elements in FHA– kaolin clay.

Element	% mass
C	2.50
O	75.00
Si	17.50
Al	5.00



(a)



(b)

Figure (3.12): (a) SEM and (b) EDS for KTD– kaolin clay with magnification 24000x.

Table (3.7): Normalized % mass of elements in KTD– kaolin clay.

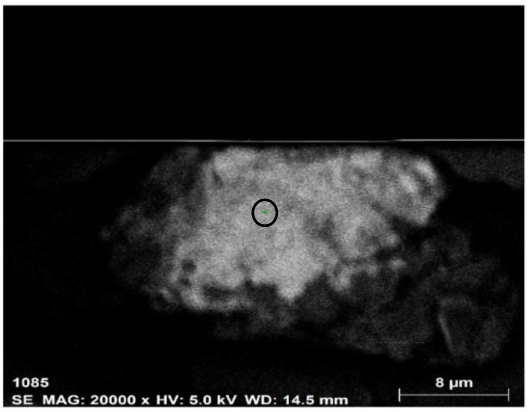
Element	% mass
C	**2.50**
N	**5.00**
O	**62.50**
Si	**22.50**
Al	**7.5**

We can notice the differences between EDS analysis of unmodified kaolin clay and the others which are modified by humic acids, the appearance of new elements such as C and N due to humic acid, which resulted in the decrease in the percentage of O and Al.

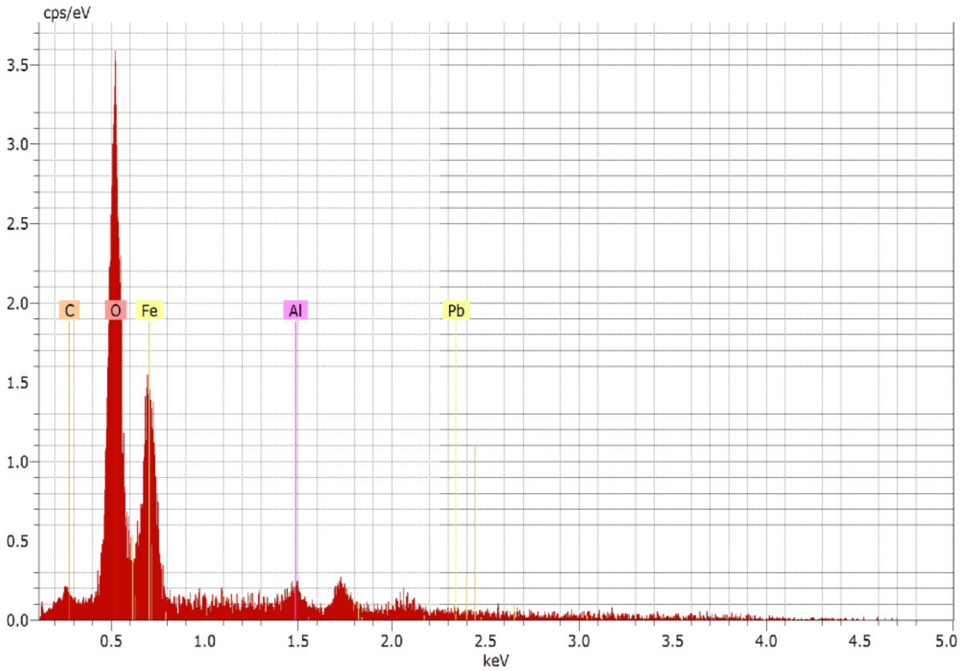
3.1.5.6. Energy dispersive X–ray spectroscopy (EDS) of modified kaolin clay with lead

The EDS for both modified kaolin clay loaded with Lead ions were done. The EDS results are shown in Figures (3.13) and (3.14) for FHA– kaolin clay and for KTD– kaolin clay loaded with lead, respectively. The EDS gives the type and weight percent of each element present in the selected point of sample in the SEM micrographs. Lead and other elements appear in both modified kaolin clay. The percentage of each element after normalization are presented in Tables (3.8) and (3.9) for FHA– kaolin clay and KTD– kaolin clay, respectively. The amount of Lead in FHA– kaolin clay (16.29%) is more than the amount in KTD– kaolin clay (12.30%). This agrees with the adsorption results, Tables (3.22) to (3.27).

High percentage (%) of Fe was appearing in both modified kaolin clay, that’s because kaolin clay in Jordan was rich in iron dioxide.



(a)

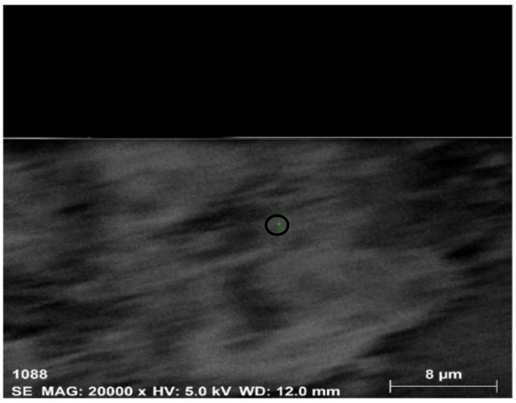


(b)

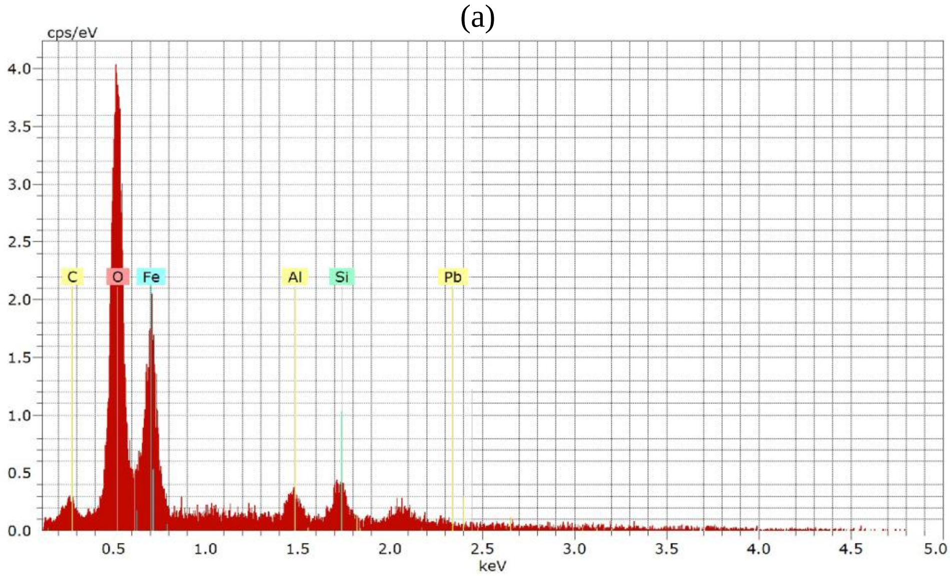
Figure (3.13): (a) SEM and (b) EDS for FHA– kaolin clay loaded with Pb(II) at 20000 x magnifications.

Table (3.8): Normalized % mass of elements in FHA– kaolin clay loaded with Pb(II).

Element	% mass
C	2.22
O	35.56
Al	1.48
Si	5.19
Fe	39.26
Pb	16.29



(a)



(b)

Figure (3.14): (a) SEM and (b) EDS for KTD– kaolin clay loaded with Pb(II) at 20000 x magnifications.

Table (3.9): Normalized % mass of elements in KTD– kaolin clay loaded with Pb(II).

Element	% mass
C	2.46
O	37.70
Al	1.64
Si	6.56
Fe	39.34
Pb	12.30

3.1.6. Surface area and porosity of unmodified and modified kaolin clay.

Surface area and porosity are important physical property that influences the quality and utility of many materials and products. Therefore, it is critically important that these characteristics be accurately determined and controlled. Likewise, knowledge of surface area and especially porosity is an important key in understanding the formation, structure, and potential application of many natural materials.

Pore sizes and porosity are usually quoted in the terms of micropore (pore diameter range < 2.0 nm), mesopore (pore diameter range 2.0–50 nm), and macropore (pore diameter range > 50 nm). The most common techniques for porosimetry analysis are Gas Adsorption Isotherm (for the micro and meso pore range) and Mercury Porosimetry (for the meso and macro pore range) (Meyer and Klobes, 1998). Figure (3.15) provides a guide for the categorization of pore diameters.

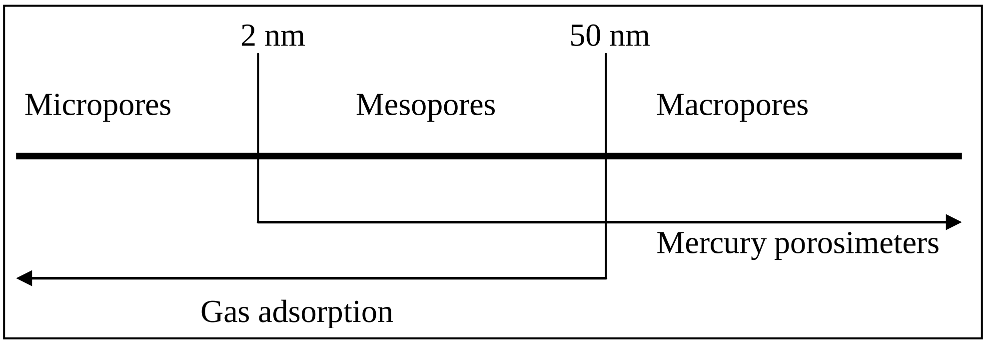


Figure (3.15): Pore size limits of gas adsorption and mercury intrusion porosimetry.

3.1.6.1. Gas Adsorption Isotherms

Probably the most widely used and studied technique for surface area determination is that of gas adsorption. The amount of gas adsorbed by a solid as a function of pressure is determined either gravimetrically or volumetrically and the surface area calculated from the adsorption isotherm by models such as Langmuir (Sudibandriyo, 2010). A common practice in determining the surface area of porous materials is using the adsorption of nitrogen gas. This inert gas interacts weakly with the solid, and then we can measure the amount of adsorbed gas enough to cover the entire surface.

The most basic theory in adsorption is the Langmuir theory. This theory describes the monolayer surface adsorption on an ideal surface. Equating the rates of adsorption and desorption (evaporation), we can obtain the Langmuir isotherm.

The surface area (A_s) of the adsorbent (m^2/g) can be calculated from the following expression:

$$A_s = L \cdot N_{av} \cdot a_m \quad (23)$$

Where L represents the maximum adsorption capacity (expressed in mol/g of adsorbent) and can be obtained from experimental isotherm data, N_{av} is avogadro's

number, and a_m is the area of the adsorbate effectively occupied by an adsorbed molecule (N_2) in the complete monolayer which is already known (Sing et al., 1985).

As shown in Figure (3.15), N_2 gas can only capture or fill some pores, the micro and meso pores only. According to Table (3.10) the unmodified kaolin clay has large number of pores in the range of micro and meso size, "small size pores". This is one of the important reasons for the modification of kaolin clay, and for the same reason we followed the procedure which was mentioned earlier in the preparation of humic acid–kaolin clay complex.

Table (3.10): Langmuir calculated surface area of unmodified and modified kaolin clay.

Type of clay	Surface area (m^2/g)
Unmodified kaolin clay	**33.5474**
FHA– kaolin clay	**12.7658**
KTD– kaolin clay	**15.7669**

Both types of modified kaolin clay have smaller number of pores with small range diameter, due to humic acid adsorption. Another conclusion is that the amount of adsorbed humic acid in FHA– kaolin clay is more than in KTD– kaolin clay. This agrees with adsorption isotherm results, Tables (3.22) to (3.27).

3.1.6.2. Mercury Porosimetry

Porosity: A dimensionless unit symbolized by (ϕ) and equal to the ratio of the void volume (V_V) to the total volume (V_T) i.e. (V_V / V_T) of the porous medium. Also it may be considered as the storage capacity of a medium such as reservoir rock. It will be measured using Mercury Porosimetry Analyzer instrument (Webb, 2001).

The operation of all mercury porosimeters is based upon the physical principle that a nonreactive, non–wetting liquid will not penetrate fine pores until sufficient pressure is applied to force its entry. The relationship between the applied pressure and the pore diameter into which mercury will intrude is given by the Washburn equation:

$$D = (-4\gamma \cos \theta)/P \quad (24)$$

Where D is the pore diameter (µm), γ is the surface tension of the mercury (480 dyne cm^{-1}), θ is the contact angle between mercury and the pore wall, usually taken as 140º and P is the applied pressure (PSI). Monitoring mercury volume intruded as a function of pressure permits the generation of pore size or pore volume distributions from the Washburn equation (http://www.quantachrome.com/science/selected_publications.html, 2008).

Knowing the bulk volume (V_B) of a sample (equal to 1.0000 cc) and total porosity (ϕ) allows percent porosity (P%) to be calculated by the simple relationship:

$$P\% = (\phi/V_B) \times 100\% \quad (25)$$

As shown in Figure (3.15), Mercury Porosimetry is suitable for the meso and macro pore range, according to Table (3.11) which summarizes the total porosity of the clays; we notice that both modified kaolin clay have large numbers of large pores diameter, because of humic acid which has polymeric structure, appearing in form of chains, and clusters. Humic acid form relatively open structure when it bonds with kaolin clay, as shown in SEM of humic acid and both modified kaolin clay, Figures (3.5) to (3.7).

Table (3.11): Total porosity [%] calculated of unmodified and modified kaolin clay.

Type of clay	Total porosity [%]
Unmodified kaolinite	**3.4434**
FHA- kaolinite	**5.6312**
KTD- kaolinite	**4.2491**
FHA-kaolinite loaded with Pb(II)	**2.6892**

FHA– kaolin clay has the highest value due to maximum adsorption of humic acid; similar result was obtained by gas adsorption isotherm, (Table 3.10) and by SEM (Tables 3.8 and 3.9). This indicates that it will have higher adsorption capacity of metal ions. The total porosity of FHA– kaolin clay loaded with Pb(II) ions has the lowest value that's because the Pb(II) ions occupy some pores in modified clay. So, increase in total porosity increases reactivity and adsorption behavior. This agrees with the adsorption results, Tables (3.22) to (3.27).

According to Table (3.12) and Figure (3.15), all metal ions are fit to occupy any pore size present in the modified kaolin clay (micro, meso or macro), because the crystal hydrate radius values for all metal ions are less than 2nm.

3.2. Part (I): Adsorption of humic acid by kaolin clay

Humic acid adsorption decreases with increasing pH, (Figures 3.16 and 3.17) in a manner typical of "ligand–like adsorption". Both the adsorbent surface and the humic acid lose their protons at increasing pH and become negatively charged, and consequently repel each other.

On the other hand, because both kaolin clay and humate are in a hydrogenated form at lower pH, the uncharged surface functional groups of the kaolinite surface and humic acid may attract each other via these protons and electronegative O atoms probably in the form of H bonds. A significant adsorption at high pH is noticed (Figures 3.18 and 3.19), means that there must be a further mechanism for humic acid uptake accompanying hydrophobic expulsion from aqueous solution. Thus humic acid reacts with silanol and aluminol groups of the surface of kaolinite (Hizal and Apak, 2006b).

In general, adsorption mechanisms of HA to mineral surfaces occur, including ligands exchange, hydrophobic effects, H–bonding and electrostatic force. Ligands exchange processes of HA fraction associated with mineral surface hydroxyl functional groups was the most significant mechanism involved in the adsorption. The functional groups (carboxyl and carbonyl groups) had two–fold effects on the adsorption (McKnight et al., 1992).

HA fractions with both hydrophobic portions as well as hydrophilic, acidic functional groups, e.g. fatty acids get increasingly hydrophobic as the acidic groups, are protonated at lower pH, and then more HA could be bound with kaolinite by the hydrophobic effect (Schwarzenbach, 1993; Gu et al., 1994; Arnarson and Keil, 2000; Hur and Schlautman, 2003).

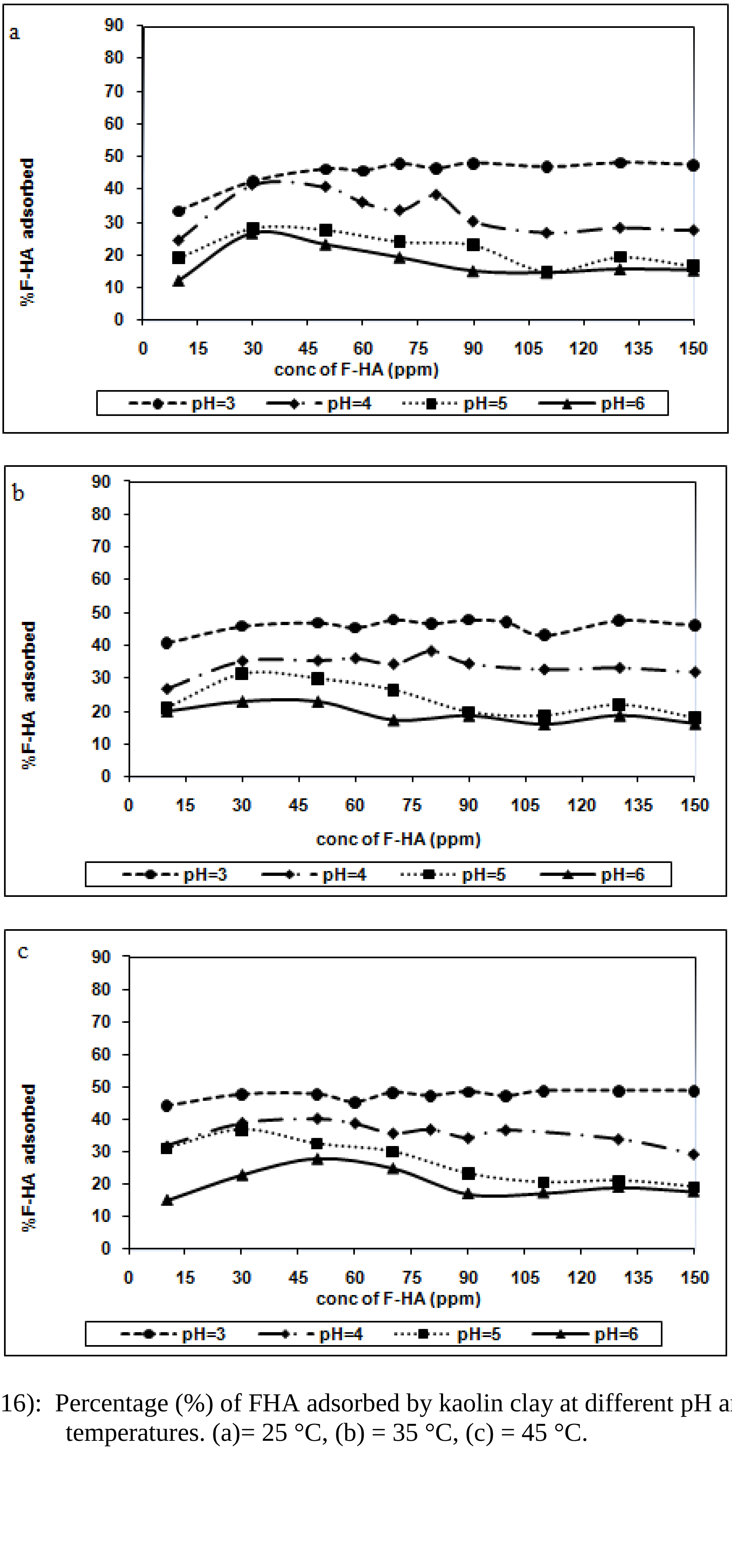


Figure (3.16): Percentage (%) of FHA adsorbed by kaolin clay at different pH and temperatures. (a)= 25 °C, (b) = 35 °C, (c) = 45 °C.

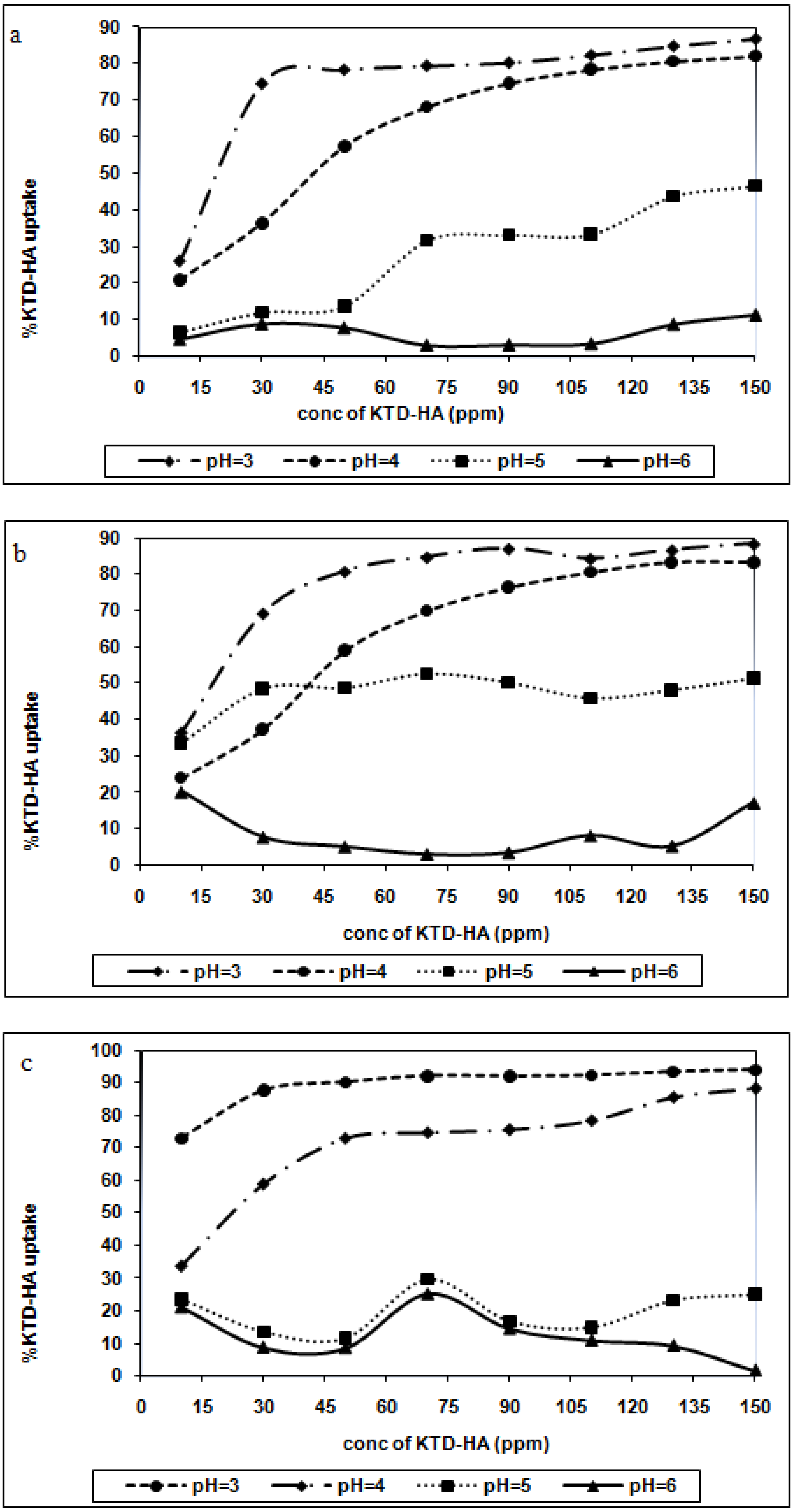
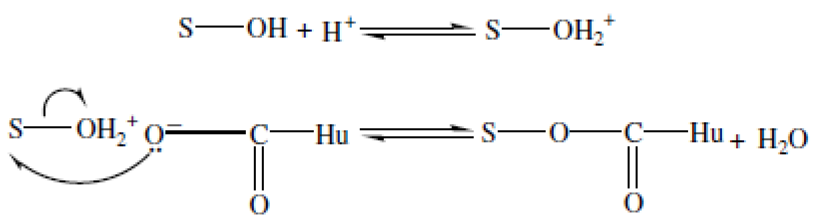


Figure (3.17): Percentage (%) of KTD humic acid adsorbed by kaolin clay at different pH and temperatures. (a)= 25 °C, (b) = 35 °C, (c) = 45 °C.

It has also been proposed in many studies (Schlautman and Morgan, 1994; Sa´nchez–Corte´s et al., 1998; Hur and Schlautman, 2004), that higher adsorption generally has been observed at lower pH.



Scheme (3.1): Adsorption mechanism of humic substances onto kaolinite, Where S is the surface of kaolinite.

The % uptakes of HA on kaolinite as a function of pH for different concentrations of humic acids are shown in Figures (3.18 and 3.19). We can notice that the % uptake becomes higher at low concentration because of the shielding effect from the coated humic acid on the neighboring site. After covering as a first layer on kaolin clay, humic acid then forms a second layer outside the first layer with the hydrophobic interaction. So, the adsorption strength of humic acid will be decreased.

On another hand, the % uptake of FHA on kaolin clay is higher than KTD–humic acid on kaolin clay, because of the higher O/C ratio of the HA fractions, (as shown earlier in elemental analysis (Table 3.4), the higher acidic functional groups such as carboxyl it contained.

The adsorption was dominated by surface complexation, stronger combination between carboxyl and carbonyl groups with surface hydroxyl sites on kaolinite**.**

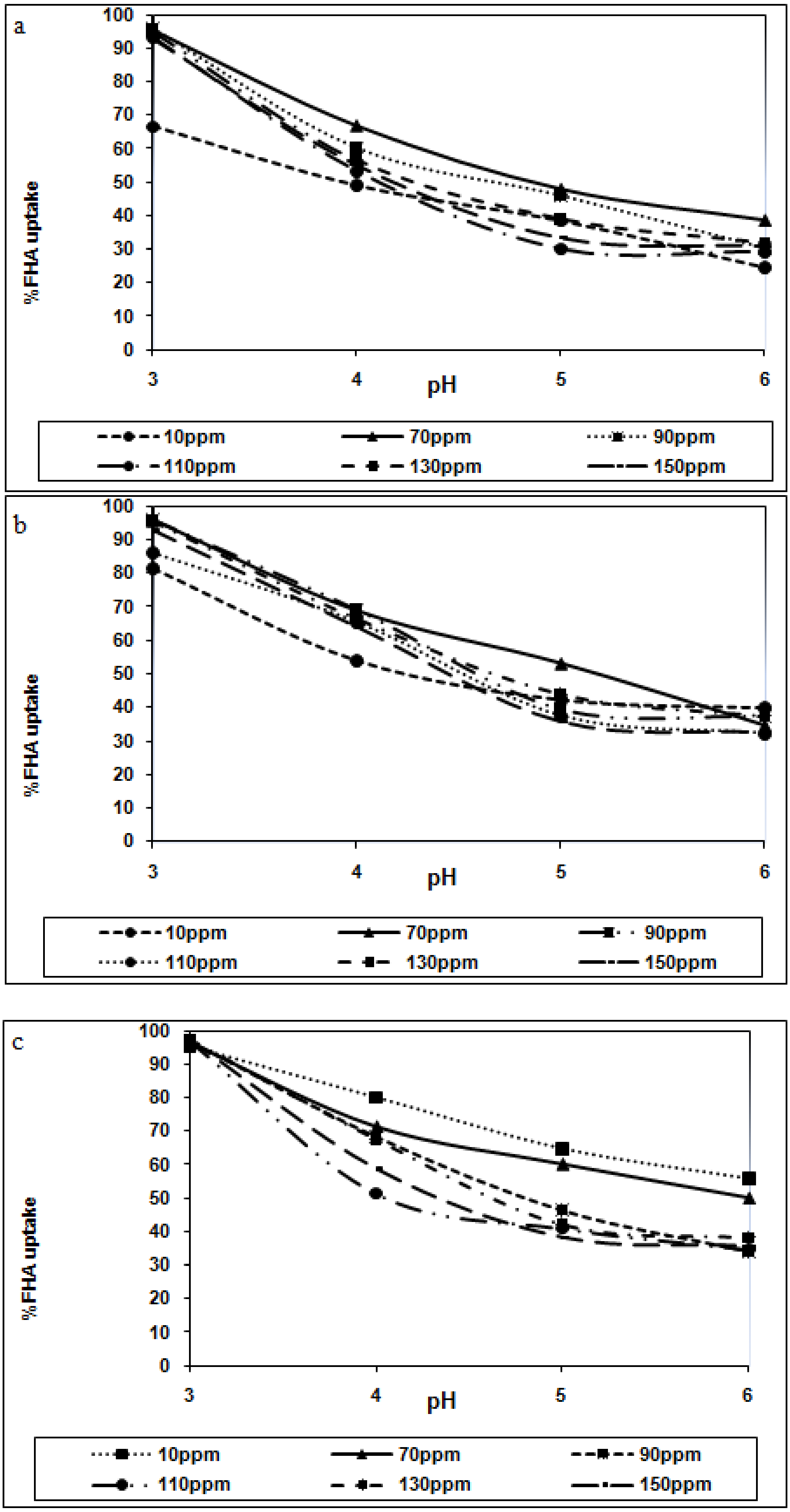


Figure (3.18): % Uptake of FHA on kaolin clay as a function of pH at (a) 25 °C, (b) 35 °C and (c) 45 °C.

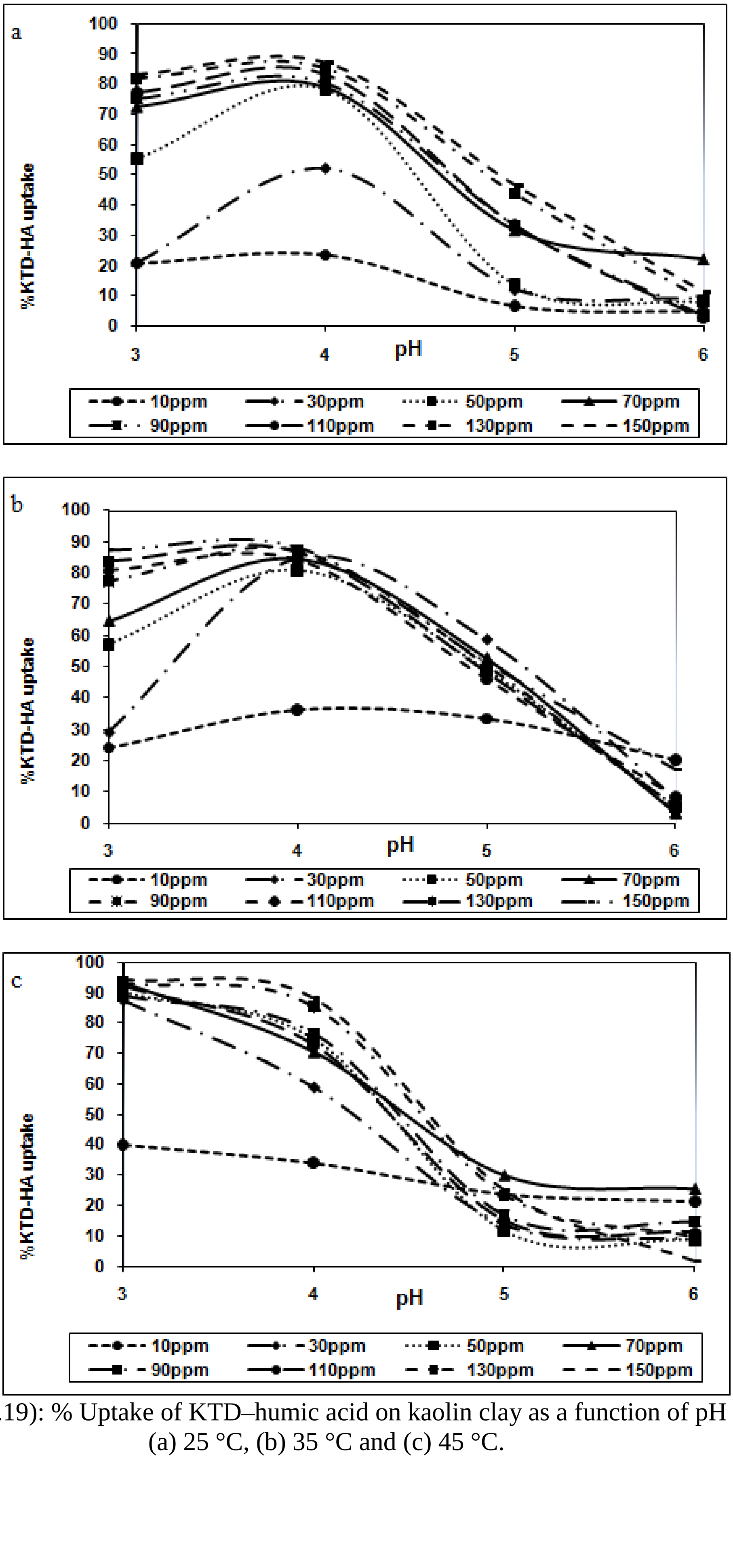


Figure (3.19): % Uptake of KTD–humic acid on kaolin clay as a function of pH at (a) 25 °C, (b) 35 °C and (c) 45 °C.

Temperature also has effect on the adsorption process of humic acid on kaolin clay. Figure (3.20) showed the % adsorbed of humic acid on kaolin clay as a function of temperature. It can be seen that the adsorption of humic acid increased with increase of the solution temperature. It is possible that increasing temperature could have increased the affinity of humic acid towards the active sites on kaolin clay. This shows that the adsorption process is an endothermic process.

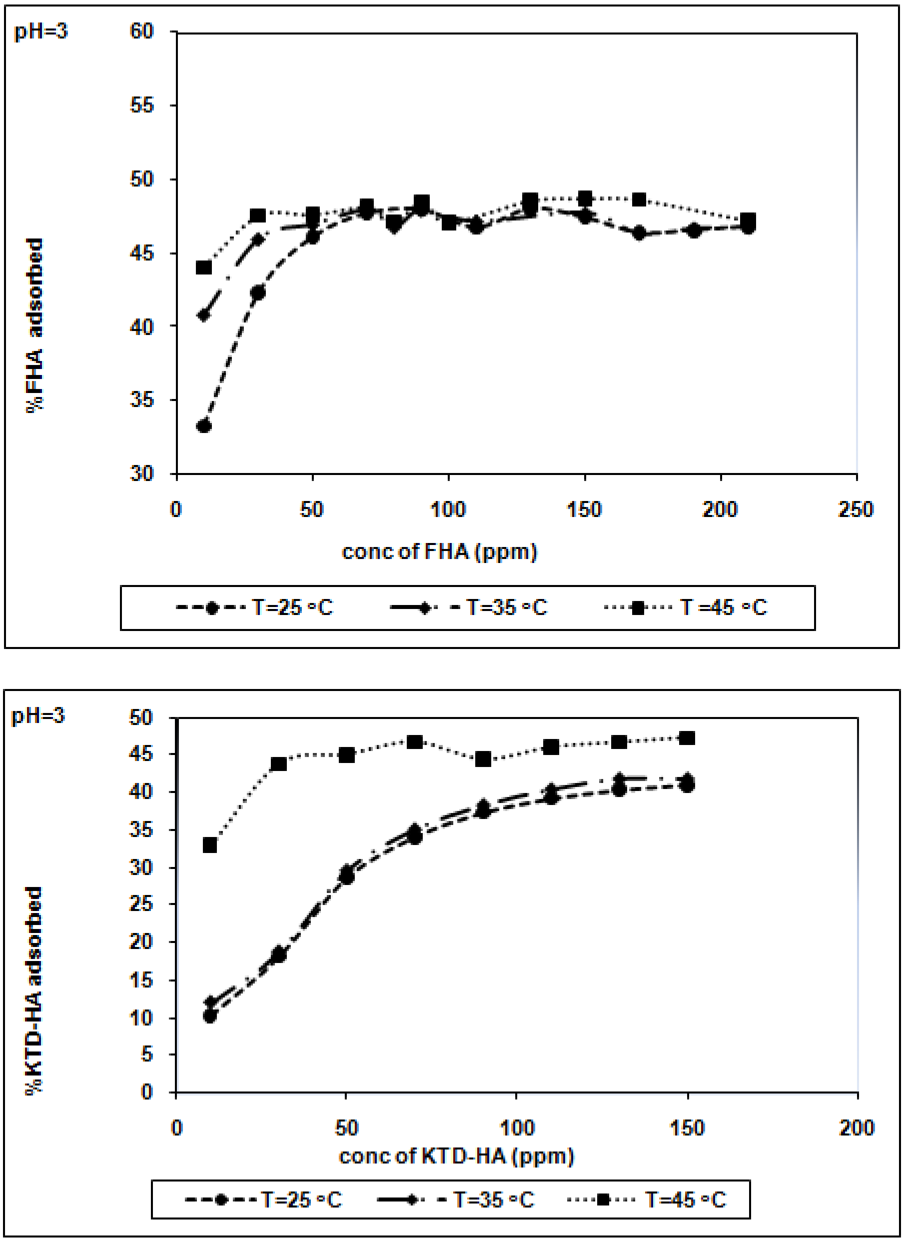


Figure (3.20): % adsorbed of FHA and KTD–humic acid on kaolin clay as a function of temperature.

Salman et al., 2007 showed in their study the isotherms of adsorption of Azraq humic acid onto Azraq bentonite that were studied at different pH (3.0–6.0) and temperature values. The adsorptivity of HA on bentonite was found to be inversely proportional to the increase in pH because of the increase in repulsion between HA and bentonite. While the adsorption of HA increased with increased temperature.

Qinyan et al., 2009, found that the percentages (%) uptake of HA adsorbed on kaolinite at constant ionic strength 0.01 M and different values of pH as follow: at pH 3, is 62.2%, at pH 5 is 38.7%, at pH 7 is 29.6% and at pH 9 is 15.4%.

3.3. Part (II): Adsorption of heavy metal ions into kaolin clay by batch technique.

3.3.1. Unmodified kaolin clay

3.3.1.1. Effect of contact time

The effect of contact time on the adsorption of Pb(II), Cd(II) and Zn(II) was investigated at different time intervals in the range of 15–1440 min with 20.0 mL of 100 ppm of metal solutions with an ionic strength of 0.01M $NaClO_4$. After they were centrifuged, the supernatant solutions were taken for metal ion analysis using AAS. As shown in Figure (3.21), the equilibrium adsorption was established within 4 hr, indicating that the initial adsorption was very fast and maximum uptake was reached within 30 min for Pb(II), Cd(II) and Zn(II). Thereafter, the amount of adsorption remained almost constant. This was due to the decrease of adsorption sites on the kaolin clay which gradually interacted with the metal ions, until all adsorption sites reached saturation.

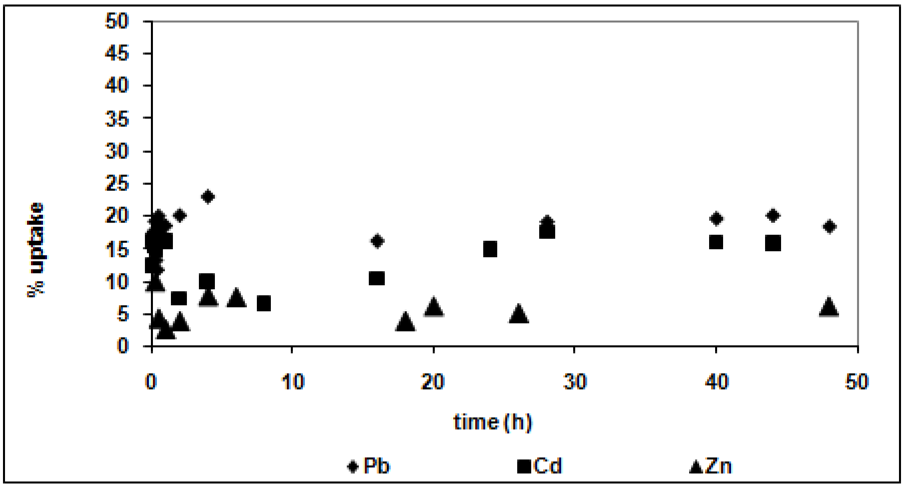


Figure (3.21): Effect of contact time on the amount of adsorption of Pb(II), Cd(II) and Zn(II) by unmodified kaolin clay. Initial concentration of metal ion is 100 ppm and temperature of 35 °C.

Schindler et al., (1987) proposed that binding of Zn(II), Cd(II) and Pb(II) on kaolinite could be described by ion exchange at the permanently charged sites on the silanol faces (SiOH), and complexation to aluminol (AlOH) and silanol groups, which occur at the crystal edges.

Another possibility for adsorption is surface complexation of hydroxyl complexes such as $CdOH^{+}$. Such reaction might involve the formation of the surface species SOCdOH, Where SO is the surface of unmodified kaolin clay (Hizal and Apak, 2006a).

Since kaolinite has strong bonding between the layers, exchange in the interlayer region cannot occur, leaving ion exchange on the siloxane faces and formation of surface complexes with SOH groups (Angove et al., 1997).

The removal capacity for different metal ions on the kaolin clay was in the order of Pb(II) >Cd(II) >Zn(II). It indicated that kaolin clay showed stronger preference for Pb(II) than Cd(II) than Zn(II).

In general, the most important factors that influence the relative selectivity of metal ions in solution are their valence and ionic radii (Puls and Bohn, 1988). From

comparison of the three elements studied, lead(II) ion has the largest ionic radius (Table 3.12). If metal adsorption on the kaolin clay were entirely electrostatic, ions of higher ionic radius should be adsorbed more strongly. The ionic radius order is Pb(II)> Cd(II)> Zn(II). And the selectivity sequence observed that Pb(II) adsorbed more than Cd(II) more than Zn(II).

Another factor that has an effect is the hydration energy, the hydration energy values decrease as the ionic radius increases (Hunt, 1965). Increasing the hydration energy values are due to the increase in the hydration shell, this makes it more difficult for metal ions to discharge the water of hydration. The formation of aqua complex $[M(OH_2)_m]^{n+}$ takes place (where m is larger than six, perhaps eight or nine), the aqua complex, having m H_2O molecules surrounding the central metal ion, has a definite structure and the cloud of water molecules (hydration shell) has another geometry than the rest of the water. A stronger hydration shell will surround small metal ion, which has smaller radius, than the metal ion with larger radius, so the adsorptivity of an ion of larger radius is higher than small radius ion.

The adsorption behavior of transition metals can also be explained by using the concept of the Lewis hard–soft acid base, in according with HSAB theory.

In the Lewis hard–soft acid base principle, a hard base indicates high electronegativity, low polarisability and small ionic size, whilst the opposite is true with soft ions. Most metal ions are Lewis acids and most anions are Lewis bases.

According to HSAB principle, hard Lewis acids prefer to react, or form complexes, with hard Lewis bases, and soft acids with soft bases (Puls and Bohn, 1988). The physical properties useful for hard–soft Lewis acid base analysis for the metals used in this study are shown in Table (3.12). Soft Lewis acids and bases tend to form

outer–sphere complexes (Sparks, 1995). So we expect that Pb(II) will form complex with kaolin clay more than other metal ions.

This indicates that main surface adsorption sites on kaolinite exhibit relatively soft Lewis base characteristics. So, soft metal ions form stable complexes.

Table (3.12): Some properties parameters of metal ions.

Metal ion	Ionic radius (A°)	Crystal hydrates radius (A°)	Pearson HSAB	Electron configuration
Pb(II)	**1.33**	**3.13**	**soft**	**$4f^{14}5d^{10}6s^{2}$**
Cd(II)	**1.09**	**2.28**	**soft**	**$4d^{10}$**
Zn(II)	**0.88**	**2.11**	**soft**	**$3d^{10}$**
Reference	**Cotton et al., 1999**	**Burgess, J. 1988**	**Pearson, R. 1968**	**Huheey et al., 1993**

3.3.1.2. Effect of pH

The adsorption of heavy metal ions on kaolin clay increased with increasing pH, (Figure (3.22) and Table (3.13)).

Several reasons may be attributed to the increased adsorption of metal ions by unmodified adsorbent relative to adsorbate solution pH. The surface of the kaolin clay sample contains a large number of active sites and may become positively charged at very low pH, thus increasing the competition between H^{+} and the metal ions for available adsorption sites. However, as pH increases, this competition decreases as these surface active sites becomes neutral and/or more negatively charged, which enhances

the adsorption of the positively charged metal ions through electrostatic force of attraction (Unuabonah et al., 2008).

We choose Cd(II) as a reference metal to compare the adsorption behavior of unmodified and modified kaolin clay, because it's properties are in between of Pb(II) and Zn(II), as shown in Table (3.12).

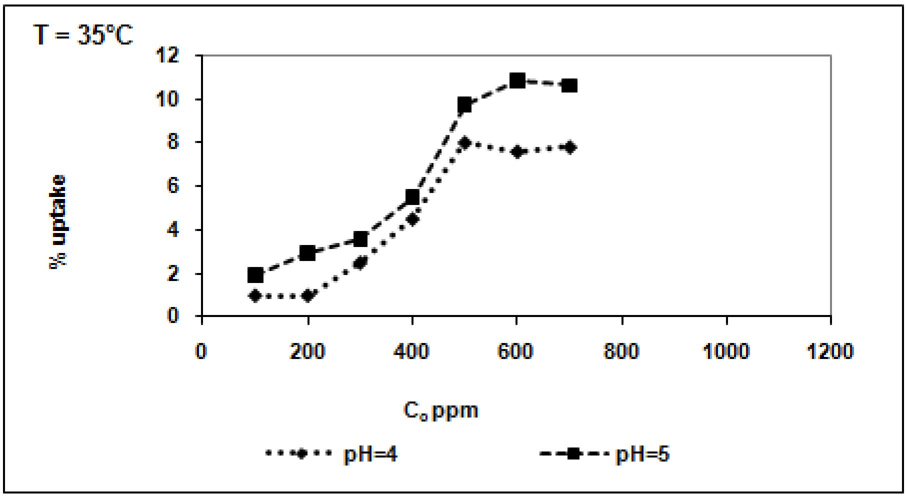


Figure (3.22): Effect of pH on the adsorption of Cd(II) onto unmodified kaolin clay at 35 °C.

3.3.1.3. Effect of temperature

It can be seen from Figure (3.23) and Table (3.13) that the adsorption of Cd(II) increased with increase of the solution temperature. It is possible that increasing temperature could have increased the affinity of the metal ion towards the active sites on kaolin clay. This shows that the adsorption process is an endothermic process.

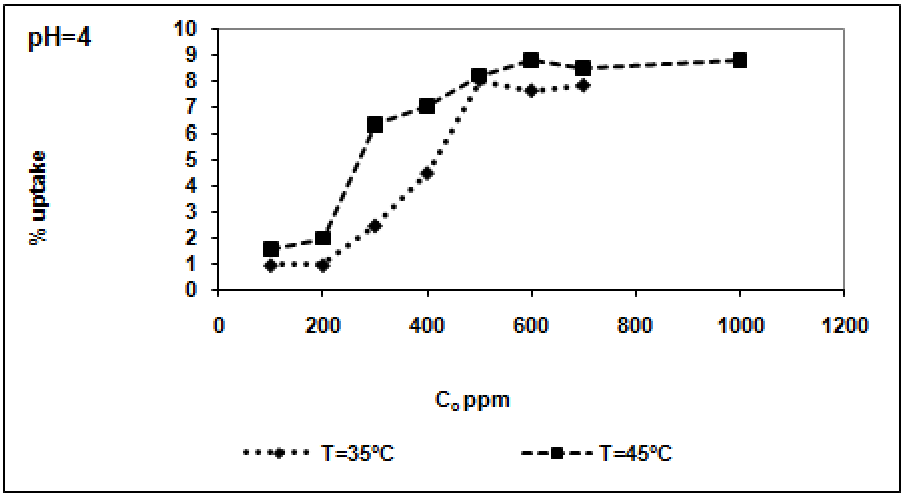


Figure (3.23): Effect of temperature on the adsorption of Cd(II) onto unmodified kaolin clay at pH=4.

Table (3.13): % Uptake of Cd(II) by unmodified kaolin clay.

T(°C)		35		45	
pH		4.00	5.00	4.00	5.00
Initial Concentration (ppm)	100.0	1.0	1.0	1.0	1.0
	200.0	1.0	1.0	1.0	1.0
	300.0	1.3	3.7	6.3	6.7
	400.0	6.3	10.3	11.5	14.8
	500.0	8.0	10.4	8.8	12.2
	600.0	7.8	8.2	7.7	10.8
	700.0	4.0	6.6	7.6	9.7
	1000.0	1.0	1.5	1.4	4.8

As shown in Table (3.13), the % uptake of Cd(II) by unmodified kaolin clay had small values, even when temperature or pH had increased. That's because kaolinite is well–packed structure, its particles are not easily broken down and the kaolinite layers are not easily separated. Hence, most adsorption activity occurs along the edges and surfaces of the structure. Kaolin clay can form a barrier that is not easily degraded and naturally occurring sediments and deposits containing an abundance of kaolinite interspersed with other minerals are effective in controlling the migration of dissolved

species (Devidal et al., 1996). Kaolinite is non–expanding and as a result of its high molecular stability, kaolinite, a 1:1 type, has little isomorphous substitution. Therefore, this is likely to account for its low capacity to adsorb cations. So we want to modify it by HA.

One research was done on kaolinite clay from Nigeria to remove Cd(II) from aqueous solutions. It was found that percentage (%) adsorbed of 300 ppm of Cd(II) at pH=4.00 is 11%, but at pH=5.00 is 36% (Adebowale et al., 2006).

Another work was done on kaolinite from Columbia to remove Pb(II), Cd(II) and Ni(II) from aqueous solutions at 303K and pH=5.50. It was found that the amount of metal ion adsorbed per 1 g of kaolinite for Pb(II) was 11.5 mg, while 6.8 mg of Cd(II) and 7.1 mg of Ni(II) (Gupta and Bhattacharyya, 2008).

3.3.2. Adsorption of heavy metal ions into modified kaolin clay by batch technique.

The adsorption properties of metal ions Pb(II), Cd(II) and Zn(II) by both modified kaolin clay (FHA– kaolin clay and KTD– kaolin clay) were studied by determination of metal ion concentration remaining in the metal ion solution using atomic absorption spectrometer after building up analytical calibration curve for each metal ion.

3.3.2.1. Adsorption parameters

3.3.2.1.1. Effect of contact time

The effect of contact time on the adsorption capacity of both modified kaolin clay was investigated in the time ranges of 15–1440 min under pH =5.00 at 35 °C. It was observed that initial adsorption of metal ions was rapid, then metal ions–clay

interactions reached equilibrium in less than 2 hr (Figures 3.24 and 3.25). The adsorption sites on the clay minerals were quickly covered by the metal ions.

No significant changes with the contact time were observed. Some authors assume the adsorption process to involve two steps, namely: a rapid, initial step where the metal ions are adsorbed at readily accessible sites on the adsorbent surface and a second, slower step typical of modified surfaces, involves co–precipitation and diffusion to inner zones (Araujoa et al., 2007).

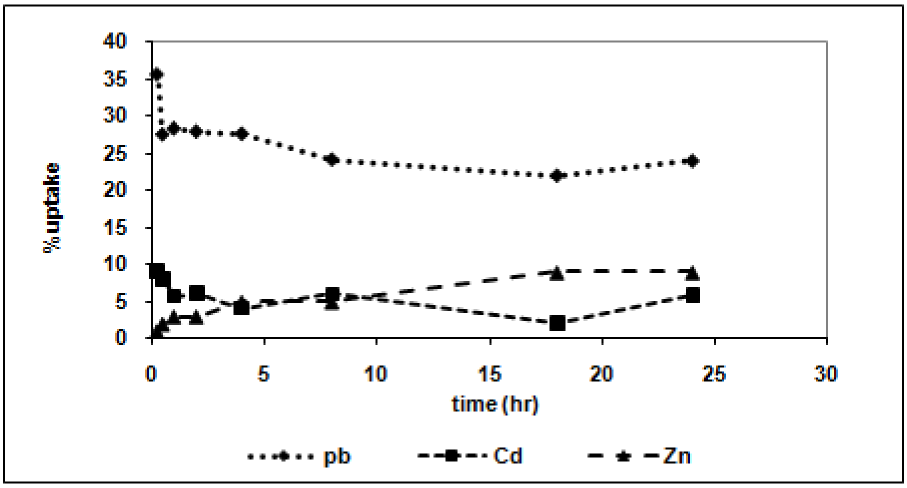


Figure (3.24): Effect of contact time on the amount of adsorption of Pb(II), Cd(II) and Zn(II) by FHA– kaolin clay. Initial concentration of metal ion is 100 ppm and temperature of 35 °C.

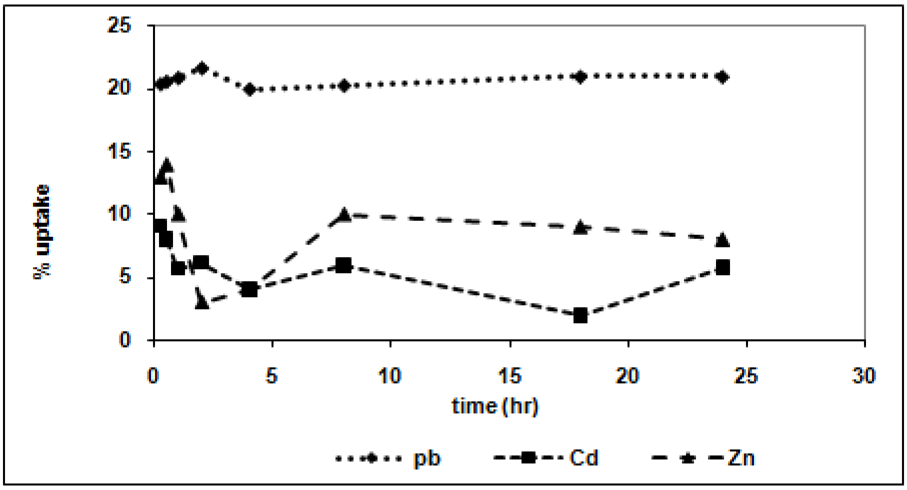


Figure (3.25): Effect of contact time on the amount of adsorption of Pb(II), Cd(II) and Zn(II) by KTD– kaolin clay. Initial concentration of metal ion is 100 ppm and temperature of 35 °C.

In comparison with effect of contact time on the amount of adsorption of Pb(II), Cd(II) and Zn(II) by unmodified kaolin clay, modified kaolin clay adsorbed metal ions and reached equilibrium faster. This is due to humic acid, where a lot of macro pores size is available.

3.3.2.1.2. Effect of adsorbent dose

Increase in adsorbent dose of FHA– kaolin clay, from (0.1–1.0) g ± 0.1 mg resulted in a decrease in equilibrium adsorption capacity, (q_e) equation (16), Table (3.13).

The increased percentage of adsorption of metal ions with increasing FHA– kaolin clay dose could be due to increased surface negative charge and decrease in the electrostatic potential near the solid surface that favors adsorbent–solute interaction. However, the decreased equilibrium adsorption capacity, q_e, of FHA– kaolin clay for the metal ions as its mass was increased can be attributed to two reasons:

First, with increasing adsorbent dose there is decreasing in the total surface area of the adsorbent and an increase in diffusion path length, which is the result of aggregation of FHA– kaolin clay particles. This aggregation becomes increasingly significant as the mass of the adsorbent is increased. Second, the increase in adsorbent dose at constant metal ion concentration and volume will lead to unsaturation of adsorption sites through the adsorption process. It is therefore clear that the equilibrium adsorption capacity of FHA– kaolin clay is a function of its mass (Adebowale et al., 2006).

A decrease in adsorbent mass allows dispersion of the particles which increases the available adsorption sites between the particles.

Table (3.14): Effect of varying FHA– kaolin clay dose on the adsorption of Pb(II) at initial pH= 5.00, initial concentration =20 ppm, temperature = 35 °C and contact time =24 hr.

Mass of FHA-kaolinite (g)	q_e (mg / g)	%Uptake
0.1	7.20	72.0
0.2	4.70	94.0
0.3	3.07	92.0
0.5	1.84	92.0
0.7	1.25	88.0
1.0	0.84	84.0

Tables (3.15–3.20) show that the adsorption behavior of metal ions is affected by pH changes, temperature and initial metal ion concentration.

3.3.2.1.3. Effect of pH

The change in H^+ and OH^- ions in the solution will cause the surface functional groups on clay minerals and HA to protonate and deprotonate by adsorption of H^+ or OH^- ions, respectively, as shown in equations (26) and (27) below (Spark, 1995).

$SOH + H^+ \rightarrow S–OH^{+2}$ Where SOH is the surface of modified kaolin clay. (26)

$SOH \rightarrow S–O^- + H^+$ (27)

Because of the protonation and deprotonation of the acidic and basic groups of the adsorbents, its adsorption behavior for metal ions is influenced by the pH value, which affects the surface structure of adsorbents, the formation of metal hydroxides which is formed in basic medium (at pH>6) , and the interaction between adsorbents and metal ions (Alkan et al., 2008).

With reference to Tables (3.15–3.20), we can observe that the adsorption behavior of metal ions is more sensitive to pH changes. It is obvious that the higher the initial pH value the larger the adsorption capacity. At very low pH, the concentrations of protons exceed that of the metal ions several times and the surface is most likely covered with H_3O^+ ions, then the metal ions can hardly compete with protons for the binding sites on the adsorbents. As pH increases, (i.e., as the solution becomes more basic) adsorption behavior can be explained on the basis of a decrease in competition between proton and metal species for the surface sites, and by the decrease in positive surface charge, which results in a lower columbic repulsion of the adsorbing metal ion, then more and more protons leave the clay mineral surface and adsorbed humic acid making the sites available to the metal ion which now increasingly bind to clay surface through a mechanism similar to that of exchange interactions (H_3O^+/metal ion(II)) (Bhattacharyya and Gupta, 2009; Jiang et al., 2009).

It is believed that the mode of adsorption of these metal ions onto the surface of the modified kaolin clay is as follows:

$$M^{2+} + 2SOH \leftrightarrow (SO)_2M + 2H^+ \qquad (28)$$

Where SOH is the surface of modified kaolin clay by HA, M is metal (Li and Dai, 2006).

The higher carboxyl and phenol–containing fractions of FHA– kaolin clay provided a greater density of sites available for complexation with metal ions.

Our results shown in Tables (3.15–3.20) show that HA– kaolin clay increased the adsorption of metal ions at high pH. This observation explains metal adsorption by the combined action of aluminol, carboxyl and phenol groups which become activated at higher pH (because of being more Lewis bases having higher pKa). Because Pb(II) exists as the unhydrolyzed ion (i.e., as the sole Pb(II)) at a higher pH, it will react with

aluminol/phenol sites which have a stronger basic character. Besides, hard and soft acids and bases principle (HSAB) put forward by Pearson et al in the early 1960's predicts that Pb(II) is a softer cation that is capable of forming stronger surface complexes with softer Lewis bases such as aluminol and phenol (Hizal and Apak, 2006b).

Our results are in accord with those of Heidmann et al., 2005, who found that addition of fulvic acid to clay strongly increased Cu(II) and Pb(II) adsorption onto kaolinite at all studied pH. Enhancement of metal ion adsorption to kaolinite by fulvic acid was strongest at low pH—similar to that reported here—where fulvic acid contributed to high–affinity binding sites of kaolinite.

Another research was studying the isotherms of adsorption of Cu(II) and Ni(II) onto solid Azraq humic acid were studied at different pH (2.0–3.7) values. The contribution of low affinity sites to binding of metal ions increases with decreasing pH and increasing metal ion loading. The aggregation of HA, which is facilitated by decreasing pH and increasing metal ion loading, may increase the ability of low–affinity sites to encapsulate metal ions (El–Eswed and Khalili, 2006).

3.3.2.1.4. Effect of initial metal ion concentration

The percentage (%) of metal ion adsorbed decreased with increasing initial metal ion concentration, as shown in Tables (3.15–3.20). This indicates a decrease in active sites on modified kaolin clay as more metal ions are adsorbed.

3.3.2.2. Metal ions uptake

The adsorption of metals on modified kaolin clay was studied in the initial pH range 4.00–6.00, at different temperatures 25, 35, 45 °C for (0.2g ± 0.1mg) adsorbent dose and 20.0 mL of different initial concentrations 10, 20, 30, 40, 50, 60, 80 and 100 ppm at a constant ionic strength (0.01M) of $NaClO_4$.

Table (3.15): % Uptake of Pb(II) by FHA– kaolin clay.

T(°C)		**25**			**35**			**45**		
pH		**4.00**	**5.00**	**6.00**	**4.00**	**5.00**	**6.00**	**4.00**	**5.00**	**6.00**
Initial Concentration (ppm)	**10.0**	**90.0**	**94.0**	**96.0**	**94.0**	**95.0**	**96.0**	**95.0**	**96.0**	**96.0**
	20.0	**90.0**	**95.0**	**95.5**	**94.5**	**95.5**	**96.5**	**95.5**	**96.5**	**97.0**
	30.0	**92.7**	**95.3**	**96.7**	**95.0**	**95.7**	**96.7**	**96.0**	**97.0**	**97.3**
	40.0	**94.0**	**95.8**	**96.8**	**95.3**	**95.8**	**96.8**	**96.3**	**97.5**	**97.8**
	50.0	**94.4**	**95.8**	**97.0**	**95.6**	**96.2**	**97.0**	**96.2**	**97.6**	**98.2**
	60.0	**91.7**	**95.0**	**97.2**	**95.7**	**96.7**	**97.0**	**96.5**	**97.7**	**98.2**
	80.0	**85.0**	**85.8**	**90.0**	**85.0**	**90.0**	**91.3**	**92.4**	**91.5**	**92.5**
	100.0	**74.2**	**76.1**	**78.0**	**77.0**	**78.0**	**80.9**	**78.4**	**81.3**	**84.7**

Table (3.16): % Uptake of Cd(II) by FHA– kaolin clay.

T(^{o}C)		**25**			**35**			**45**		
pH		**4.00**	**5.00**	**6.00**	**4.00**	**5.00**	**6.00**	**4.00**	**5.00**	**6.00**
Initial Concentration (ppm)	**10.0**	**67.0**	**72.0**	**72.0**	**70.0**	**80.0**	**92.0**	**80.0**	**92.0**	**99.0**
	20.0	**69.0**	**51.0**	**85.0**	**62.5**	**70.0**	**90.0**	**72.5**	**86.5**	**98.5**
	30.0	**36.7**	**42.7**	**79.0**	**50.0**	**60.0**	**84.0**	**56.7**	**83.3**	**90.0**
	40.0	**30.3**	**32.3**	**73.5**	**40.0**	**47.5**	**80.0**	**47.5**	**75.0**	**85.8**
	50.0	**28.0**	**30.0**	**68.2**	**34.0**	**40.0**	**73.0**	**44.0**	**68.0**	**79.4**
	60.0	**23.3**	**26.7**	**66.5**	**30.0**	**36.7**	**67.7**	**36.7**	**66.7**	**74.0**
	80.0	**21.3**	**25.0**	**50.0**	**23.8**	**37.5**	**68.0**	**2.5**	**10.8**	**68.8**
	100.0	**15.0**	**20.0**	**40.0**	**20.0**	**25.0**	**52.0**	**21.0**	**27.7**	**66.7**

Table (3.17): % Uptake of Zn(II) by FHA– kaolin clay.

T(^{o}C)		**25**			**35**			**45**		
pH		**4.00**	**5.00**	**6.00**	**4.00**	**5.00**	**6.00**	**4.00**	**5.00**	**6.00**
Initial Concentration (ppm)	**10.0**	**5.0**	**10.0**	**10.0**	**10.0**	**52.0**	**70.0**	**68.0**	**75.0**	**78.0**
	20.0	**32.0**	**53.0**	**65.0**	**50.0**	**62.5**	**70.0**	**58.0**	**75.0**	**76.0**
	30.0	**26.7**	**46.0**	**64.0**	**48.7**	**60.0**	**66.7**	**50.0**	**73.3**	**75.3**
	40.0	**26.5**	**45.5**	**62.5**	**47.0**	**57.5**	**65.0**	**45.8**	**68.0**	**73.5**
	50.0	**24.4**	**42.8**	**60.8**	**47.6**	**56.0**	**64.0**	**40.0**	**68.6**	**72.8**
	60.0	**23.3**	**41.0**	**59.5**	**46.0**	**53.3**	**63.3**	**38.3**	**65.0**	**72.7**
	80.0	**21.3**	**37.5**	**59.3**	**32.5**	**50.0**	**61.3**	**25.0**	**62.5**	**71.3**
	100.0	**20.0**	**32.0**	**50.0**	**26.0**	**50.0**	**53.0**	**28.0**	**60.0**	**70.0**

Table (3.18): % Uptake of Pb(II) by KTD– kaolin clay.

T(°C)		25			35			45		
pH		4.00	5.00	6.00	4.00	5.00	6.00	4.00	5.00	6.00
Initial Concentration (ppm)	10.0	87.0	90.0	90.0	90.0	90.0	90.0	90.0	90.0	90.0
	20.0	90.5	95.0	93.0	93.0	95.0	95.0	94.5	95.0	95.0
	30.0	93.3	95.0	95.3	96.7	96.3	96.0	96.7	96.7	96.7
	40.0	94.3	97.5	95.0	97.3	97.5	96.0	97.5	95.5	97.5
	50.0	96.4	96.0	97.2	97.8	98.0	97.2	98.0	97.6	98.0
	60.0	93.3	93.3	97.3	91.7	96.7	98.3	96.7	98.3	98.3
	80.0	81.3	82.5	88.8	85.0	87.5	91.3	87.5	88.8	97.5
	100.0	70.0	74.0	79.0	76.0	78.0	83.0	77.0	79.0	93.0

Table (3.19): % Uptake of Cd(II) by KTD– kaolin clay.

T(°C)		25			35			45		
pH		4.00	5.00	6.00	4.00	5.00	6.00	4.00	5.00	6.00
Initial Concentration (ppm)	10.0	50.0	50.0	60.0	60.0	70.0	50.0	40.0	40.0	60.0
	20.0	45.0	55.0	75.0	50.0	65.0	75.0	60.0	65.0	85.0
	30.0	40.0	50.0	76.7	46.7	40.0	76.7	53.3	63.3	80.0
	40.0	37.5	40.0	70.0	40.0	47.5	71.3	45.0	50.0	77.5
	50.0	32.0	34.0	70.0	36.0	42.0	70.0	40.0	44.0	76.0
	60.0	26.7	43.3	66.7	38.3	38.3	66.7	33.3	36.7	71.7
	80.0	27.5	31.3	66.3	25.0	33.8	60.0	31.3	33.8	70.0
	100.0	26.0	25.0	68.0	22.0	27.0	59.0	25.0	28.0	70.0

Table (3.20): % Uptake of Zn(II) by KTD– kaolin clay.

T(^{o}C)		25			35			45		
pH		4.00	5.00	6.00	4.00	5.00	6.00	4.00	5.00	6.00
Initial Concentration (ppm)	10.0	50.0	64.0	80.0	60.0	80.0	90.0	70.0	90.0	90.0
	20.0	45.0	61.0	70.0	55.0	85.0	75.0	70.0	92.5	80.0
	30.0	43.3	56.7	66.7	50.0	70.0	73.3	56.7	93.3	76.7
	40.0	37.5	48.5	65.0	45.0	60.0	70.0	55.0	85.0	75.0
	50.0	36.0	42.4	64.0	44.0	58.0	68.0	52.0	72.0	72.0
	60.0	10.0	43.3	60.0	13.3	60.0	65.0	18.3	68.3	70.0
	80.0	7.5	43.8	57.5	10.0	51.3	65.0	16.3	72.5	77.5
	100.0	6.0	40.0	56.0	10.0	48.0	60.0	15.0	60.0	66.0

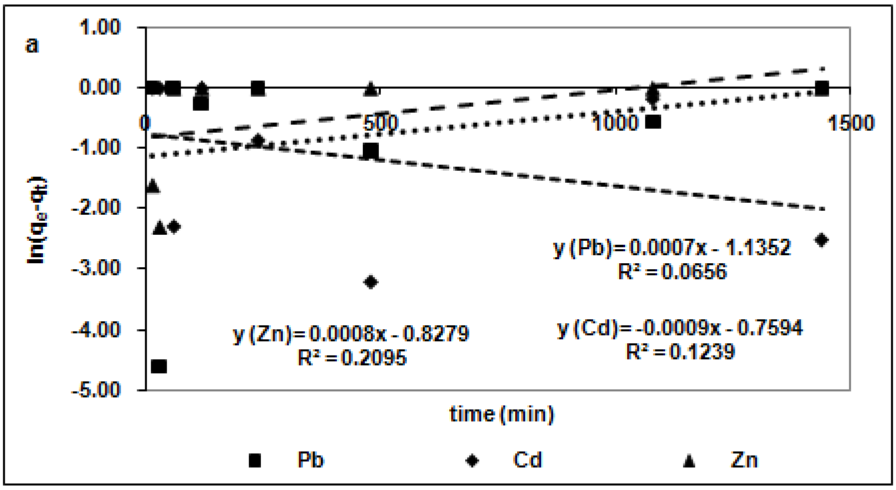
3.3.2.3. Kinetics of adsorption

Adsorption of the metal ions at (308.15 K) was initially very fast and the maximum uptake was recorded within 30 min. The initial uptake rate for the metal ions was very high as a large number of adsorption sites were available for adsorption at the beginning of the process, where adsorption proceeded with a high rate. As the sites were gradually filled up, the number of sites become less and metal ions have to fiercely compete among themselves for getting adsorbed, so adsorption became slow and the kinetics became more dependent on the rate at which the metal ionic species were transported from the exterior to the interior sites of the clay mineral particles or from the bulk of the solution to the clay surface.

In the present work, various kinetic models starting from Lagergren's pseudo first order equation and second order equation were tested to find out which model is in

agreement with the experimental results of kinetic study. On comparison, it was found that the second order kinetics (Figures 3.27 and 3.28) yielded the best results.

The linearity of the plots (Figures 3.27 and 3.28) of the pseudo–second–order model with R^2 values greater than 0.90 for all metal ions indicating that one of the mechanisms or rate determining step of the adsorption of metal ions by kaolin clay may be by chemisorption (Jiang et al., 2009).



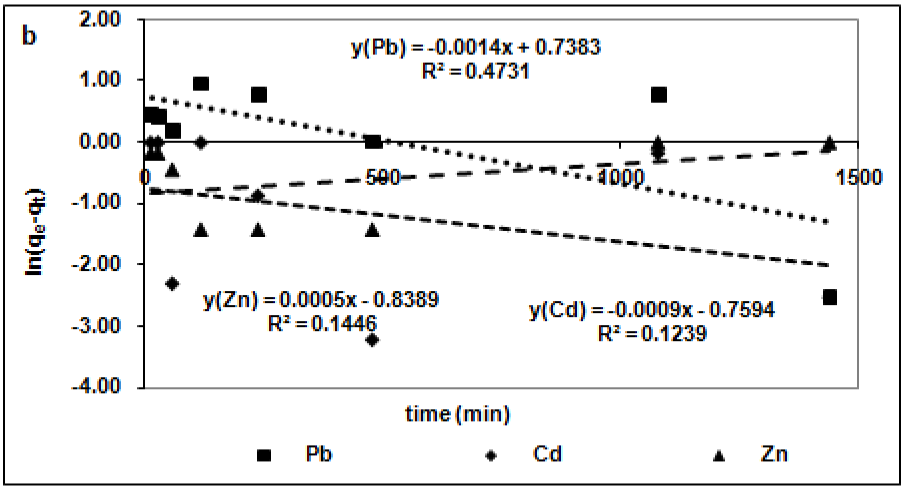


Figure (3.26): Pseudo–first–order kinetic plots for the adsorption of metal ions by (a) FHA– kaolin clay and (b) KTD– kaolin clay.

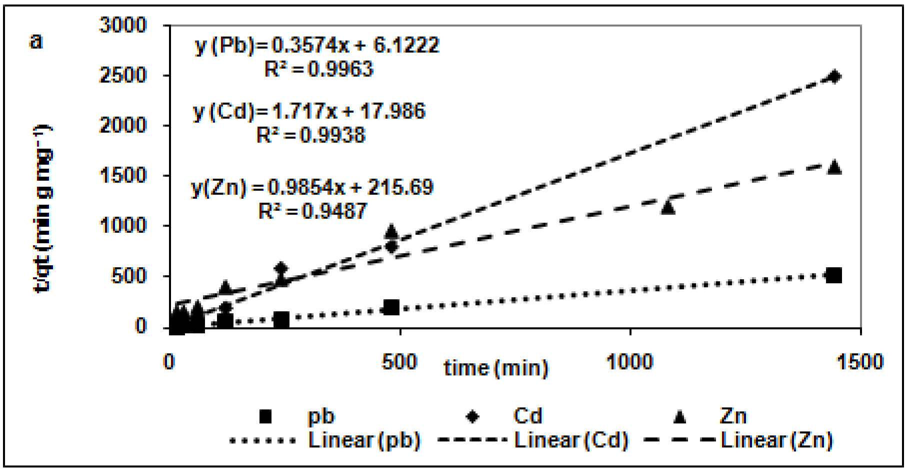


Figure (3.27): Pseudo–second–order kinetic plots for the adsorption of metal ions by (a) FHA– kaolin clay.

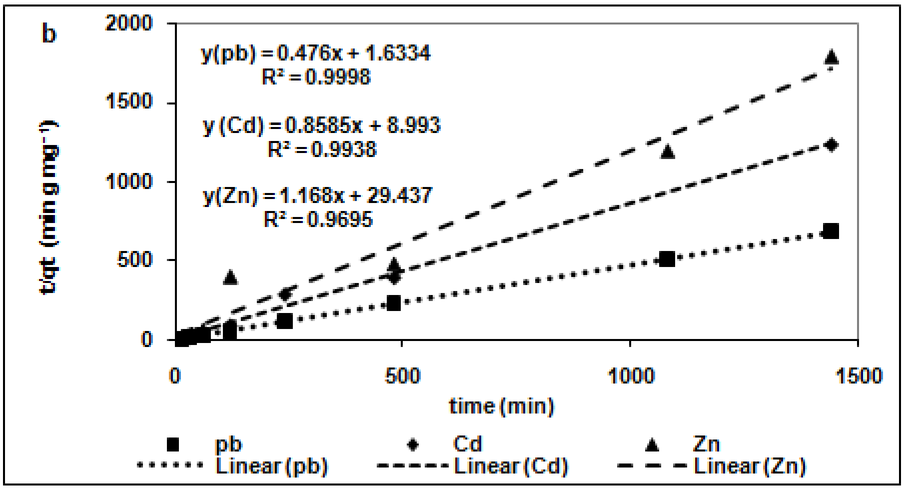


Figure (3.28): Pseudo–second–order kinetic plots for the adsorption of metal ions by (b) KTD– kaolin clay.

Moreover, the experimental q_e values (when q_e reach's plateau) were equal to the calculated values of the pseudo–second–order kinetic plots (Figures 3.27 and 3.28) as obtained from equation (15), Table (3.20), which indicate that pseudo–second–order kinetic model is considered appropriate to represent the kinetic data.

Table (3.21): Calculated and experimental q_e values for both modified kaolin clay.

Modified Clay	**Metal(II)** / **q_e (mg/g)**	**Pb(II)**	**Cd(II)**	**Zn(II)**
FHA-kaolinite	**Calculated**	**2.7979**	**0.5824**	**1.0148**
	Experimental	**2.8000**	**0.5800**	**0.9000**
KTD-kaolinite	**Calculated**	**2.1008**	**1.1648**	**0.8562**
	Experimental	**2.1000**	**1.2400**	**0.9000**

3.3.2.4. Adsorption isotherms

The isotherm plots for metal ions adsorption on both modified kaolin clay with a fixed adsorbent dose at different pH values 4.00, 5.00 and 6.00 and different temperature 25, 35 and 45 °C are shown in Figures (3.29–3.34). They were analyzed using Langmuir, Freundlich and D–R isotherm models.

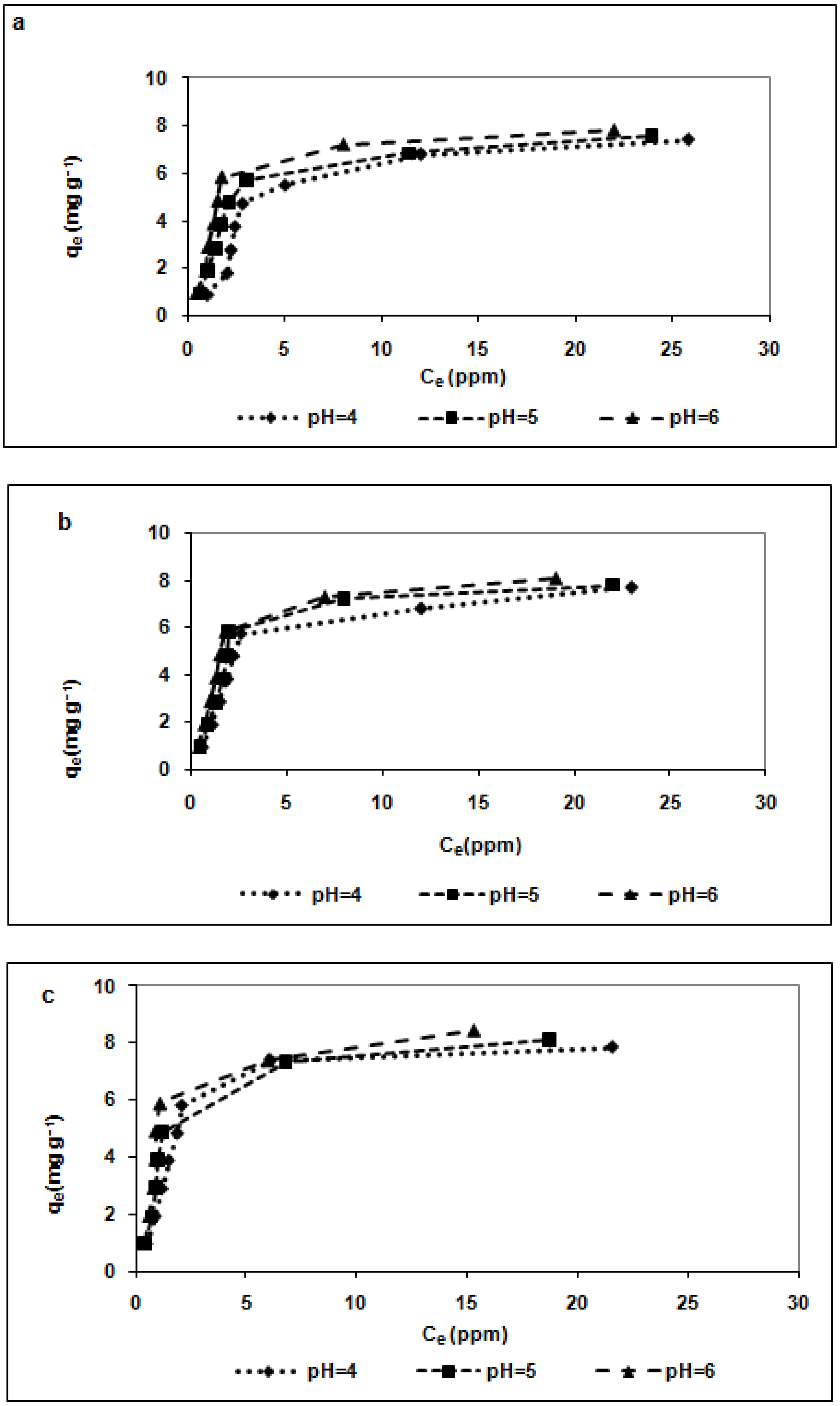


Figure (3.29): Plot of adsorption isotherm of Pb(II) on FHA– kaolin clay at (a) 25 °C, (b) 35 °C and (c) 45 °C.

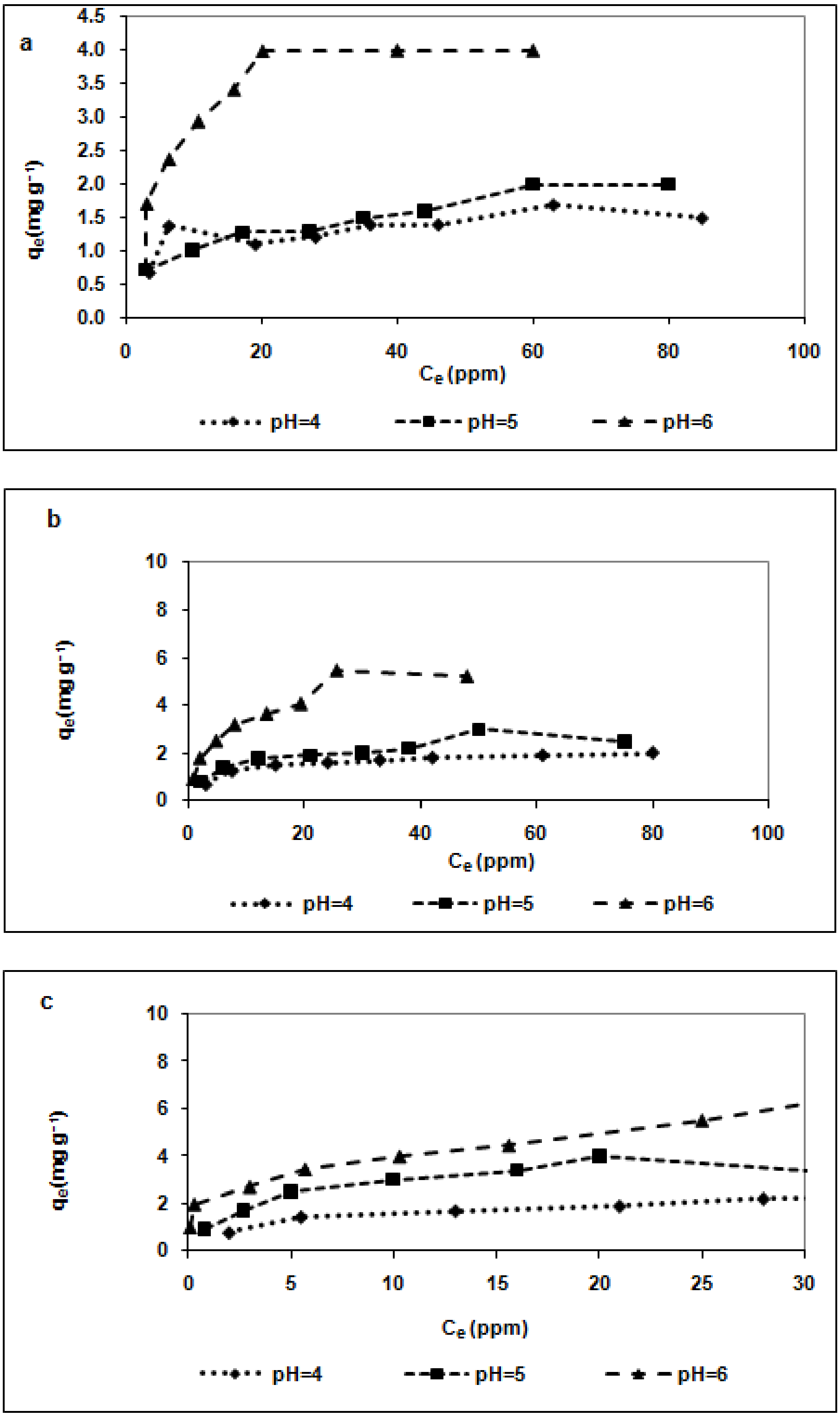


Figure (3.30): Plot of adsorption isotherm of Cd(II) on FHA– kaolin clay at (a) 25 °C, (b) 35 °C and (c) 45 °C.

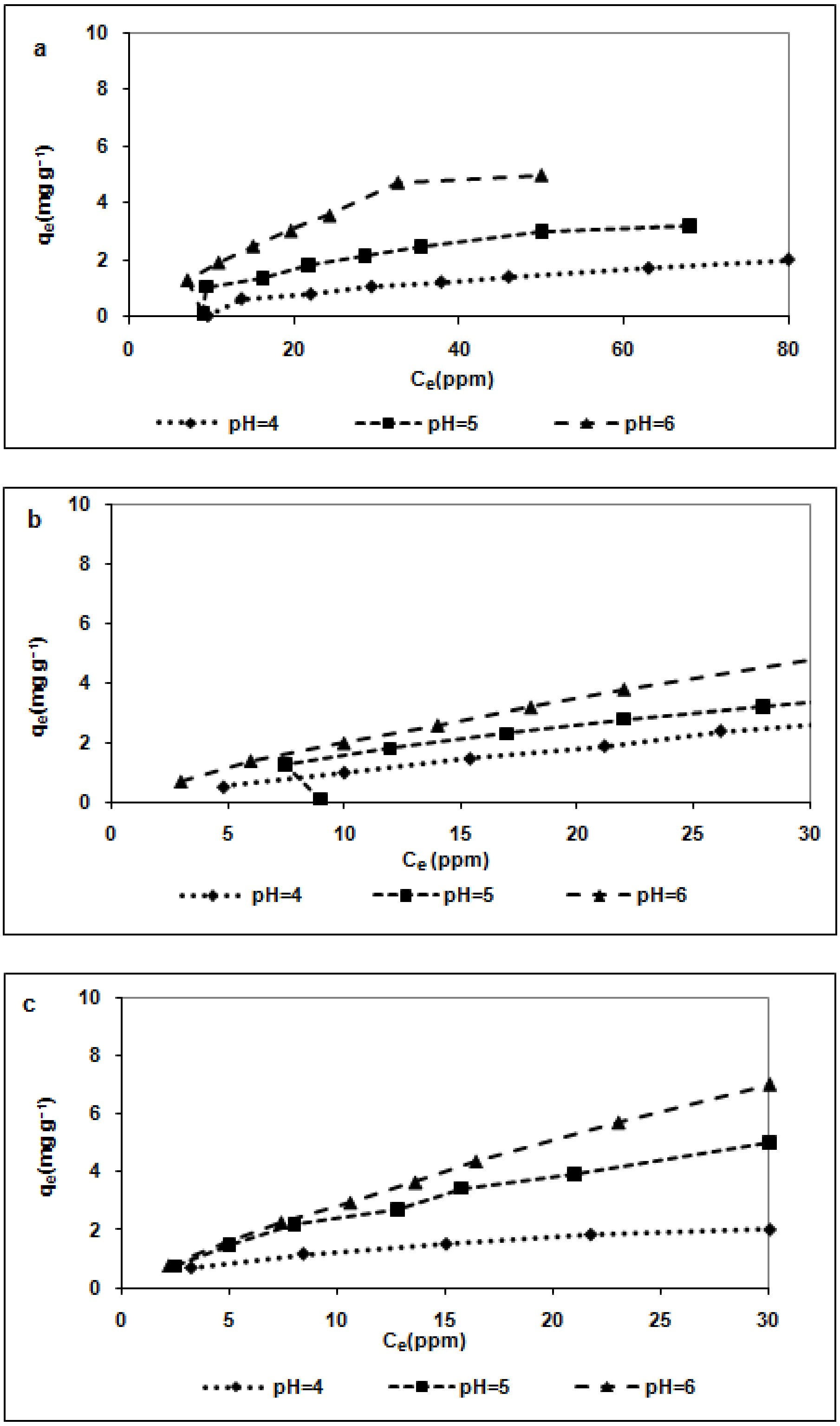
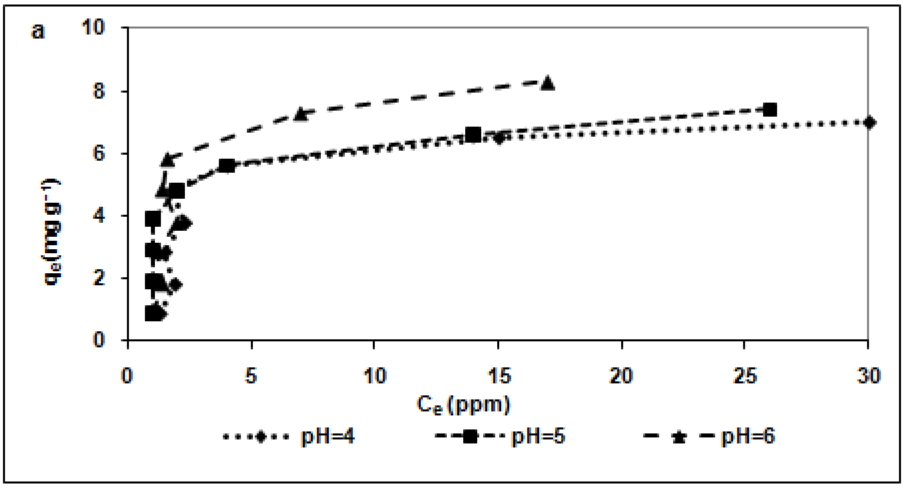
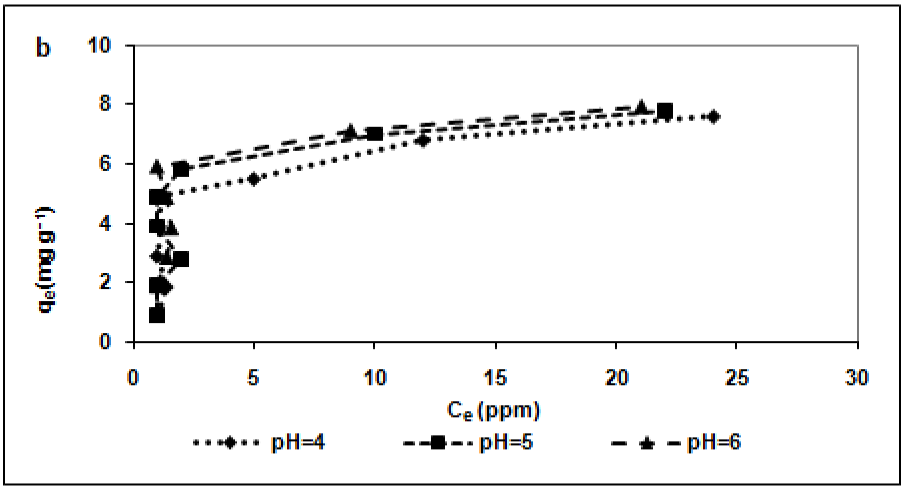


Figure (3.31): Plot of adsorption isotherm of Zn(II) on FHA– kaolin clay at (a) 25 °C, (b) 35 °C and (c) 45 °C.





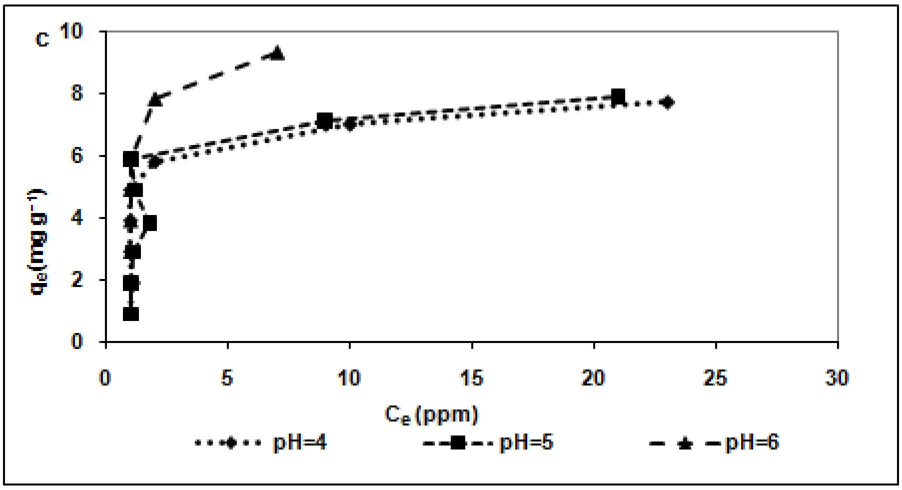


Figure (3.32): Plot of adsorption isotherm of Pb(II) on KTD– kaolin clay at (a) 25 °C, (b) 35 °C and (c) 45 °C.

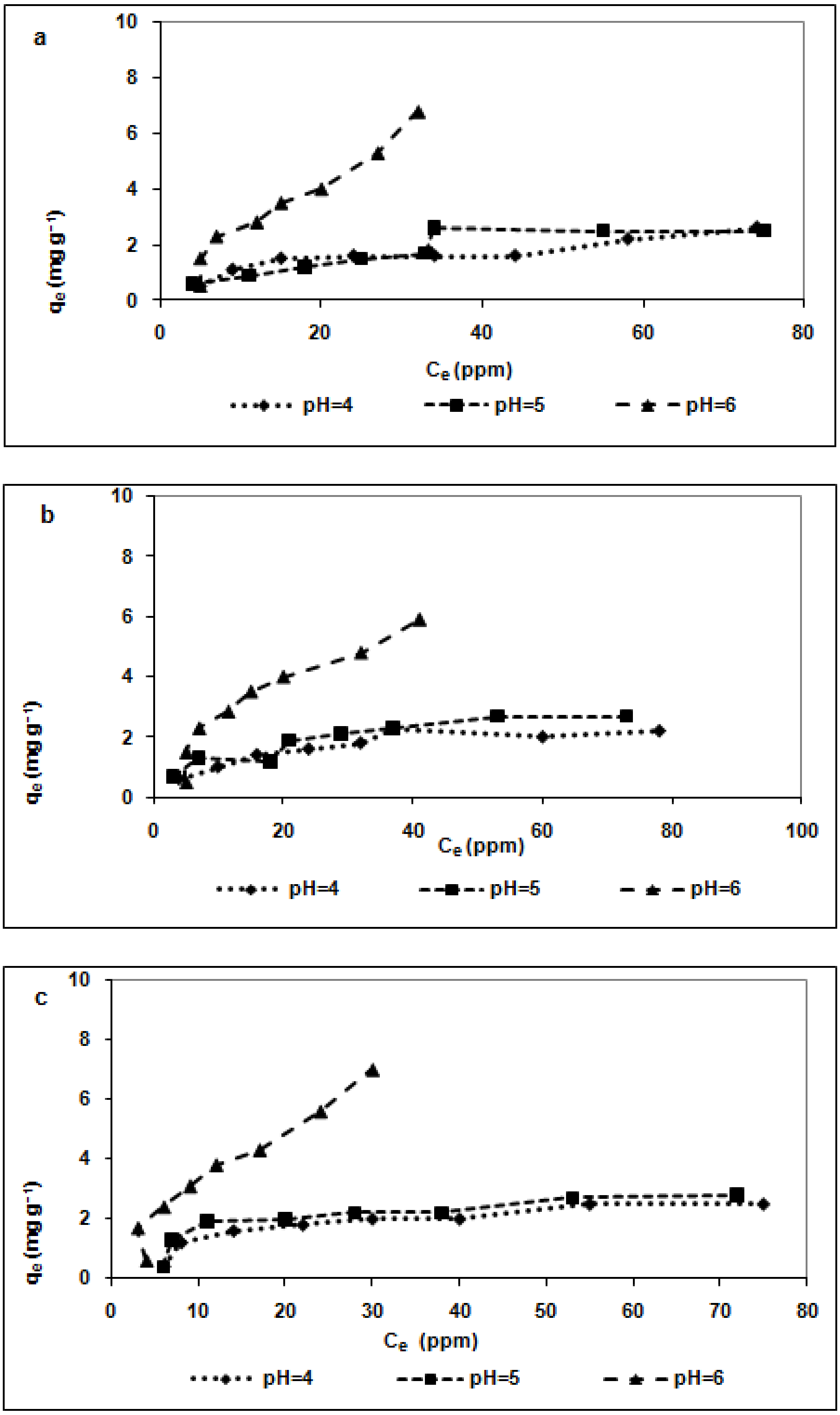


Figure (3.33): Plot of adsorption isotherm of Cd(II) on KTD– kaolin clay at (a) 25 °C, (b) 35 °C and (c) 45 °C.

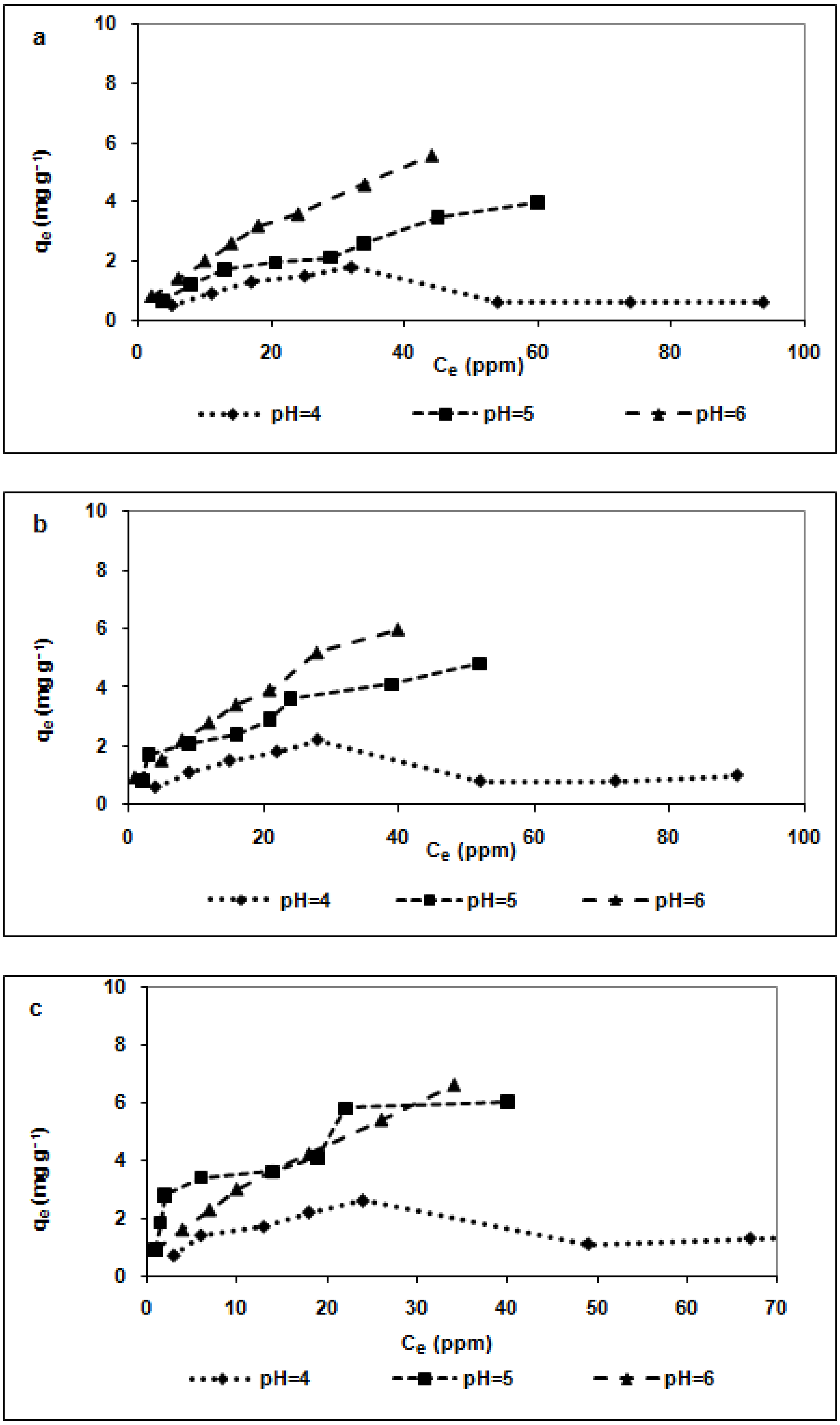


Figure (3.34): Plot of adsorption isotherm of Zn(II) on KTD– kaolin clay at (a) 25 °C, (b) 35 °C and (c) 45 °C.

It is clear from Figures ((3.29) to (3.34)) that as the metal ion concentration remaining in the metal ion solution decreased, adsorption increased first rapidly, then slowed down, and saturation was reached. This occurs because of the more efficient utilization of the adsorptive capacities of the adsorbent.

The shape of isotherm for Pb(II) adsorption on both modified kaolin clay is L–curve, which is the most common type and it describes the case where the solid (modified kaolin clay) has a high affinity for the solute (metal ion) especially in the initial stages of the isotherm. As more sites in the substrate (modified kaolin clay) are filled, it becomes increasingly difficult for solute molecules to find a vacant site available. This implies either that the adsorbed solute molecules are not vertically oriented or that there is no strong competition from the solvent (Giles et al., 1960, 1974).

While the shape of isotherm for Cd(II) and Zn(II) adsorption on both modified kaolin clay is C–curve which is given by solutes which penetrate into the solid more readily than the solvent does. These curves are characterized by the constant partition of solute between solution (solvent) and substrate (solid), right up to the maximum possible adsorption, where an abrupt change to horizontal plateau occurs.

3.3.2.4.1. Langmuir adsorption isotherm model

The adsorption of metal ions on modified kaolin clay was analyzed using Langmuir model. The Langmuir isotherm plots are shown in Figures (3.35) to (3.40), and the Linearized Langmuir (II) and (III) isotherms are shown in Tables ((3.22) to (3.27)).

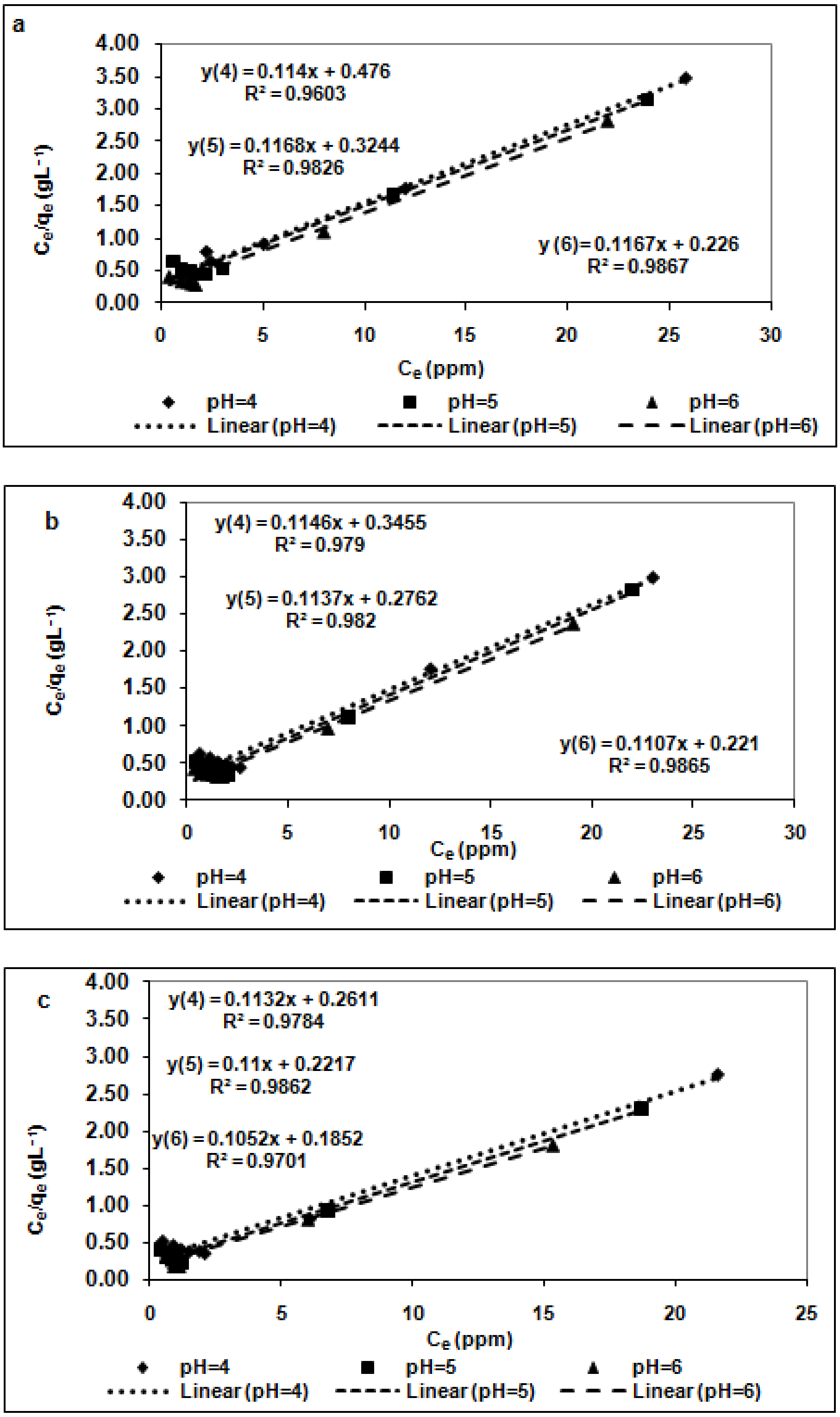


Figure (3.35): Plots of linearized Langmuir isotherm (II) for Pb(II) adsorbed by FHA–kaolin clay at (a) 25 °C, (b) 35 °C and (c) 45 °C.

Table (3.22): Linearized Langmuir isotherm parameters for Pb(II) adsorbed by FHA–kaolin clay.

T(°C)	pH	Langmuir Isotherm (C vs. C/q)				Langmuir Isotherm (1/C vs. 1/q)			
		R^2	K_L	R_L	q_m	R^2	K_L	R_L	q_m
25	4.00	0.9932	0.3351	0.0289	8.33	0.9423	0.3872	0.0257	8.32
	5.00	0.9826	0.3602	0.0270	8.56	0.9349	0.5666	0.0173	8.34
	6.00	0.9867	0.5162	0.0190	8.57	0.9419	0.7385	0.0134	8.44
35	4.00	0.9790	0.3317	0.0293	8.73	0.9706	0.3520	0.0276	8.70
	5.00	0.9820	0.4117	0.0237	8.79	0.9797	0.3591	0.0271	9.41
	6.00	0.9865	0.5008	0.0196	9.03	0.9804	0.4744	0.0206	9.42
45	4.00	0.9784	0.4336	0.0225	8.83	0.9668	0.5160	0.0190	9.19
	5.00	0.9862	0.5565	0.0177	8.99	0.9595	0.9058	0.0109	8.66
	6.00	0.9701	0.5679	0.0173	9.51	0.9999	0.5497	0.0179	9.56

Units for the parameters: K_L (L mg^{-1}), q_m (mg g^{-1}) and R_L unitless.

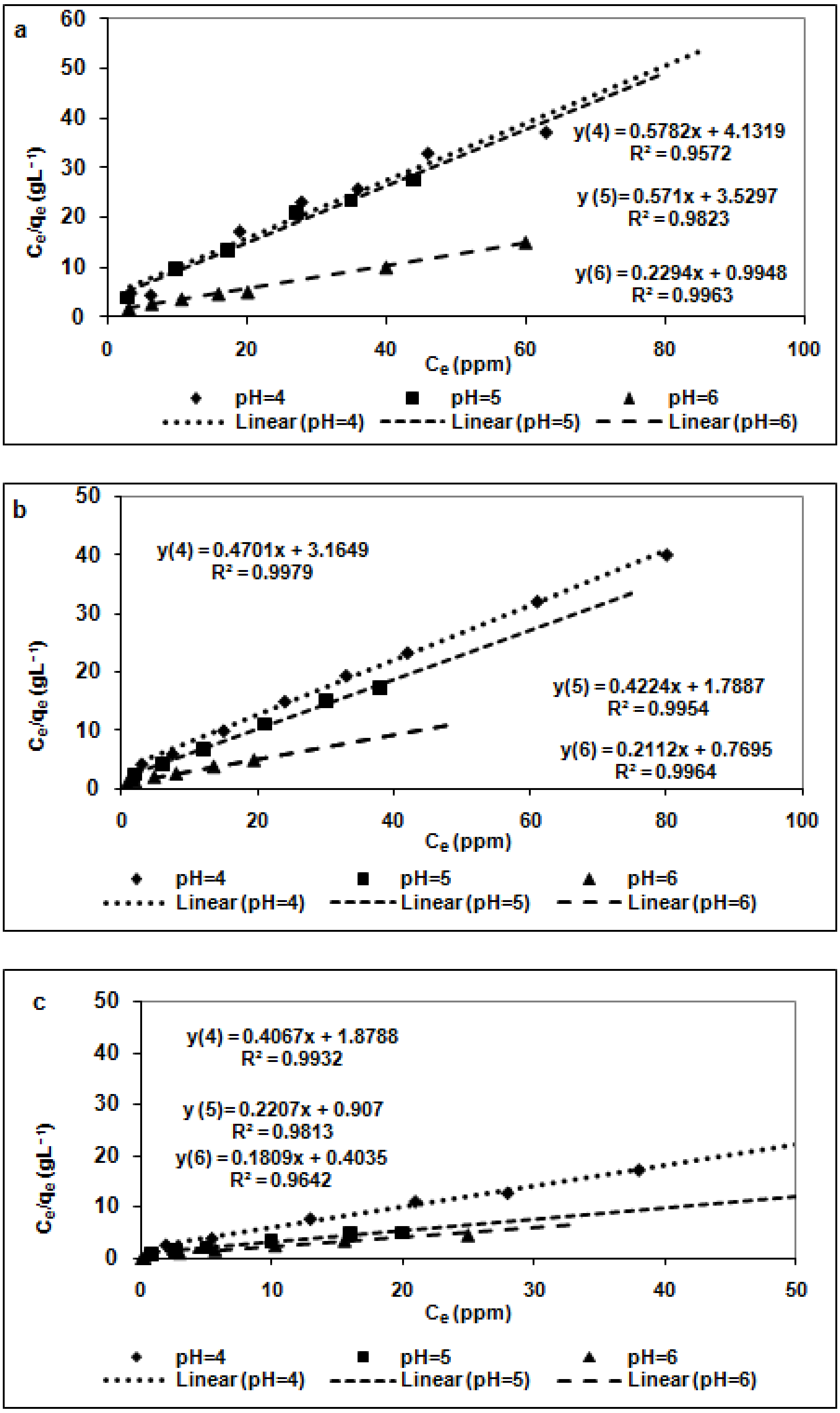


Figure (3.36): Plots of linearized Langmuir isotherm (II) for Cd(II) adsorbed by FHA–kaolin clay at (a) 25 °C, (b) 35 °C and (c) 45 °C.

Table (3.23): Linearized Langmuir isotherm parameters for Cd(II) adsorbed by FHA–kaolin clay.

T(°C)	pH	Langmuir Isotherm (C vs. C/q)				Langmuir Isotherm (1/C vs. 1/q)			
		R^2	K_L	R_L	q_m	R^2	K_L	R_L	q_m
25	4.00	0.9572	0.1399	0.0667	1.73	0.9440	0.2364	0.0406	1.51
	5.00	0.9823	0.1618	0.0582	1.75	0.9432	0.3069	0.0316	1.53
	6.00	0.9963	0.2306	0.0416	4.36	0.9841	0.1993	0.0478	4.48
35	4.00	0.9979	0.1485	0.0631	2.13	0.9927	0.1751	0.0540	2.05
	5.00	0.9954	0.2362	0.0406	2.37	0.9723	0.2355	0.0407	2.47
	6.00	0.9964	0.2745	0.0352	4.73	0.9909	0.2869	0.0337	4.89
45	4.00	0.9932	0.2165	0.0442	2.46	0.9911	0.2573	0.0374	2.37
	5.00	0.9813	0.2433	0.0395	4.53	0.9859	0.3881	0.0251	3.82
	6.00	0.9642	0.4484	0.0218	5.53	0.9795	2.6979	0.0033	4.62

Units for the parameters: K_L (L mg^{-1}), q_m (mg g^{-1}) and R_L unitless.

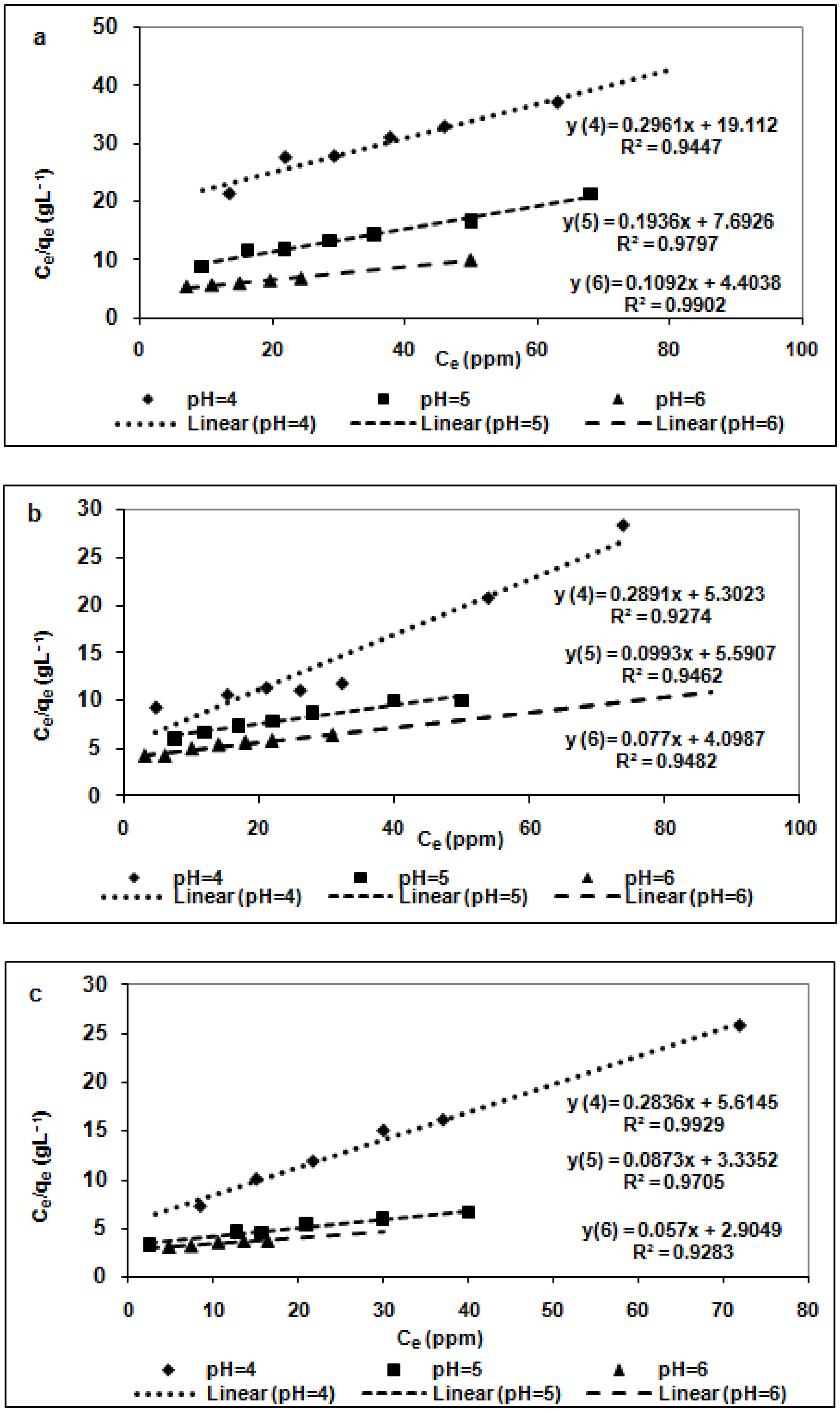


Figure (3.37): Plots of linearized Langmuir isotherm (II) for Zn(II) adsorbed by FHA–kaolin clay at (a) 25 °C, (b) 35 °C and (c) 45 °C.

Table (3.24): Linearized Langmuir isotherm parameters for Zn(II) adsorbed by FHA–kaolin clay.

T(°C)	**pH**	**Langmuir Isotherm (C vs. C/q)**				**Langmuir Isotherm (1/C vs. 1/q)**			
		R^2	**K_L**	**R_L**	**q_m**	**R^2**	**K_L**	**R_L**	**q_m**
25	**4.00**	**0.9447**	**0.0155**	**0.3923**	**3.38**	**0.9747**	**0.0187**	**0.3481**	**3.02**
	5.00	**0.9797**	**0.0252**	**0.2844**	**5.17**	**0.9793**	**0.0298**	**0.2512**	**4.67**
	6.00	**0.9902**	**0.0248**	**0.2873**	**9.15**	**0.9966**	**0.0178**	**0.3598**	**11.81**
35	**4.00**	**0.9355**	**0.0545**	**0.1549**	**3.46**	**0.9718**	**0.0493**	**0.1687**	**3.49**
	5.00	**0.9940**	**0.0178**	**0.3602**	**10.07**	**0.9940**	**0.0196**	**0.3380**	**9.34**
	6.00	**0.9981**	**0.0188**	**0.3474**	**12.99**	**0.9981**	**0.0209**	**0.3237**	**11.95**
45	**4.00**	**0.9929**	**0.0505**	**0.1652**	**3.53**	**0.9710**	**0.0459**	**0.1789**	**3.60**
	5.00	**0.9705**	**0.0262**	**0.2763**	**11.45**	**0.9964**	**0.0318**	**0.2390**	**10.32**
	6.00	**0.9283**	**0.0196**	**0.3375**	**17.54**	**0.9984**	**0.0179**	**0.3572**	**19.04**

Units for the parameters: K_L (L mg^{-1}), q_m (mg g^{-1}) and R_L unitless.

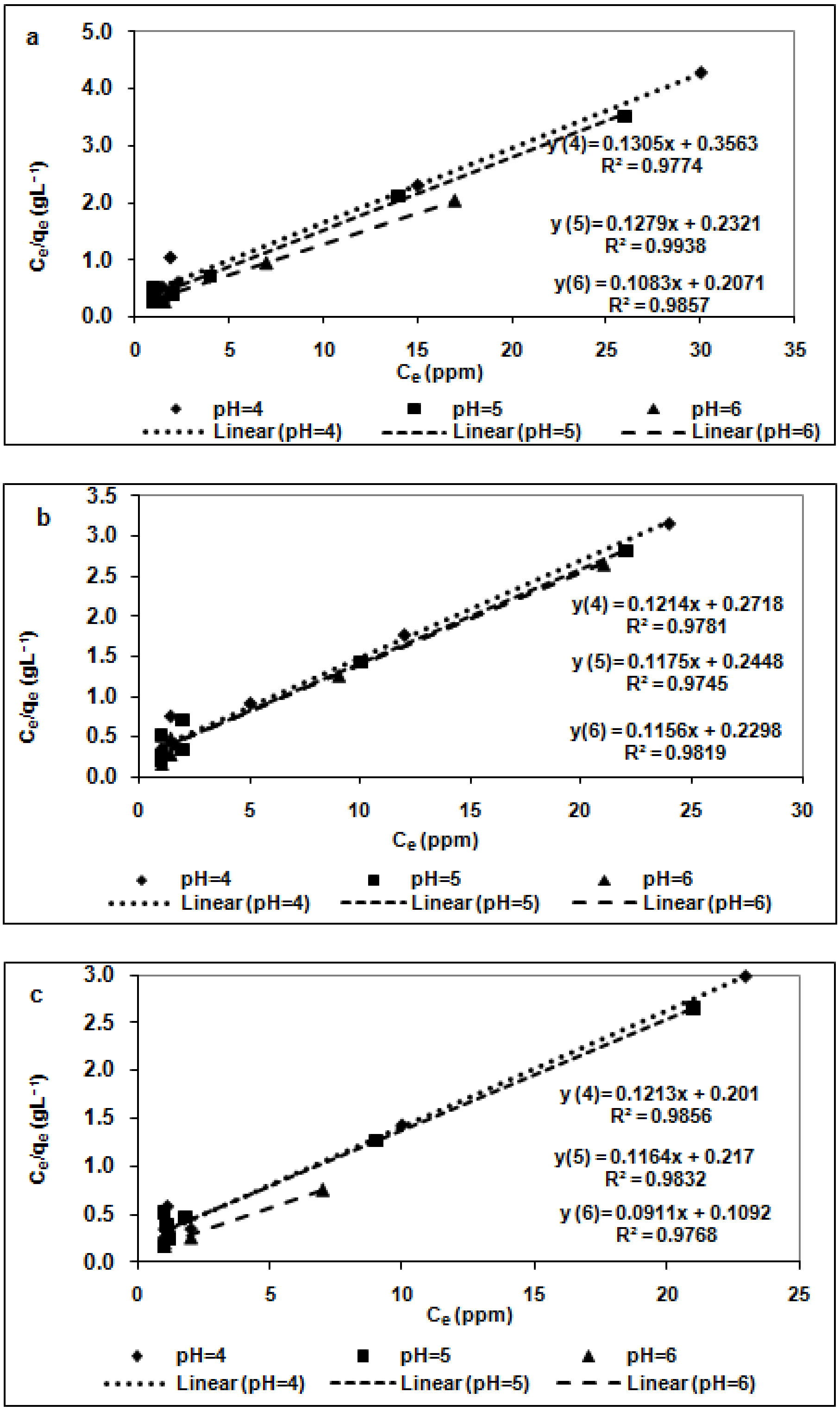


Figure (3.38): Plots of linearized Langmuir isotherm (II) for Pb(II) adsorbed by KTD–kaolin clay at (a) 25 °C, (b) 35 °C and (c) 45 °C.

Table (3.25): Linearized Langmuir isotherm parameters for Pb(II) adsorbed by KTD–kaolin clay.

T(^{o}C)	pH	Langmuir Isotherm (C vs. C/q)				Langmuir Isotherm (1/C vs. 1/q)			
		R^2	K_L	R_L	q_m	R^2	K_L	R_L	q_m
25	4.00	0.9774	0.3662	0.0266	7.66	0.9979	0.4043	0.0241	7.64
	5.00	0.9938	0.5511	0.0178	7.82	0.9750	0.6044	0.0163	7.93
	6.00	0.9857	0.5228	0.0187	9.24	0.9940	0.3346	0.0290	9.89
35	4.00	0.9781	0.4466	0.0219	8.24	0.9954	0.5975	0.0165	7.72
	5.00	0.9745	0.4798	0.0204	8.51	0.9879	0.2640	0.0365	8.86
	6.00	0.9819	0.5031	0.0195	8.65	0.9404	0.3621	0.0269	9.27
45	4.00	0.9856	0.6034	0.0163	8.25	0.9699	0.9738	0.0102	8.11
	5.00	0.9832	0.5362	0.0183	8.59	0.9991	0.4434	0.0221	8.75
	6.00	0.9768	0.8343	0.0118	10.98	0.9912	1.304	0.0076	10.51

Units for the parameters: K_L (L mg^{-1}), q_m (mg g^{-1}) and R_L unitless.

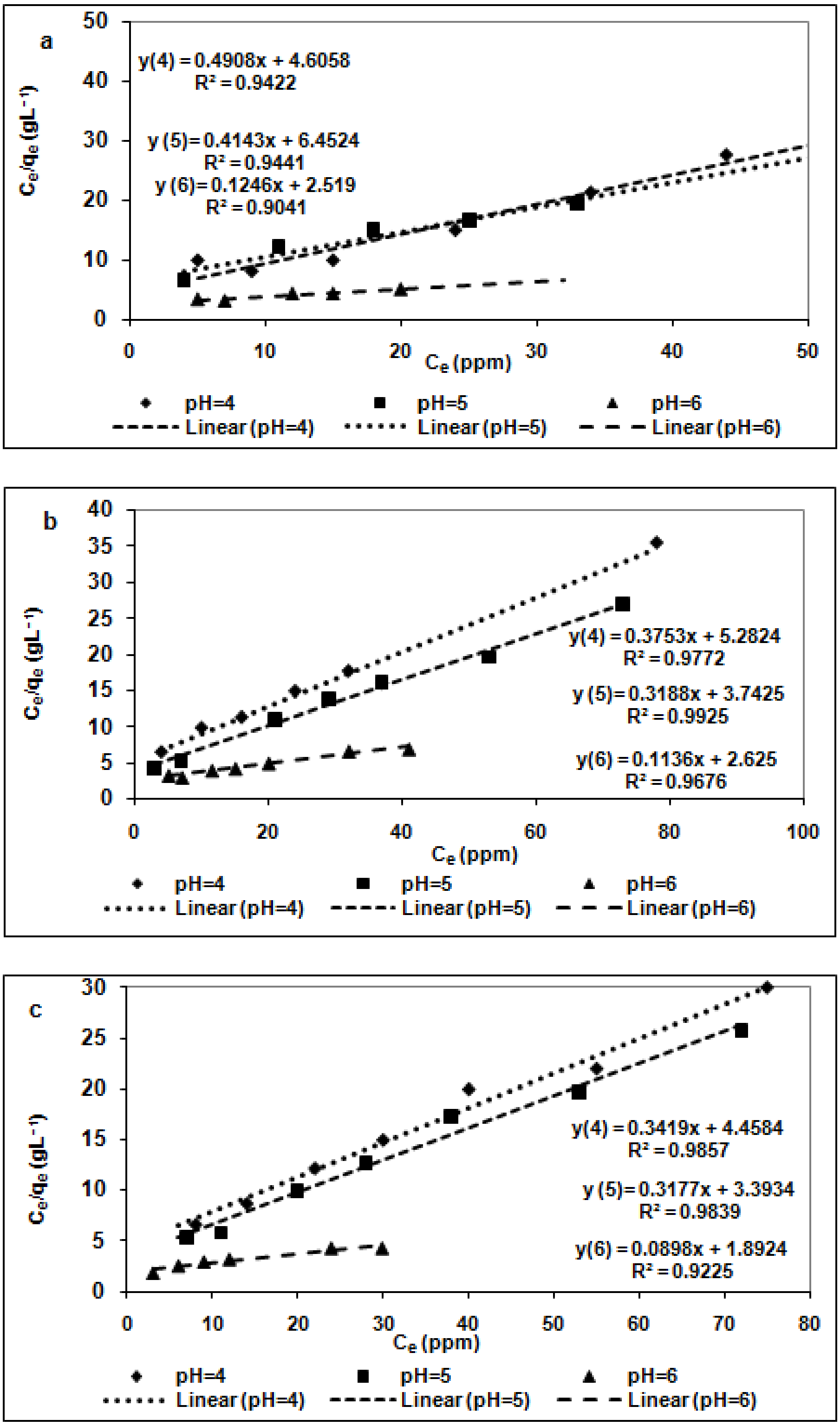


Figure (3.39): Plots of linearized Langmuir isotherm (II) for Cd(II) adsorbed by KTD–kaolin clay at (a) 25 °C, (b) 35 °C and (c) 45 °C.

Table (3.26): Linearized Langmuir isotherm parameters for Cd(II) adsorbed by KTD–kaolin clay.

T(^{o}C)	pH	Langmuir Isotherm (C vs. C/q)				Langmuir Isotherm (1/C vs. 1/q)			
		R^2	K_L	R_L	q_m	R^2	K_L	R_L	q_m
25	4.00	0.9422	0.1066	0.0858	2.04	0.9659	0.0375	0.2104	3.24
	5.00	0.9441	0.064	0.1347	2.41	0.9473	0.0711	0.1232	2.66
	6.00	0.9041	0.0494	0.1681	8.02	0.9681	0.0386	0.2054	9.62
35	4.00	0.9772	0.0711	0.1234	2.66	0.9845	0.0747	0.1176	2.56
	5.00	0.9925	0.0852	0.1051	3.13	0.9954	0.1044	0.0874	2.95
	6.00	0.9676	0.0433	0.1877	8.80	0.9768	0.0431	0.1884	8.87
45	4.00	0.9857	0.0767	0.1154	2.92	0.9738	0.0973	0.0932	2.73
	5.00	0.9839	0.0936	0.0965	3.15	0.9764	0.1098	0.0835	2.97
	6.00	0.9225	0.0474	0.1741	11.14	0.9818	0.0492	0.1689	10.32

Units for the parameters: K_L (L mg^{-1}), q_m (mg g^{-1}) and R_L unitless.

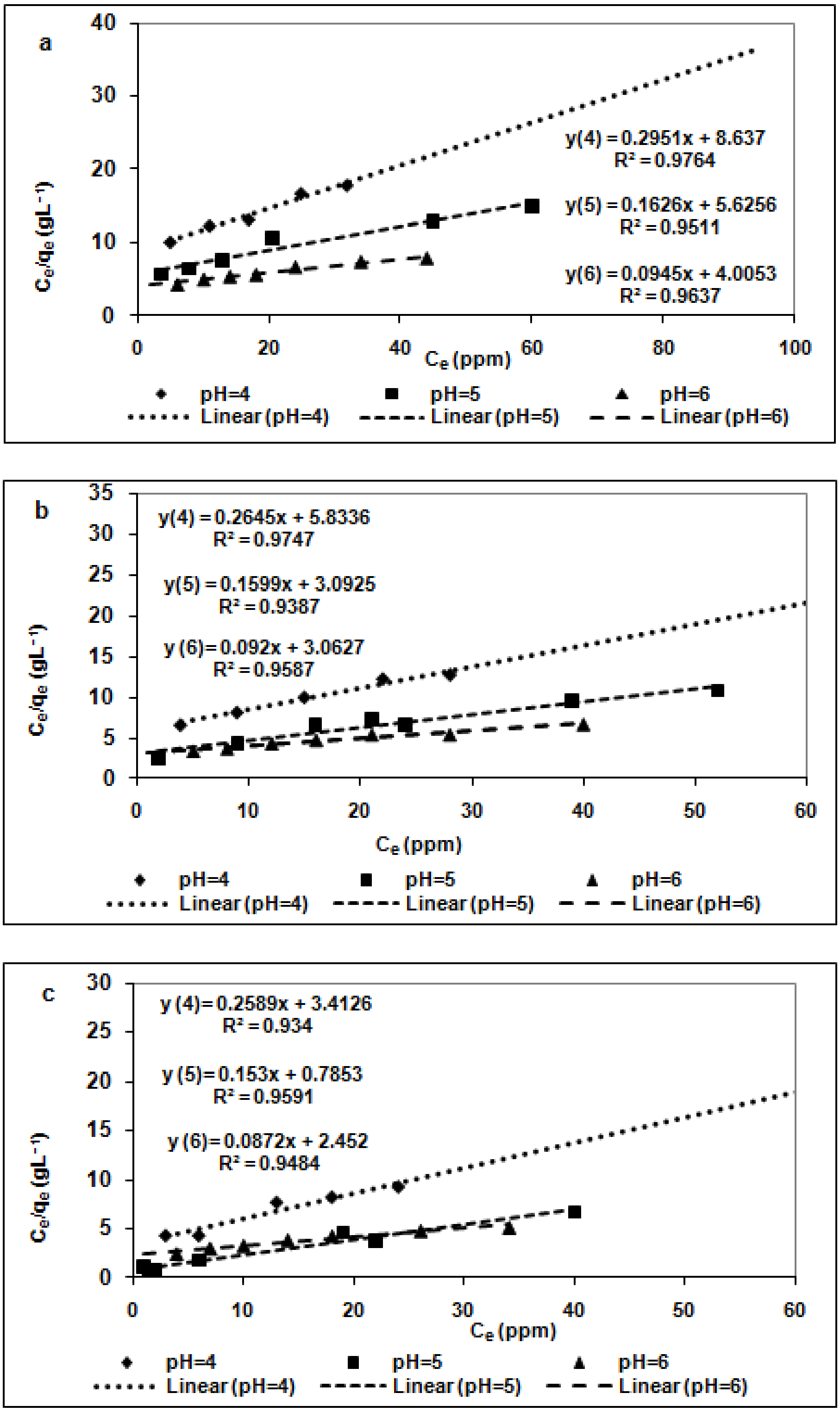


Figure (3.40): Plots of linearized Langmuir isotherm (II) for Zn(II) adsorbed by KTD–kaolin clay at (a) 25 °C, (b) 35 °C and (c) 45 °C.

Table (3.27): Linearized Langmuir isotherm parameters for Zn(II) adsorbed by KTD–kaolin clay.

T(°C)	pH	Langmuir Isotherm (C vs. C/q)				Langmuir Isotherm (1/C vs. 1/q)			
		R^2	K_L	R_L	q_m	R^2	K_L	R_L	q_m
25	4.00	0.9764	0.0342	0.2264	3.39	0.9977	0.0356	0.2194	3.30
	5.00	0.9511	0.0289	0.2571	6.15	0.9973	0.0398	0.2008	5.10
	6.00	0.9637	0.0236	0.2977	10.58	0.9954	0.0291	0.2556	9.23
35	4.00	0.9747	0.0453	0.1807	3.78	0.9985	0.0518	0.1619	3.49
	5.00	0.9387	0.0517	0.1621	6.26	0.9545	0.0609	0.1411	5.82
	6.00	0.9587	0.0300	0.2498	10.87	0.9846	0.0354	0.2201	9.70
45	4.00	0.9340	0.0759	0.1165	3.86	0.9736	0.0745	0.1184	3.94
	5.00	0.9591	0.1948	0.0488	6.54	0.9918	0.1720	0.0549	6.14
	6.00	0.9484	0.0356	0.2195	11.47	0.9919	0.0384	0.2068	10.74

Units for the parameters: K_L (L mg^{-1}), q_m (mg g^{-1}) and R_L unitless.

The adsorption of metal ions on modified kaolin clay fitted Langmuir model. In addition to that there is a good agreement in q_m values between linearized Langmuir (II) and (III) isotherms as shown in Tables (3.22) to (3.27).

The Langmuir isotherms plots (Figures (3.35) to (3.40)) had excellent linearity (R^2 >0.90). When the experimental values for the metal ions were fitted to both the Langmuir model, the following observations were obtained according to Langmuir model postulates:

(1) The metal ions were adsorbed on some sites whose binding energies are uniform and therefore formed a layer on the surface of the adsorbents.

(2) There is no interaction between the adsorbed ions (Adebowale et al., 2005).

From the Langmuir constant, the value of R_L indicates the type of the isotherm to be either unfavorable adsorption ($R_L > 1$), linear adsorption ($R_L = 1$), favorable adsorption ($0 < R_L < 1$) or irreversible adsorption ($R_L = 0$) (Anirudhan and Suchithra, 2010; Unuabonaha, et al., 2007).

So as shown in Tables ((3.22) to (3.27)), the values for Pb(II) are ($0.0118 < R_L < 0.0293$), for Cd(II) are ($0.0218 < R_L < 0.1877$) and for Zn(II) are ($0.1549 < R_L < 0.3923$). The R_L values for all metal ions adsorbed by both modified kaolin clay are in between 0 and 1, so the adsorption process of all metal ions is favorable.

So the adsorption coefficients (R_L and q_m) agreed well with the conditions supporting favorable adsorption.

From Tables (3.22) to (3.27), the values of q_m which related to adsorption capacity indicated that increasing of temperatures and pH lead to increase in the adsorption capacities of both modified kaolin clay for all metal ions. These results agree with that obtained from Tables (3.15 – 3.20) of metal ions uptake with the same trend (Pb(II)> Cd(II) > Zn(II)).

Adebowale et al., 2006, modified kaolinite with orthophosphate enhanced adsorption of Pb and Cd ions from aqueous solutions of the metal ions. Adsorption data were fitted against Langmuir, they found that the values of q_m at 0.01 M of $NaNO_3$ for Pb(II) was 17.89 mg/g, and for Cd(II) was 8.39 mg/g. Besides to that, they calculated K_L values for both metal ions and were equal to 0.0437 L/g for Pb(II) and 0.0290 L/g for Cd(II).

Amer et al., 2010, determined the potential of application of sodium polyphosphate modified kaolinite as an adsorbent for the removal of lead(II), zinc(II) and cadmium(II) ions from aqueous solutions. The adsorption isotherms of all three metal ions followed well Langmuir equation.

The Langmuir constants were calculated at different temperatures. For Pb(II) the K_L values were equal to 0.062, 0.106 and 0.111 L/mg at 25 °C, 35 °C and 45 °C, respectively. While for Zn(II), K_L values were equal to 0.032 , 0.044 and 0.044 L/mg, and for Cd(II) were 0.014, 0.015 and 0.016 L/mg, at 25 °C, 35 °C and 45 °C, respectively.

Polyphosphate–kaolinite was found to remove heavy metal ions efficiently from aqueous solutions with selectivity in the order of Pb(II) > Zn(II) > Cd(II). The q_m values were found to be 25.13, 22.83 and 10.37mg/g, for Pb(II), Zn(II) and Cd(II), respectively.

3.3.2.4.1.1. Explanation of the order of adsorption of metal ions by modified kaolin clay

The results from metal ions uptake Tables (3.15 – 3.20) and Langmuir model show that Pb(II) had the highest adsorption affinity onto both modified kaolin clay. We explained the factors that influence the relative selectivity of metal ions in solution in section 3.3.1.1. In addition to that there are other factors due to the presence of humic acid,

According to HSAB principle, hard Lewis acids prefer to react, or form complexes, with hard Lewis bases, and soft acids with soft bases (Puls and Bohn, 1988). Soft Lewis acids and bases tend to form outer–sphere complexes (Sparks, 1995). Main surface adsorption sites on kaolinite exhibit relatively soft Lewis base characteristics. So, metal ions form stable complexes with carboxylic and phenolic groups of organic fractions of modified kaolin clay by humic acid. In addition, organic functional groups such as carboxyl or phenol of humic acid incorporated in the kaolinite material may behave in conjunction with the inorganic Lewis basic sites, and react with heavy metals

in solution, exhibiting a complementary behavior of Lewis bases at the adsorbent surface.

Metal adsorption by the combined action of aluminol and phenol groups which become activated at higher pH (because of being more potent Lewis bases having higher pKa). The metal ion–binding sites (possibly silanol and –COOH deprotonated at lower pH) are occupied first with a higher overall binding constant (Unuabonaha, et al., 2007).

The values of electronegativity for the metal ion are Pb(II)> Cd(II) >Zn(II). This means that the Pb(II) binding onto the negative surface strongly, then the adsorption capacity of modified kaolin clay will be increase (kaolinite (in nature) has small negative charge, in addition, with increasing pH it becomes negatively charged) so q_m values should be higher than other metal ions.

Another view that supports the order of adsorption of metal ions by both modified kaolin clay is by using Langmuir parameter (R_L). If ($0 < R_L < 1$) then the adsorption process is favorable.

Plots of (R_L) values for the metal ions as given in Figures (3.41) and 3.42) indicated that adsorption is more favorable for Pb(II) than Cd(II) than Zn(II) for both modified kaolin clay.

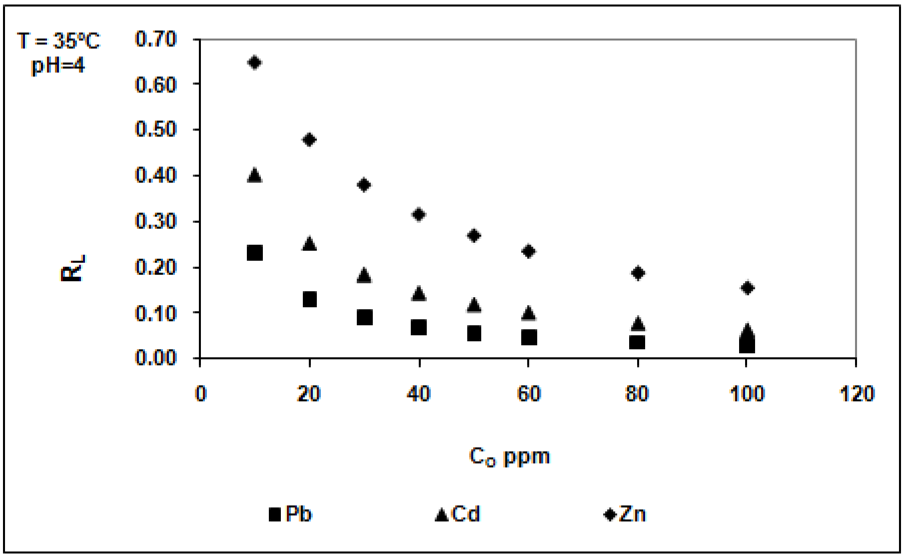


Figure (3.41): Values of the separation factor, R_L, for the adsorption of Pb(II), Cd(II) and Zn(II) by FHA– kaolin clay, at 35 °C and pH=4.00.

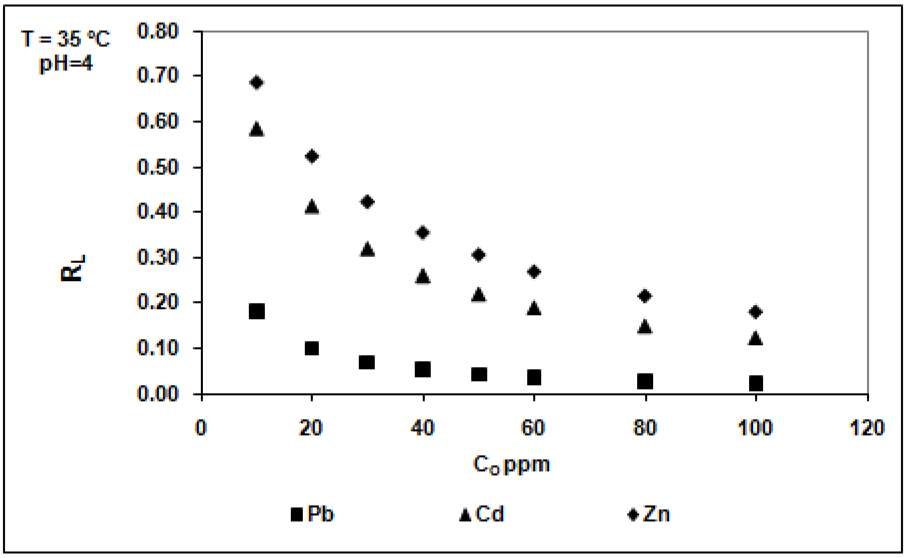


Figure (3.42): Values of the separation factor, R_L, for the adsorption of Pb(II), Cd(II) and Zn(II) by KTD– kaolin clay, at 35 °C and pH=4.00.

3.3.2.4.2. Freundlich adsorption isotherm model

The adsorption of metal ions on modified kaolin clay was analyzed using Freundlich model, the Freundlich isotherm plots are shown in Figures (3.43) to (3.48) and Tables (3.28–3.33).

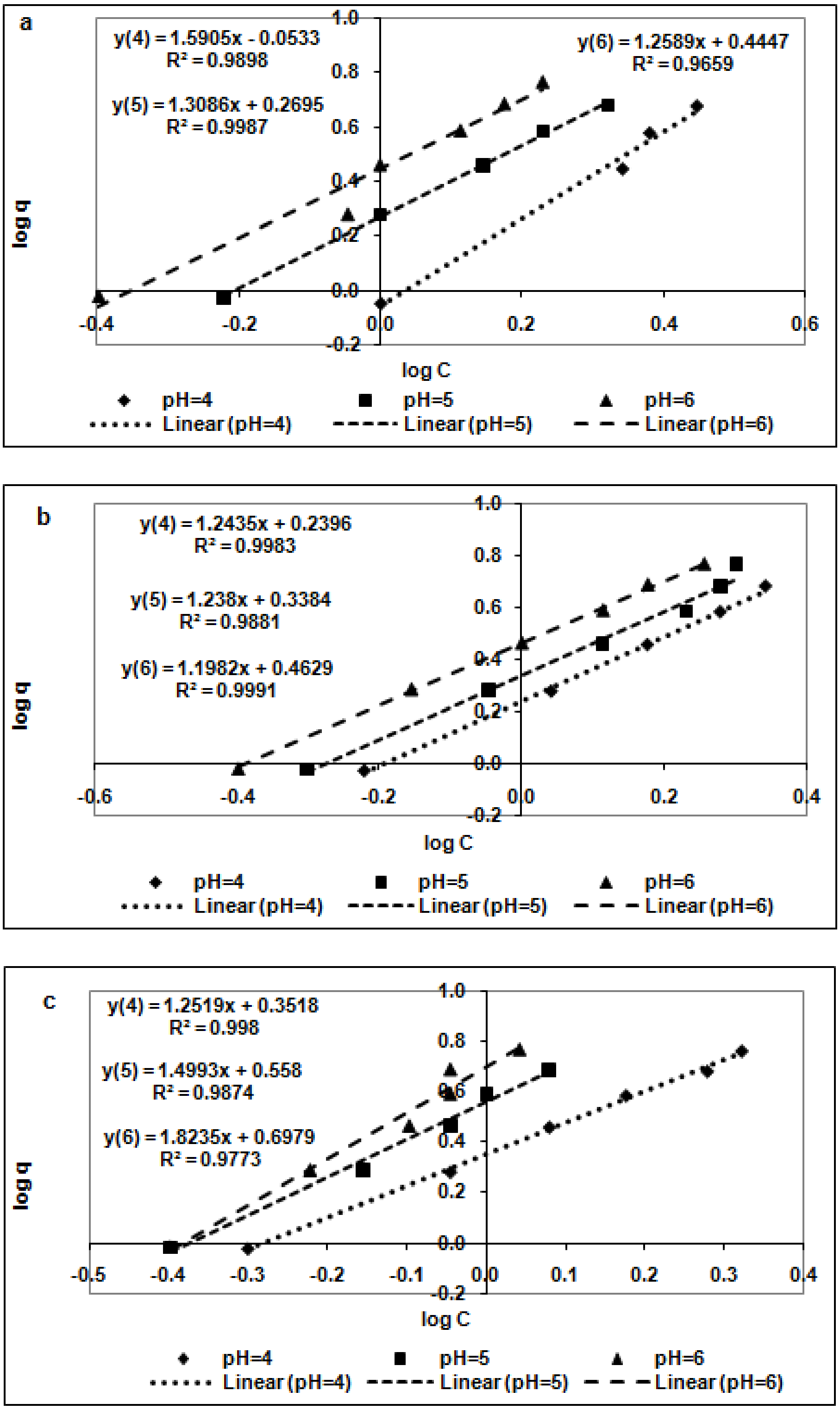


Figure (3.43): Plots of linearized Freundlich isotherm for Pb(II) adsorbed by FHA–kaolin clay at (a) 25 °C, (b) 35 °C and (c) 45 °C.

Table (3.28): Freundlich isotherm parameters for Pb(II) adsorbed by FHA– kaolin clay.

T(°C)	**pH**	**Freundlich Isotherm**		
		R^2	**n**	**K_F**
25	**4.00**	**0.9898**	**0.629**	**0.88**
	5.00	**0.9987**	**0.764**	**1.86**
	6.00	**0.9659**	**0.794**	**2.78**
35	**4.00**	**0.9983**	**0.804**	**1.74**
	5.00	**0.9881**	**0.808**	**2.18**
	6.00	**0.9991**	**0.835**	**2.90**
45	**4.00**	**0.9980**	**0.799**	**2.25**
	5.00	**0.9874**	**0.672**	**3.59**
	6.00	**0.9773**	**0.548**	**4.99**

Units for the parameters: n (gL^{-1}) and K_F ($L\ g^{-1}$).

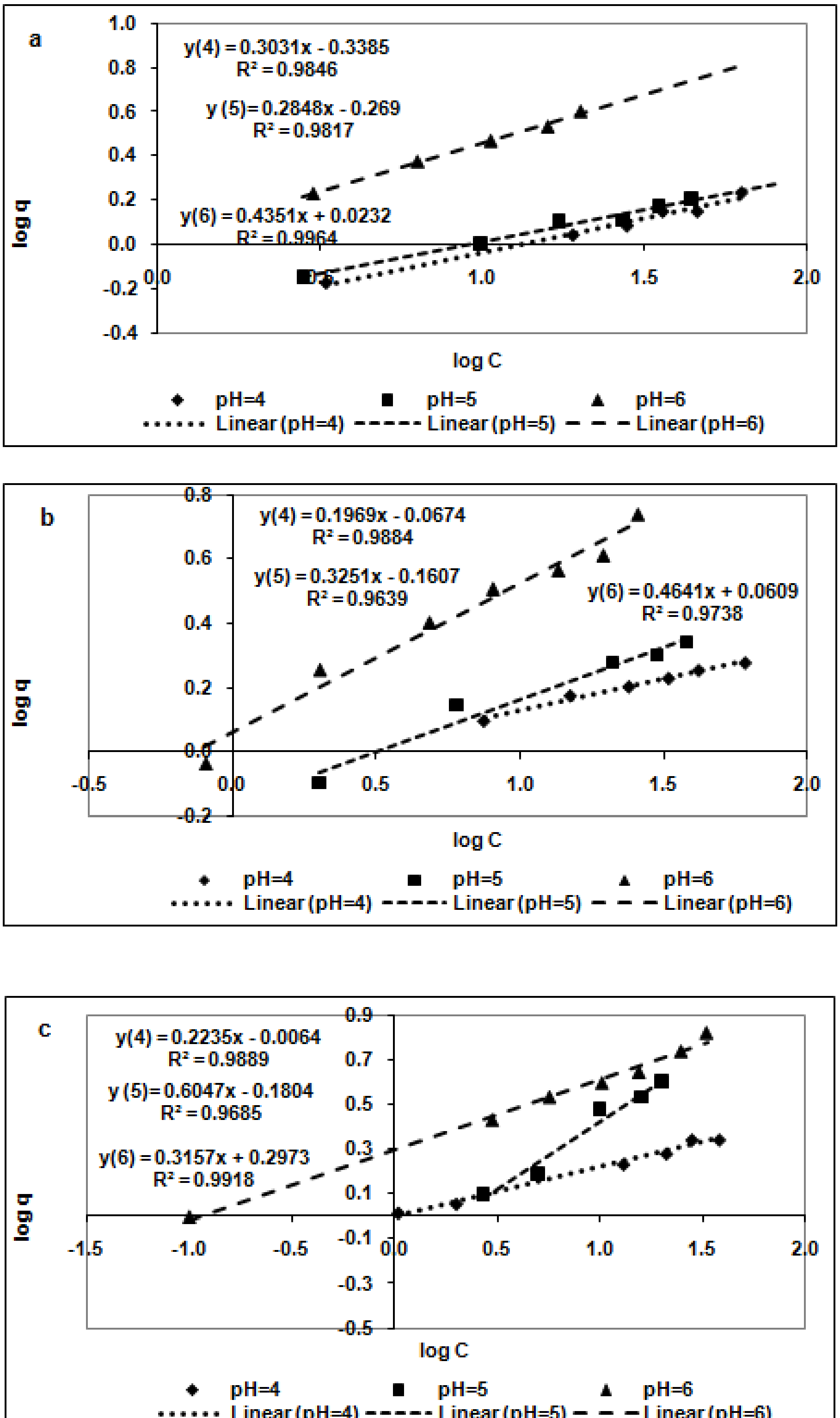


Figure (3.44): Plots of linearized Freundlich isotherms for Cd(II) adsorbed by FHA–kaolin clay at (a) 25 °C, (b) 35 °C and (c) 45 °C.

Table (3.29): Freundlich isotherm parameters for Cd(II) adsorbed by FHA– kaolin clay.

T(^{o}C)	pH	Freundlich Isotherm		
		R^2	n	K_F
25	4.00	0.9846	3.299	0.46
	5.00	0.9817	3.511	0.54
	6.00	0.9964	2.298	1.05
35	4.00	0.9884	5.079	0.86
	5.00	0.9639	3.076	0.69
	6.00	0.9738	2.155	1.15
45	4.00	0.9889	4.475	0.99
	5.00	0.9685	1.654	0.66
	6.00	0.9918	3.167	1.98

Units for the parameters: n (gL^{-1}) and K_F ($L\ g^{-1}$).

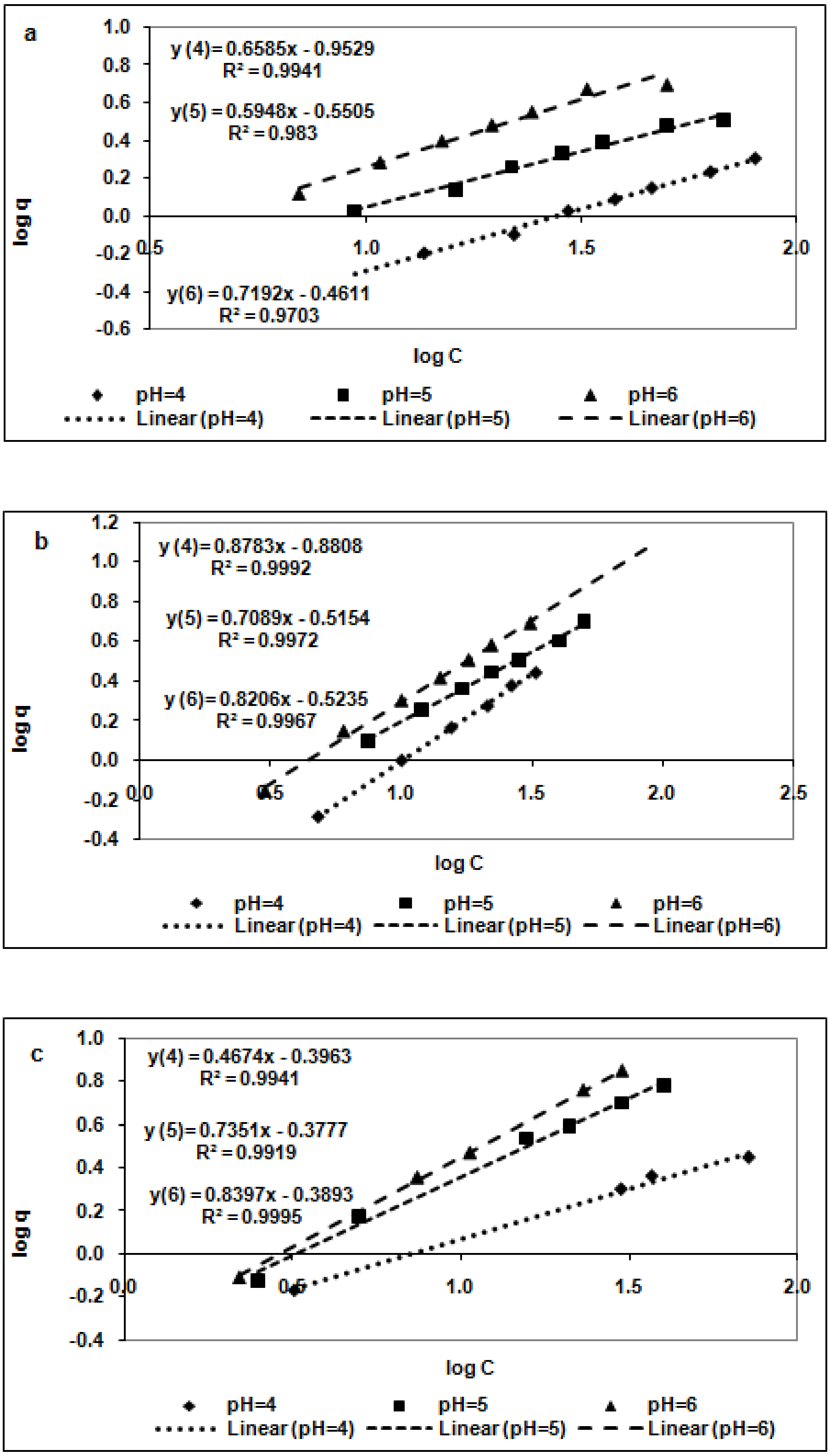


Figure (3.45): Plots of linearized Freundlich isotherms for Zn(II) adsorbed by FHA–kaolin clay at (a) 25 °C, (b) 35 °C and (c) 45 °C.

Table (3.30): Freundlich isotherm parameters for Zn(II) adsorbed by FHA– kaolin clay.

T(^{o}C)	**pH**	**Freundlich Isotherm**		
		R^2	**n**	**K_F**
25	**4.00**	**0.9941**	**1.519**	**0.11**
	5.00	**0.9830**	**1.681**	**0.28**
	6.00	**0.9703**	**1.390**	**0.35**
35	**4.00**	**0.9992**	**1.139**	**0.13**
	5.00	**0.9972**	**1.411**	**0.31**
	6.00	**0.9967**	**1.219**	**0.29**
45	**4.00**	**0.9941**	**2.139**	**0.40**
	5.00	**0.9919**	**1.360**	**0.42**
	6.00	**0.9995**	**1.191**	**0.41**

Units for the parameters: n (gL^{-1}) and K_F ($L\ g^{-1}$).

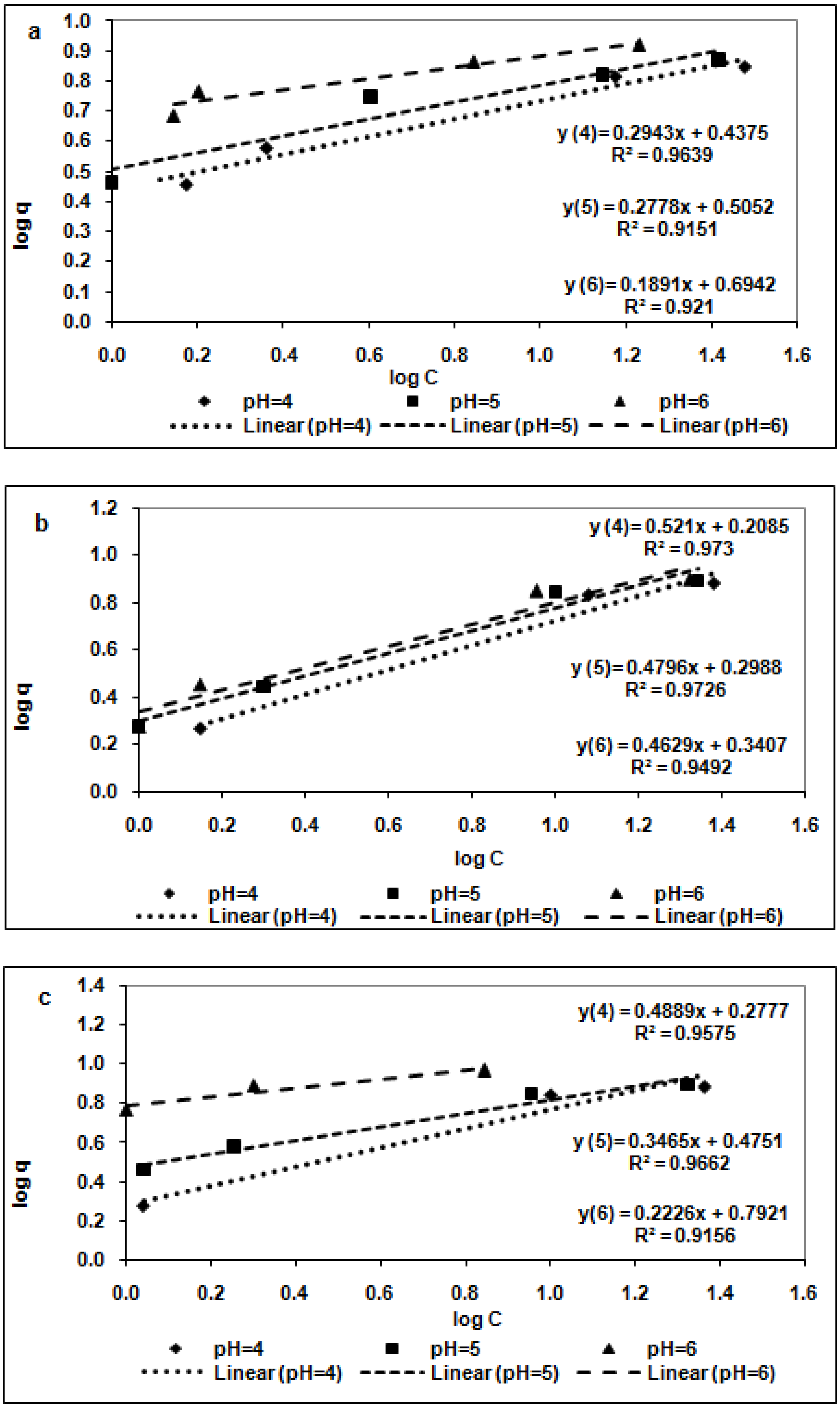


Figure (3.46): Plots of linearized Freundlich isotherms for Pb(II) adsorbed by KTD–kaolin clay at (a) 25 °C, (b) 35 °C and (c) 45 °C.

Table (3.31): Freundlich isotherm parameters for Pb(II) adsorbed by KTD– kaolin clay.

T(°C)	pH	Freundlich Isotherm		
		R^2	n	K_F
25	4.00	0.9639	3.398	2.74
	5.00	0.9151	3.599	3.20
	6.00	0.9210	5.287	4.94
35	4.00	0.9730	1.919	1.62
	5.00	0.9726	2.085	1.99
	6.00	0.9492	2.161	2.19
45	4.00	0.9575	2.045	1.89
	5.00	0.9662	2.886	2.99
	6.00	0.9156	4.492	6.19

Units for the parameters: n (gL^{-1}) and K_F ($L\ g^{-1}$).

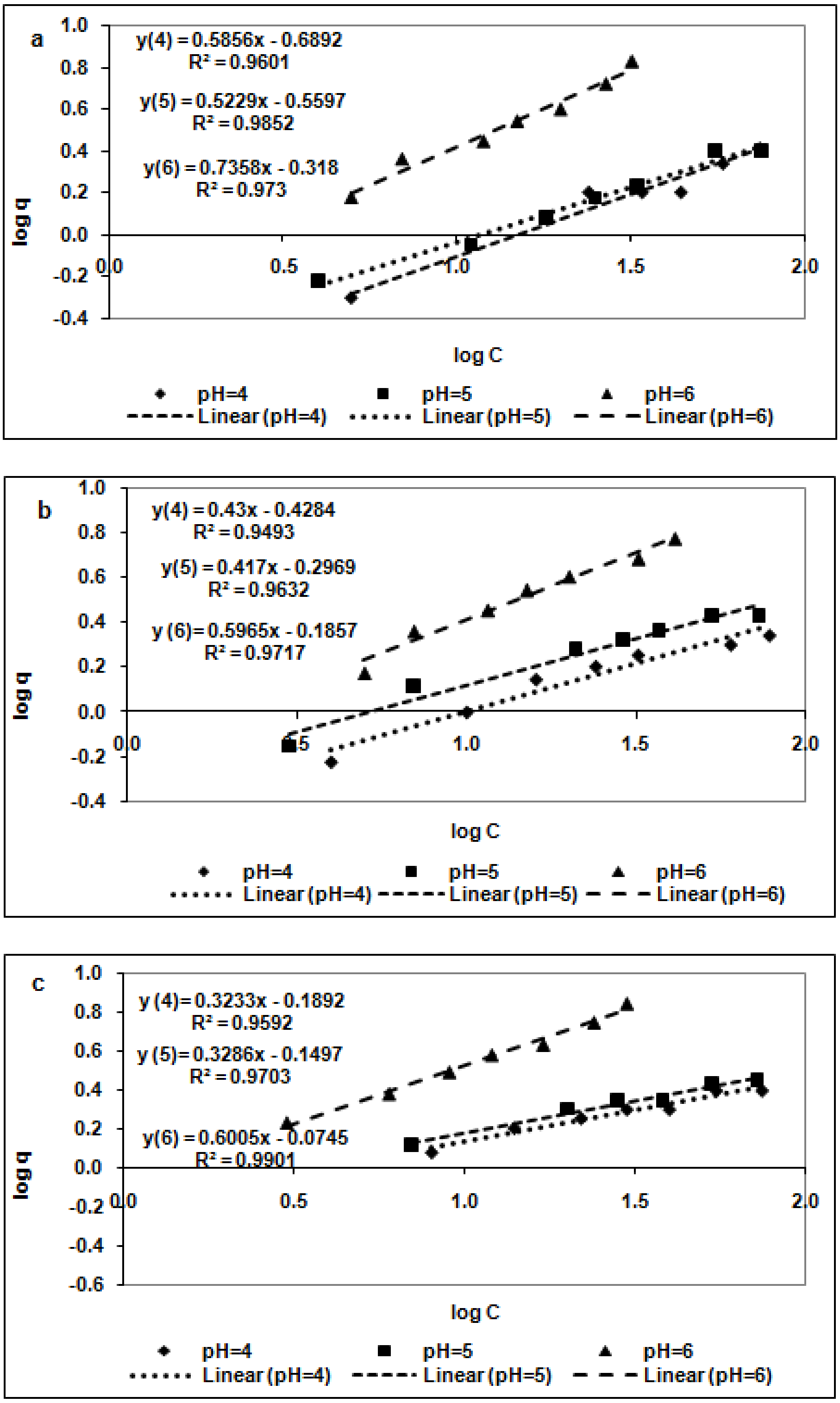


Figure (3.47): Plots of linearized Freundlich isotherms for Cd(II) adsorbed by KTD–kaolin clay at (a) 25 °C, (b) 35 °C and (c) 45 °C.

Table (3.32): Freundlich isotherm parameters for Cd(II) adsorbed by KTD– kaolin clay.

T(°C)	**pH**	**Freundlich Isotherm**		
		R^2	**n**	**K_F**
25	**4.00**	**0.9852**	**1.708**	**0.20**
	5.00	**0.9852**	**1.912**	**0.28**
	6.00	**0.973**	**1.359**	**0.48**
35	**4.00**	**0.9493**	**2.326**	**0.37**
	5.00	**0.9632**	**2.398**	**0.50**
	6.00	**0.9717**	**1.677**	**0.65**
45	**4.00**	**0.9592**	**3.090**	**0.65**
	5.00	**0.9703**	**3.040**	**0.71**
	6.00	**0.990**	**1.665**	**0.84**

Units for the parameters: n (gL^{-1}) and K_F ($L\ g^{-1}$).

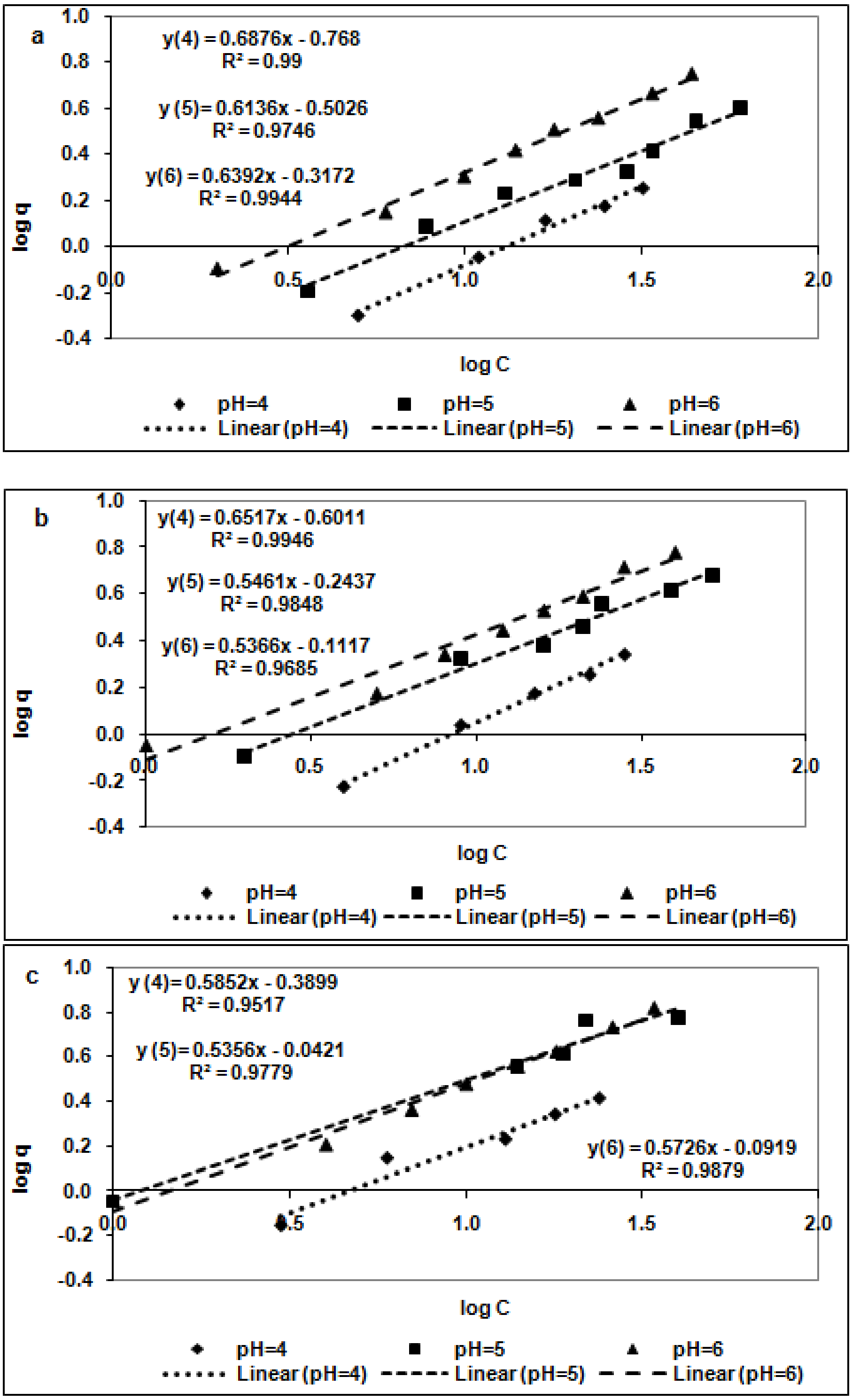


Figure (3.48): Plots of linearized Freundlich isotherms for Zn(II) adsorbed by KTD–kaolin clay at (a) 25 °C, (b) 35 °C and (c) 45 °C.

Table (3.33): Freundlich isotherm parameters for Zn(II) adsorbed by KTD– kaolin clay.

T(^oC)	pH	Freundlich Isotherm		
		R^2	n	K_F
25	4.00	0.9900	1.454	0.17
	5.00	0.9746	1.629	0.31
	6.00	0.9944	1.565	0.48
35	4.00	0.9946	1.534	0.25
	5.00	0.9848	1.831	0.57
	6.00	0.9685	1.864	0.77
45	4.00	0.9517	1.709	0.41
	5.00	0.9779	1.867	0.91
	6.00	0.9879	1.746	0.81

Units for the parameters: n (gL^{-1}) and K_F ($L\ g^{-1}$).

The adsorption of metal ions on modified kaolin clay fitted Freundlich model, the Freundlich isotherm plots (Figures (3.43) to (3.48)) had excellent linearity (R^2 >0.90). When the experimental values for the metal ions were fitted to the Freundlich model, the following observations were obtained:

There is an indication that some other adsorption sites were non–uniform and nonspecific in nature. It was in conformity with the existence of different types of possible adsorption sites on clay surface and humic acid with considerable difference in energy if the site was on an edge and surface or was located in a defect position. This agrees with the hypothesis of Freundlich model (Jiang, et al., 2010).

The adsorption coefficients (K_F, n) agreed well with the conditions supporting favorable adsorption.

From the Freundlich model, the better the adsorption the higher the K_F value. With reference to Tables (3.28) to (3.33), K_F values increase with increasing both temperature and pH for all metal ions.

These results agree with that obtained in Tables (3.15 – 3.20) of metal ions uptake with the same trend (Pb(II)> Cd(II) > Zn(II)). Similar explanation of this trend as in section (3.3.2.4.1.1).

The values of n represent the degree of favorability of adsorption. The value of n was greater than one, indicating that the adsorption was favorable (Unuabonah, et al., 2008; Kaya and Oren, 2005). The values of n which shown in Tables ((3.28) to (3.33)) for Pb(II) are (0.672–5.287), for Cd(II) are (1.359–5.079) and for Zn(II) are (1.191–2.139), which indicate that the adsorption is favorable.

Jiang et al., 2009, Modified kaolinite with aluminium sulphate to remove Pb(II) from aqueous solution. The results show that amount of Pb(II) adsorbed onto modified kaolinite is 20 mg/g under the optimized condition. In addition, the Freundlich model was used to describe equilibrium isotherm. The n value from Freundlich model was 3.56 g/L.

3.3.2.4.3. D–R adsorption isotherm model

The adsorption of metal ions on modified kaolin clay was analyzed using the D–R model, the D–R isotherm plots are shown in Figures (3.49) to (3.54) and Tables (3.34–3.36).

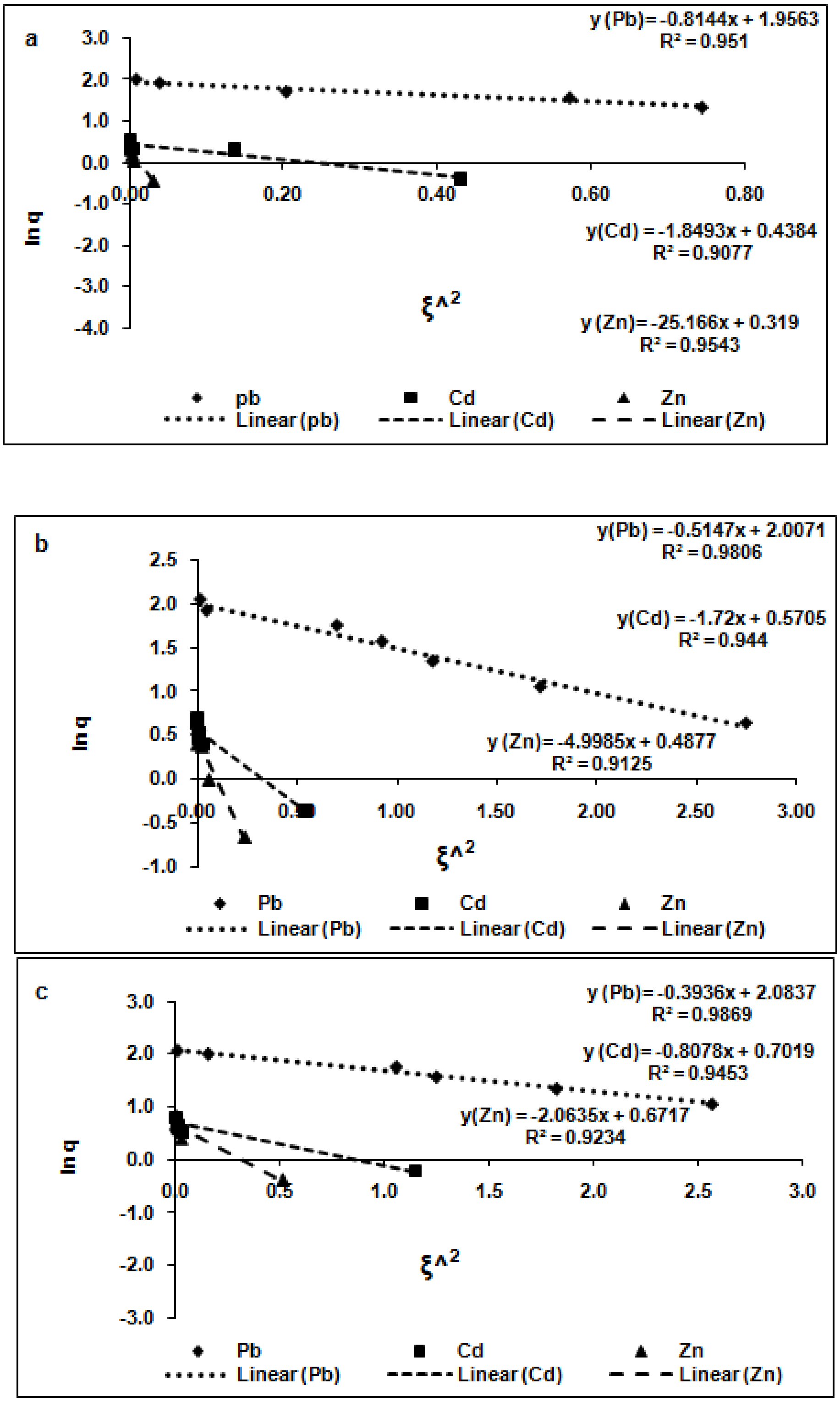


Figure (3.49): Plots of D–R isotherms for all metal ions by FHA– kaolin clay at pH=4, (a) 25 °C, (b) 35 °C and (c) 45 °C.

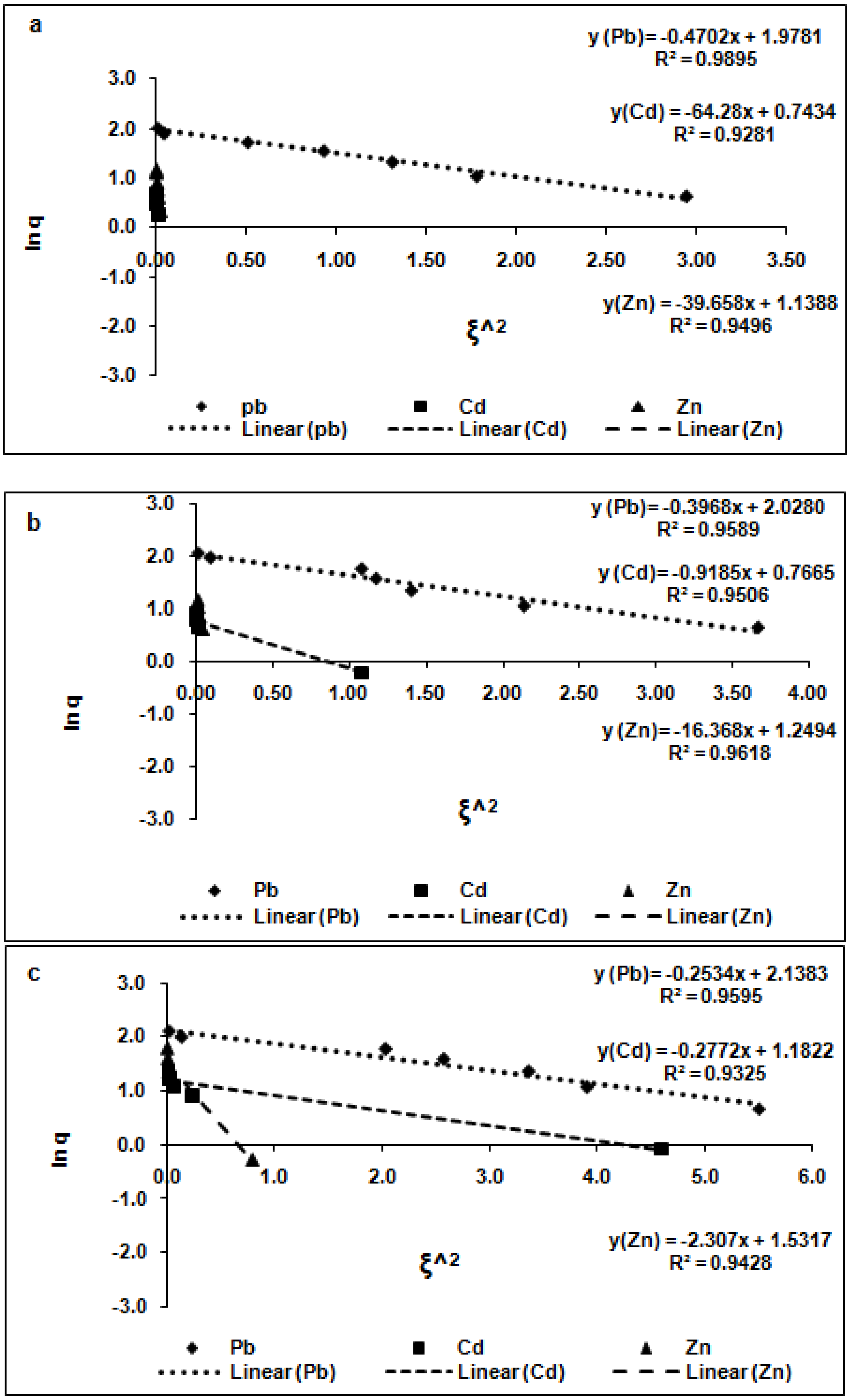


Figure (3.50): Plots of D–R isotherms for all metal ions by FHA– kaolin clay at pH=5, (a) 25 °C, (b) 35 °C and (c) 45 °C.

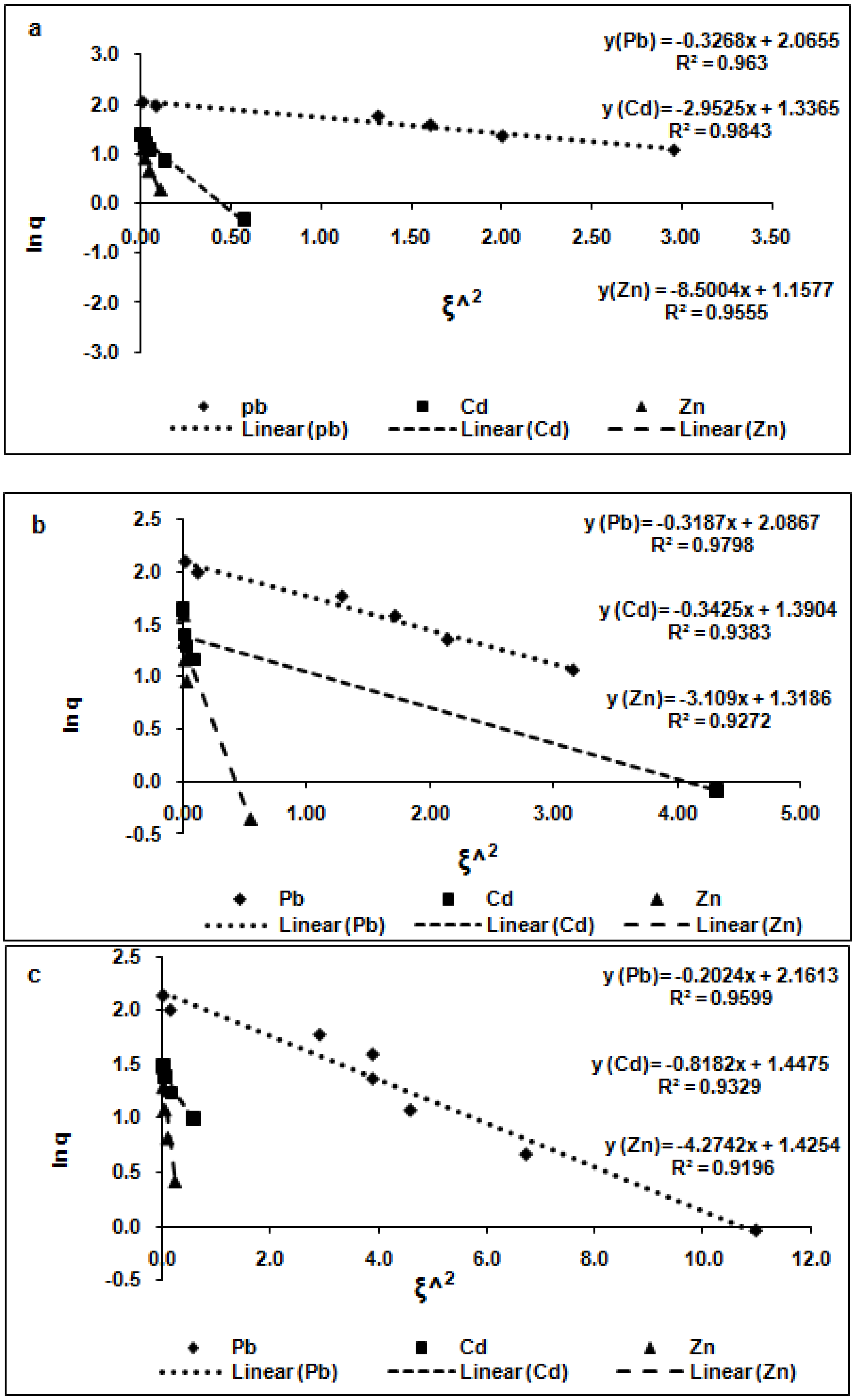


Figure (3.51): Plots of D–R isotherms for all metal ions by FHA– kaolin clay at pH=6, (a) 25 °C, (b) 35 °C and (c) 45 °C.

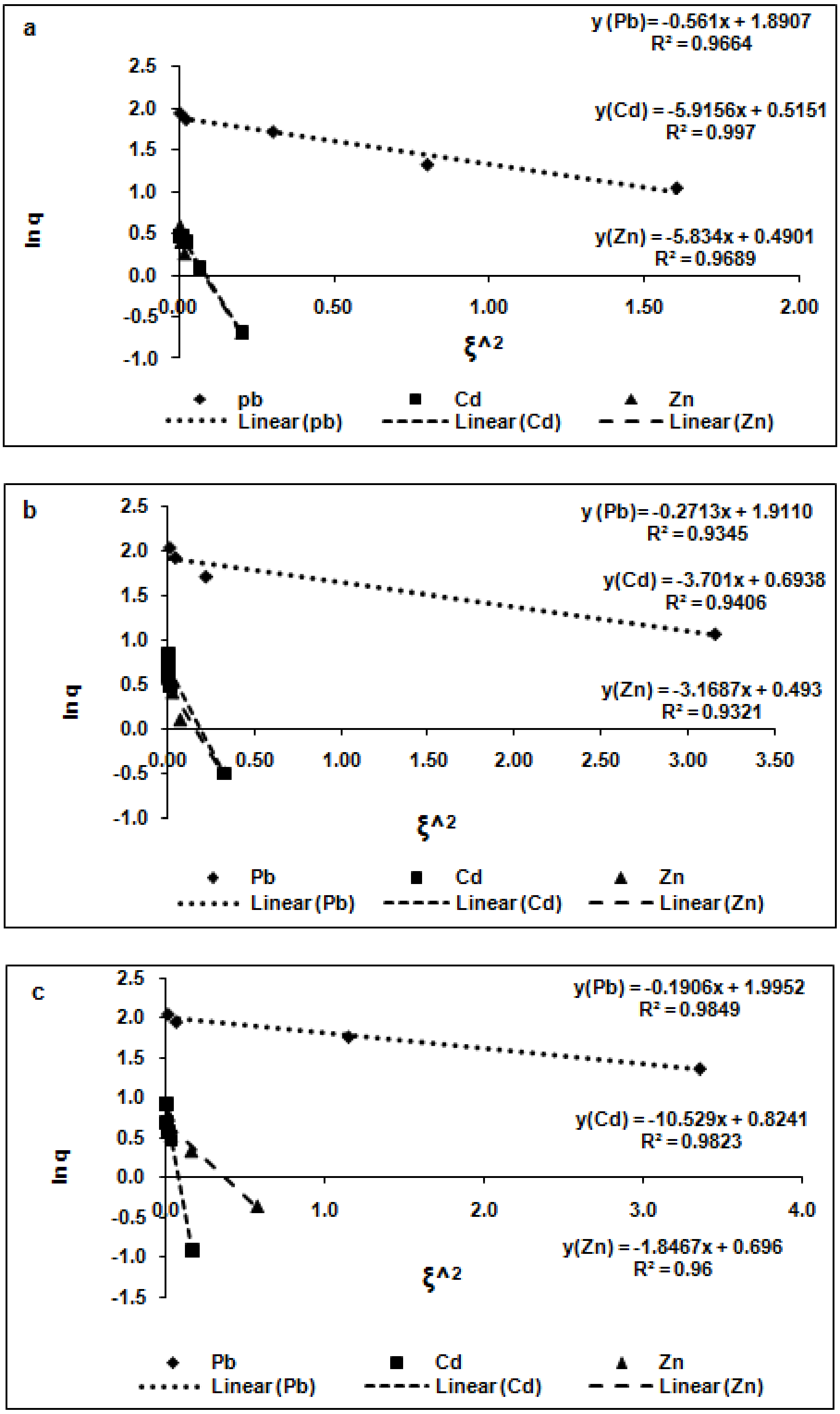


Figure (3.52): Plots of D–R isotherms for all metal ions by KTD– kaolin clay at pH=4, (a) 25 °C, (b) 35 °C and (c) 45 °C.

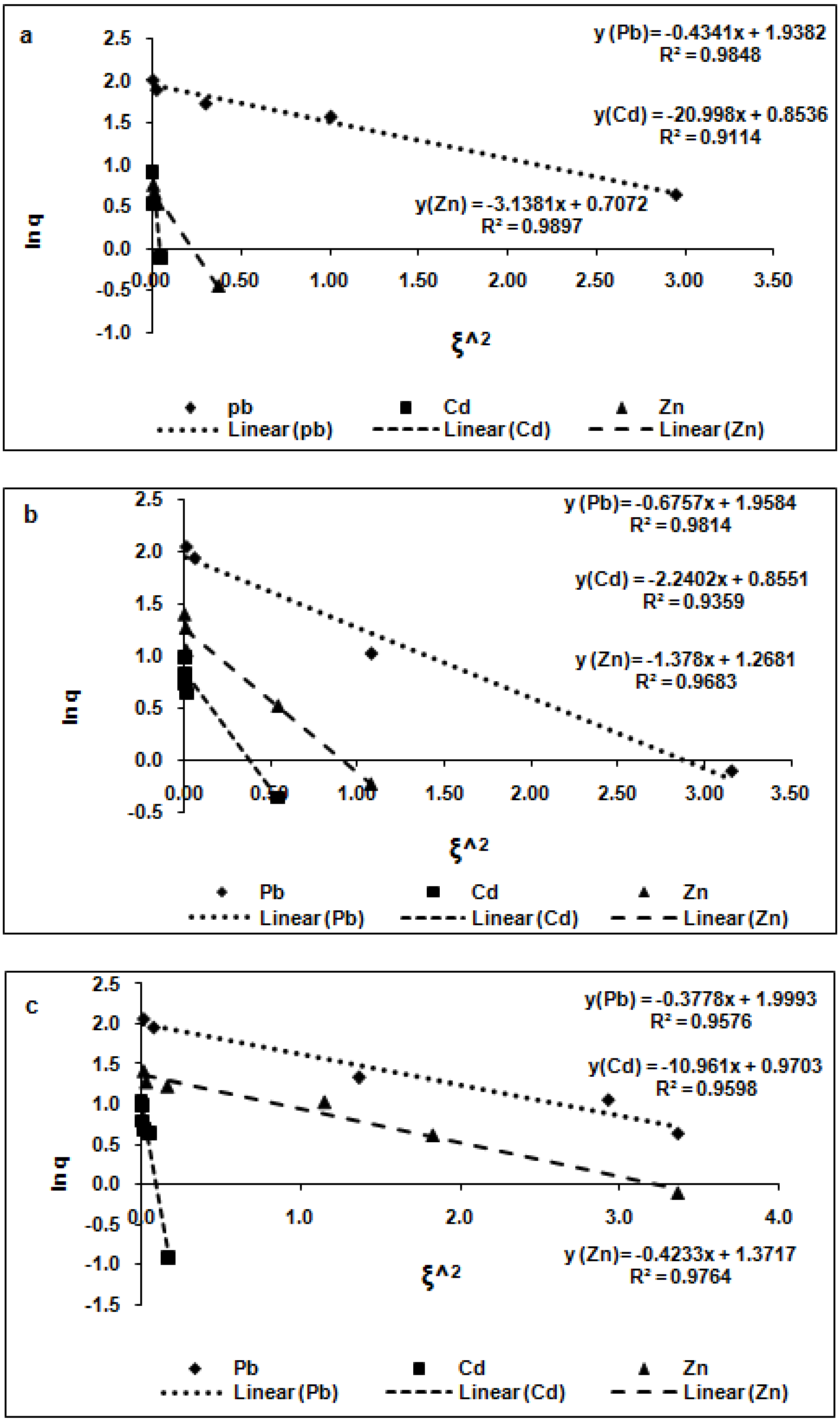


Figure (3.53): Plots of D–R isotherms for all metal ions by KTD– kaolin clay at pH=5, (a) 25 °C, (b) 35 °C and (c) 45 °C.

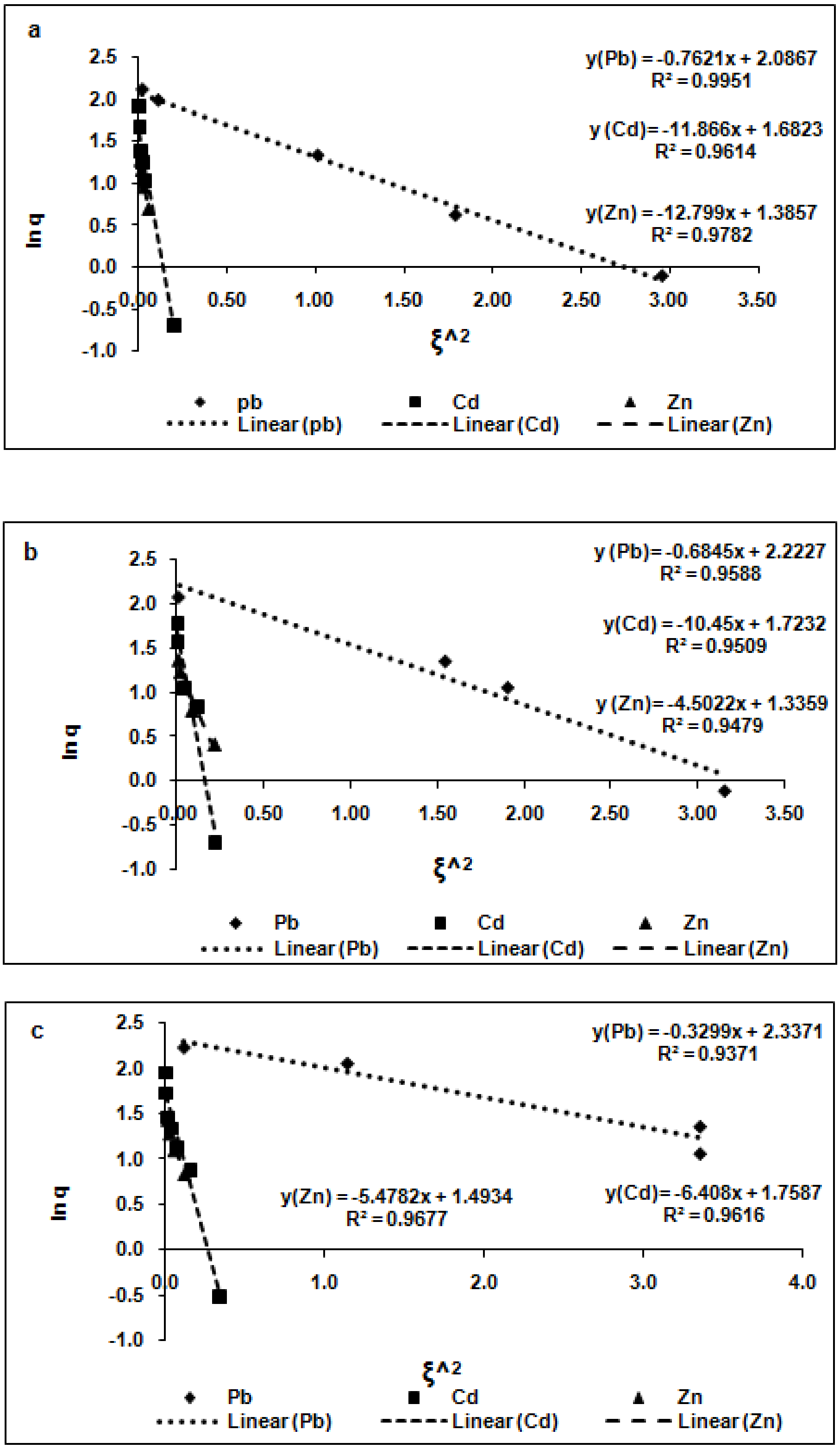


Figure (3.54): Plots of D–R isotherms for all metal ions by KTD– kaolin clay at pH=6, (a) 25 °C, (b) 35 °C and (c) 45 °C.

Table (3.34): D–R isotherm parameters for Pb(II) adsorbed by both modified kaolin clay.

D – R Isotherm Constants									
T(°C)	pH	FHA-kaolinite				KTD-kaolinite			
		R^2	β	E	q_m	R^2	β	E	q_m
25	4.00	0.9510	0.814	0.784	7.07	0.9664	0.561	0.944	6.62
	5.00	0.9895	0.470	1.031	7.23	0.9848	0.434	1.073	6.95
	6.00	0.9630	0.327	1.237	7.89	0.9951	0.762	0.820	8.06
35	4.00	0.9806	0.515	0.986	7.44	0.9345	0.271	1.358	6.78
	5.00	0.9589	0.397	1.123	7.60	0.9814	0.676	0.860	7.09
	6.00	0.9798	0.319	1.253	8.06	0.9588	0.685	0.855	9.23
45	4.00	0.9914	0.394	1.127	8.03	0.9849	0.191	1.619	7.35
	5.00	0.9595	0.253	1.405	8.49	0.9576	0.378	1.150	7.38
	6.00	0.9599	0.202	1.572	8.68	0.9371	0.240	1.443	9.86

Units for the parameters: β (mol^2kJ^{-2}), E ($kJmol^{-1}$) and q_m (mgg^{-1}).

Table (3.35): D–R isotherm parameters for Cd(II) adsorbed by both modified kaolin clay.

D – R Isotherm Constants									
T(°C)	pH	FHA-kaolinite				KTD-kaolinite			
		R^2	β	E	q_m	R^2	β	E	q_m
25	4.00	0.9077	1.849	0.520	1.55	0.9970	5.916	0.291	1.67
	5.00	0.9281	64.280	0.088	2.10	0.9114	20.998	0.154	2.34
	6.00	0.9843	2.953	0.412	3.81	0.9614	11.866	0.205	5.38
35	4.00	0.9440	1.720	0.539	1.77	0.9406	3.701	0.368	2.00
	5.00	0.9506	0.919	0.738	2.15	0.9359	2.240	0.472	2.35
	6.00	0.9383	0.343	1.208	4.02	0.9509	10.450	0.219	5.60
45	4.00	0.9453	0.808	0.787	2.02	0.9823	10.529	0.218	2.28
	5.00	0.9325	0.277	1.343	3.26	0.9598	10.961	0.214	2.64
	6.00	0.9329	0.818	0.782	4.25	0.9616	6.408	0.279	5.80

Units for the parameters: β (mol^2kJ^{-2}), E ($kJmol^{-1}$) and q_m (mgg^{-1}).

Table (3.36): D–R isotherm parameters for Zn(II) adsorbed by both modified kaolin clay.

D – R Isotherm Constants									
T(°C)	pH	FHA-kaolinite				KTD-kaolinite			
		R^2	β	E	q_m	R^2	β	E	q_m
25	4.00	0.9543	25.166	0.141	1.38	0.9689	5.834	0.293	0.61
	5.00	0.9496	39.658	0.112	3.12	0.9897	3.138	0.399	2.03
	6.00	0.9555	8.500	0.243	3.18	0.9568	1.125	0.667	2.47
35	4.00	0.9125	4.999	0.316	1.63	0.9321	3.169	0.397	1.64
	5.00	0.9618	16.368	0.175	3.49	0.9683	1.378	0.602	3.55
	6.00	0.9272	3.109	0.401	3.74	0.9923	0.496	1.004	4.42
45	4.00	0.9234	2. 064	0.492	1.96	0.9600	1.847	0.520	2.01
	5.00	0.9428	2.307	0.466	4.63	0.9764	0.423	1.087	3.94
	6.00	0.9196	4.274	0.342	4.16	0.9106	5.478	0.302	4.45

Units for the parameters: β (mol^2kJ^{-2}), E ($kJmol^{-1}$) and q_m (mgg^{-1}).

The R^2 values shown in Figures (3.49 to 3.54) and Tables (3.34 to 3.36) are greater than 0.90, indicating that D–R model can describe the adsorption data very well, which means that the adsorption on both homogeneous and heterogeneous surfaces. If we notice the trend of q_m values for all metal ions and both modified kaolin clay vs. temperature and pH, we will see that as temperature and pH increases q_m values will increase. Similar trend was obtained by Langmuir parameter (q_m), and Freundlich parameter (K_F). (Notice that there are no significant differences between q_m values obtained from Langmuir and D–R models).

These results agree with that obtained in Tables (3.15 – 3.20) of metal ions uptake with same trend (Pb(II)> Cd(II) > Zn(II)). The explanation of this trend is in section (3.3.2.4.1.1).

The magnitude of E from D–R isotherm can give a good idea about the overall mechanism of the adsorption. If E is in the range of 8 – 16 kJ/mol, the adsorption is governed by chemical ion exchange, but in the case of E < 8 kJ/mol, physical forces may affect the adsorption. On the other hand, adsorption may be dominant by particle diffusion if E > 16 kJ/mol (Donat et al., 2005; Xu et al., 2007). As illustrated in Tables (3.34) to (3.36), the values of E for Pb(II) are (0.784–1.619), for Cd(II) are (0.088–0.154) and for Zn(II) are (0.112–1.087). All values are less than 8.00 kJ/mol, this indicates that physical forces affect the adsorption.

The obtained adsorption data showed fitting very well for Langmuir more than other adsorption isotherm models.

3.3.2.5. Adsorption thermodynamics

3.3.2.5.1. Effect of temperature

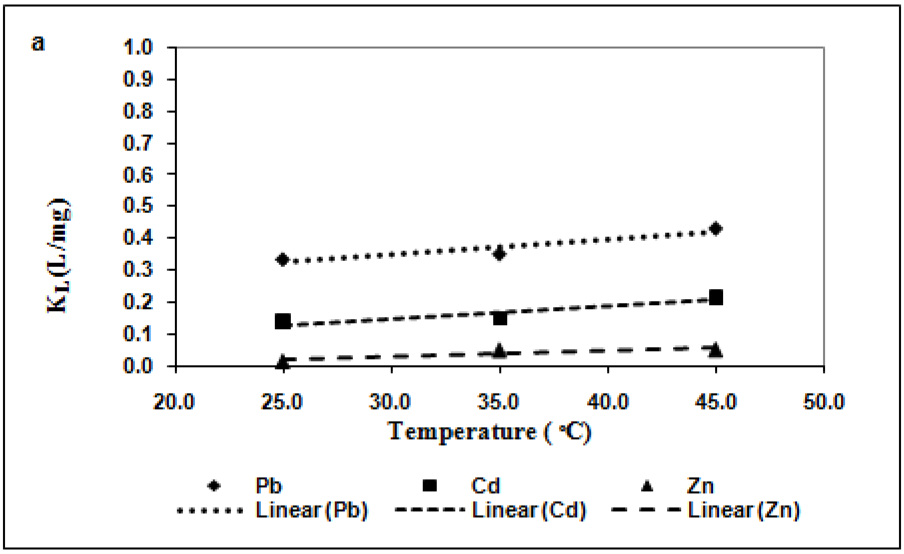
The effect of temperature on adsorption is important not only because it affects the rate and extent of adsorption but also due to the fact that temperature dependence of adsorption provides information about possible adsorbate–adsorbent interaction.

The metal ions adsorption isotherms onto both modified kaolin clay were conducted at temperatures of 25, 35 and 45 °C, and the adsorption capacity of modified kaolin clay for the metal ion was determined. The results of the studies on the influence of temperature on metal ions adsorption are presented in Tables (3.15–3.20) in terms of the amount of metal ions removed versus temperature. The results indicate that the adsorption removal increased with increase of the solution temperature. This shows that the adsorption process is an endothermic one.

It is possible that increasing temperature could have increased the driving force of the metal ions towards the active sites on kaolinite. (Ho and McKay, 1999 a; Ho and McKay, 1999 b).

Figure (3.55) presents the plots of the K_L–Langmuir parameter against temperature for heavy metal ions adsorption on both modified kaolin clay.

The K_L parameter is the adsorption equilibrium constant which gives information on both adsorption rate, compared to desorption rate of the system, and the heat of adsorption. For exothermic reactions, K_L should decrease with increasing temperature of the system (Faust and Aly, 1987). An opposite trend depicts endothermic reactions. Figure (3.55) implies that adsorption of most heavy metal ions onto kaolin clay is an endothermic process. Endothermic adsorption was also supported by previous studies, such as Orumwense (1996), Marzal et al., (1996) and (Singh and Tiwari, 1997).



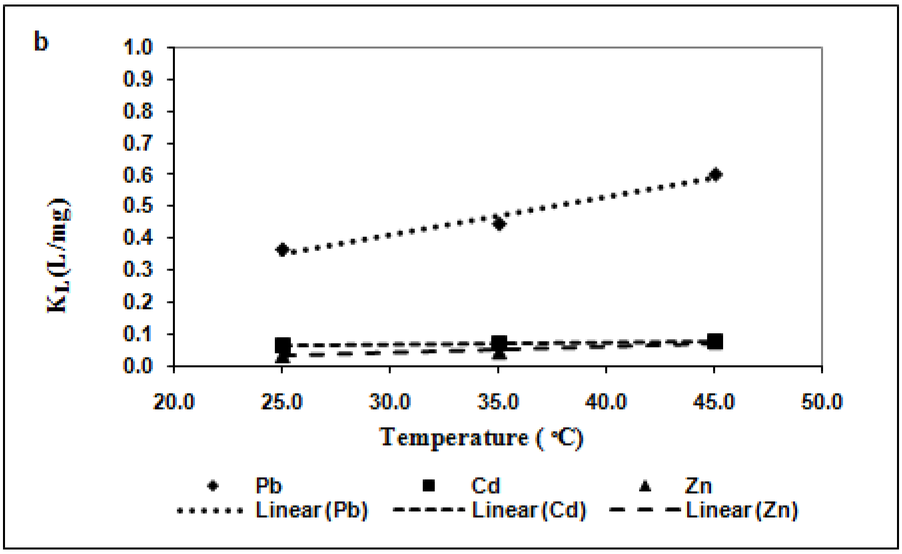


Figure (3.55): Langmuir parameters of Pb(II), Cd(II) and Zn(II) on (a) FHA– kaolin clay and (b) KTD– kaolin clay.

In order to understand the thermodynamics of adsorption process, thermodynamic functions for the system, including changes in Gibbs free energy (ΔG), enthalpy of adsorption (ΔH) and entropy of adsorption (ΔS), were calculated from Figures (3.56) to (3.61), for metal ion concentrations of 10, 20, 30, 40, 50, 60, 80 and 100 ppm with an adsorbent amount of 0.2 g ± 0.1mg and temperature range of 298.15 to 318.15 K at pH= 4.00, 5.00 and 6.00. These values are shown in Table (3.37).

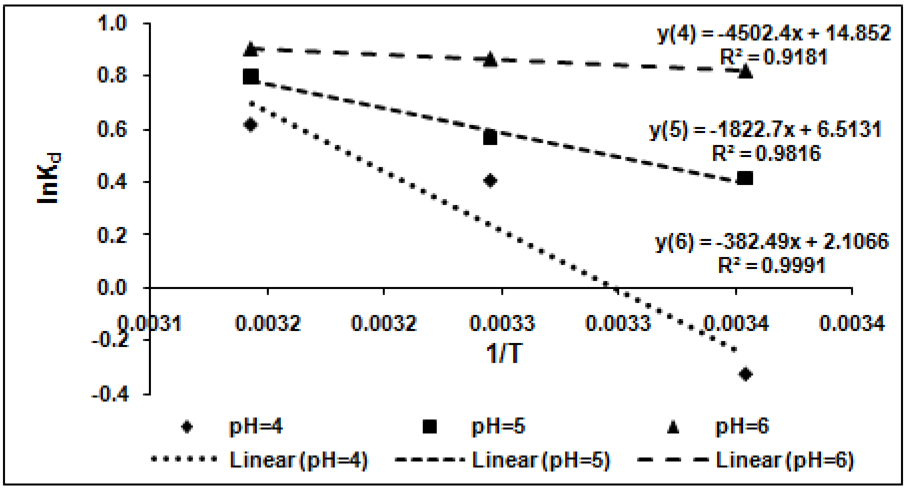


Figure (3.56): Thermodynamic plots of ln K_d against 1/T (K) for the adsorption of Pb(II) onto FHA– kaolin clay.

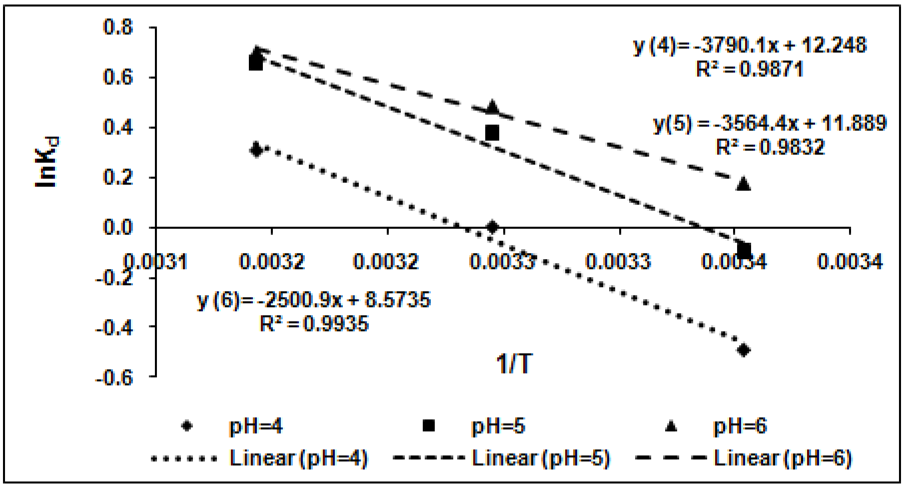


Figure (3.57): Thermodynamic plots of ln K_d against 1/T (K) for the adsorption of Cd(II) onto FHA– kaolin clay.

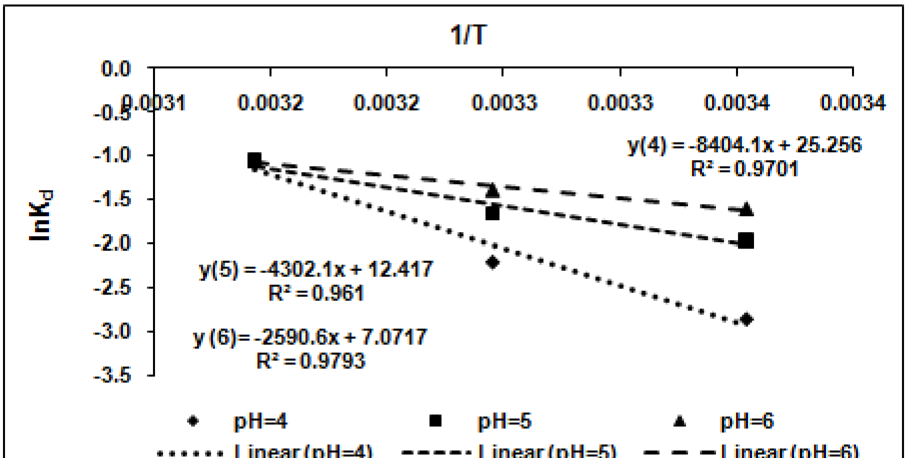


Figure (3.58): Thermodynamic plots of ln K_d against 1/T (K) for the adsorption of Zn(II) onto FHA– kaolin clay.

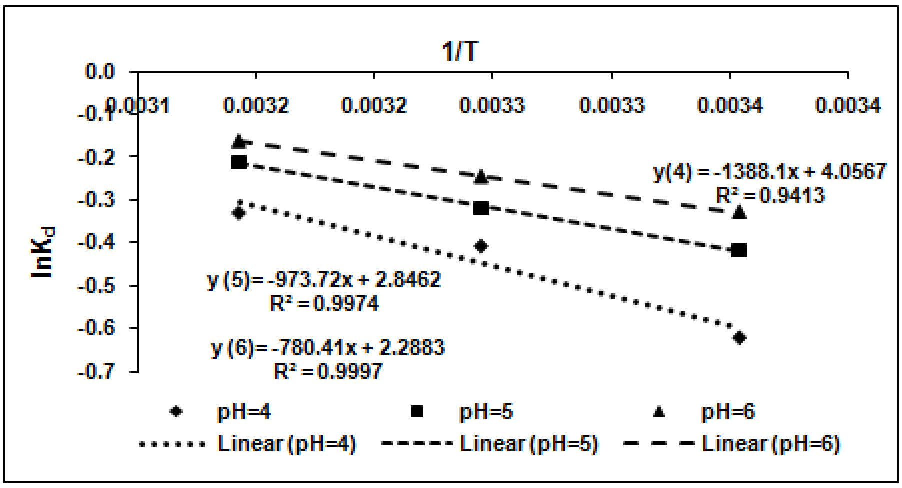


Figure (3.59): Thermodynamic plots of ln K_d against 1/T (K) for the adsorption of Pb(II) onto KTD– kaolin clay.

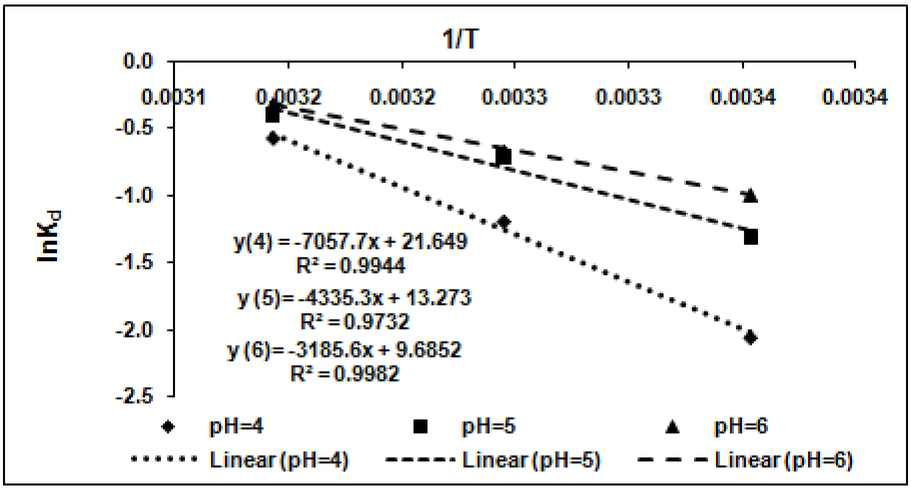


Figure (3.60): Thermodynamic plots of ln K_d against 1/T for the adsorption of Cd(II) onto KTD– kaolin clay.

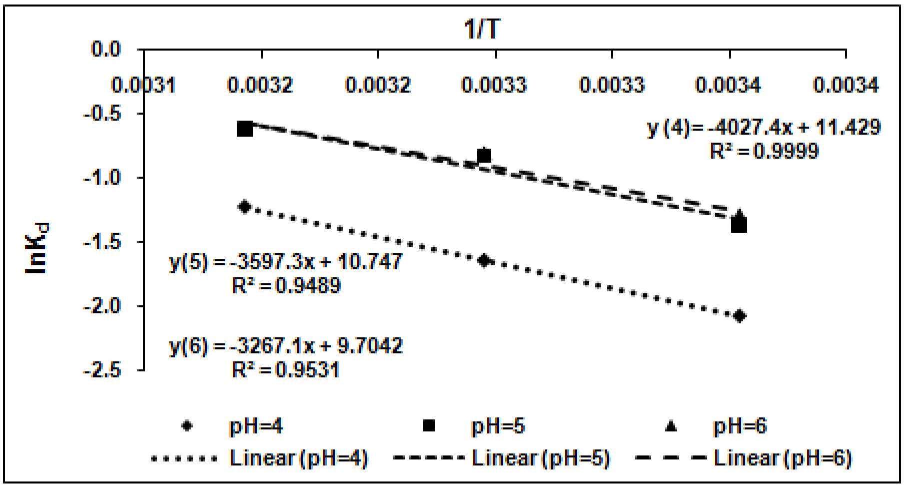


Figure (3.61): Thermodynamic plots of ln K_d against 1/T for the adsorption of Zn(II) onto KTD– kaolin clay.

Table (3.37): Thermodynamic functions for metal ions adsorbed by both modified kaolin clay. The ΔG values are at 25 °C.

Metal ion	**pH**	**FHA-kaolinite**			**KTD-kaolinite**		
		ΔG (kJ/mol)	**ΔH (kJ/mol)**	**ΔS (J/mol.K)**	**ΔG (kJ/mol)**	**ΔH (kJ/mol)**	**ΔS (J/mol.K)**
Pb	**4.00**	**0.8153**	**37.4352**	**123.5**	**1.5355**	**11.5414**	**33.7**
	5.00	**-1.0270**	**15.1548**	**54.2**	**1.0330**	**8.0960**	**23.7**
	6.00	**-2.0404**	**3.1802**	**17.5**	**0.8141**	**6.4887**	**19.0**
Cd	**4.00**	**1.2142**	**31.5128**	**101.8**	**5.0912**	**58.6812**	**180.0**
	5.00	**0.2313**	**29.6362**	**98.9**	**3.2476**	**36.0459**	**110.4**
	6.00	**-0.4301**	**20.7937**	**71.3**	**2.4572**	**26.4867**	**80.5**
Zn	**4.00**	**7.0519**	**69.8759**	**210.0**	**5.1485**	**33.4858**	**95.0**
	5.00	**4.8615**	**35.7698**	**103.2**	**3.3904**	**29.9098**	**89.4**
	6.00	**3.9540**	**21.5395**	**58.8**	**3.2139**	**27.1643**	**80.7**

Spontaneity of the adsorption process is established by decrease in Gibbs free energy values, ΔG. They were found to be small and negative indicating that the adsorption of metal ions onto both modified kaolin clay was spontaneous and favorable (Table 3.37). The decrease was more at higher pH such that the interactions were favored by an increase in pH in agreement with the nature of metal ion adsorption on the clays (as found in metal ions uptake, Tables (3.15 to 3.20), Langmuir parameter (q_m), Tables (3.22 to 3.27), Freundlich constant (K_F), Tables (3.28 to 3.33) and (q_m) values of D–R model, Tables (3.34 to 3.36)). This is because the deprotonation of humic acid functional groups increases the negative charge on the clay surface.

The decrease of ΔG values of Pb(II)> Cd(II)> Zn(II), and the trend of selectivity sequence of metal ions toward modified kaolin clay, agrees with those found, previously from the three models, sections number 3.3.2.4.1, 3.3.2.4.2 and 3.3.2.4.3.

The ΔG values obtained were small and positive which suggests that the adsorption of metal ions onto both modified kaolin clay samples require some small amount of energy to convert reactants into products (Scheckel and Donald, 2001). This is agreeing with values of n which represent to the degree of favorability of adsorption, the values of n were less than one for Pb(II) adsorbed by FHA– kaolin clay, as shown in Table (3.28).

And this is further supported by the positive ΔH values obtained for the adsorption of Pb(II) and Cd(II) at low pH, and Zn(II) at all pH values onto both adsorbents (Table 3.37).

It can be noticed that FHA– kaolin clay is better for adsorption of heavy metal ions than KTD– kaolin clay. This is supported by results obtained by elemental analysis where % of oxygen in KTD is less than FHA, Table (3.3), EDS analysis, Tables (3.8 and 3.9), surface area and porosity measurements, Table(3.11).

As shown in Table (3.37) all ΔH values are positive, this mean that as temperature increase, the adsorption capacity was increased. This result agrees with results obtained in metal ions uptake, Tables (3.15 to 3.20), Langmuir parameter (q_m), Tables (3.22 to 3.27), Freundlich constant (K_F), (3.28 to 3.33) and (q_m) values of D–R model, Tables (3.34 to 3.36). This suggests that the adsorption of Pb(II), Cd(II) and Zn(II) onto both modified kaolin clay adsorbent is endothermic in nature.

One possible explanation of the endothermic enthalpy of adsorption is the well–known fact that heavy metal ions used are well solvated in water. The endothermic enthalpy gives indication of interaction between adsorbate and adsorbent. This can be

explained by the fact that each ion of adsorbate has to release more than one molecule of water. This dehydration process of ions requires energy. We assume that this energy of dehydration exceeds the exothermic energy of the ions adsorb on the surface (Alkaram, et al., 2009).

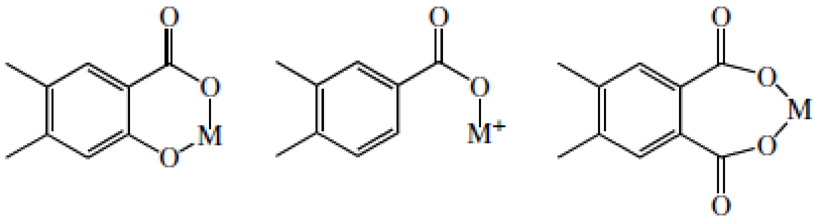
The endothermic interactions between kaolin clay and metal ions were accompanied by small positive values of entropy, which was the driving force for adsorption. The positive values of ΔS signify an increased state of randomness at the solid–solution interface following adsorption. Also positive entropy of adsorption reflects the affinity of adsorbent for metal ions used. The adsorbed water molecules, which are displaced by the adsorbate species, gain more translational energy than is lost by the adsorbate ions, thus allowing the prevalence of randomness in the system (Donat, et al., 2005).

The entropy changes were most likely to be due to structural changes and adjustments in the adsorbate as well as the adsorbent. The structural changes arise from the release of ions like H^+ and K^+ from the clay surface into the solution and also from partial solvation of the metal ions in water. The adsorptions of Pb(II), Cd(II) and Zn(II) on both modified kaolin clay were associated with entropy decrease in conformity with the general situation of ions existing in a more chaotic random distribution in aqueous solution compared to their adsorbed and immobilized states (Bhattacharyya and Gupta, 2006).

3.4. Comparison between modified and unmodified kaolin clay

From Tables (3.12), (3.15–3.20), it was observed that modification of kaolin clay enhanced adsorption of the metal ions. Also Figure (3.62) support this observation.

Two factors may be responsible for the greater enhancement of adsorption of metal ions. Firstly, HA–coated kaolin clay has a greater density of adsorption sites e.g. carboxyl and phenolic hydroxyl sites. Secondly, the adsorbed HA fractions could profoundly alter the surface charge, and contribute to the electrostatic attraction between kaolin clay and metal ions, because of their negative charge.



Scheme (3.2): Formation of metal–humic substance complexes in river (natural) water (Katsumata et al., 2003).

As shown in Table (3.11) which summarizes the total porosity of the clays; we notice that both modified kaolin clay have large numbers of large pores diameter, and form relatively open structure when it bonds with kaolin clay. This is shown in the SEM of humic acid and both modified kaolin clay, Figures (3.6) to (3.8). So the humic acid affect the pore size in clay and the modified structure of kaolin clay is more suitable to adsorb metal ions especially in the hydrated form.

Because the enhancement of HA loaded on kaolin clay would lead to an increase in metal complexation abilities in the aqueous phase and formed stable metal ions–HA complexes and diminish the precipitation of the metal itself.

For example, our results show that the percentage (%) uptake of 100 ppm of Cd(II) adsorbed by unmodified kaolin clay at pH 4.00 and 35 °C is 1%, while 20% by FHA– kaolin clay and 22% by KTD– kaolin clay, under the same conditions.

A similar observation was obtained by Christl and Kretzschmar (2001), who found that below pH 6, adsorption of Cu(II) to the solid phase increased by up to 40% compared with the pure hematite.

Some experimental results (Taylor and Theng, 1995) demonstrated that the adsorption of heavy metal ions onto minerals increased with an increase in the HA concentration and solution pH. Plavsic and Cosovic (1999) found that the interaction of copper ions with alumina particles was enhanced in the presence of HA.

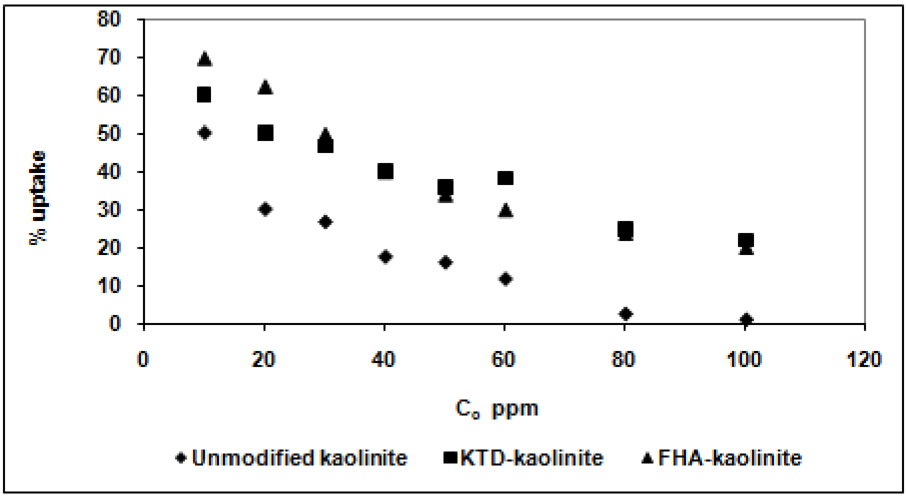


Figure (3.62): Comparison between unmodified and modified kaolin clay adsorption of Cd(II) at pH= 4 and 35 °C.

3.5. Column techniques

3.5.1. Adsorption studies

The adsorption of metal ions by unmodified and modified kaolin clay using column experiments for Pb(II), Cd(II) and Zn(II) were determined at pH 4.00 and 25 °C, initial concentration of 1000 ppm and a flow rate of 1 mL/min. The percent of uptake for metal ions are represented in Figures (3.63 and 3.65) and Tables (3.38 to 3.40).

Table (3.38): Loaded concentration of Cd(II) ion adsorbed by unmodified kaolin clay by column technique.

10 mL of 1000 ppm (Initial conc.) of Cd(II)	**Loaded Conc. (ppm) of Cd(II)**
1st	**201**
2nd	**7**
3rd	**6**
4th	**4**
5th	**3**
6th	**3**
7th	**2**
8th	**2**
9th	**1**
10th	**1**
Cumulative load (mg Cd(II)/2g clay)	**23**

Table (3.39): Loaded concentration of metal ions adsorbed by FHA– kaolin clay by column technique.

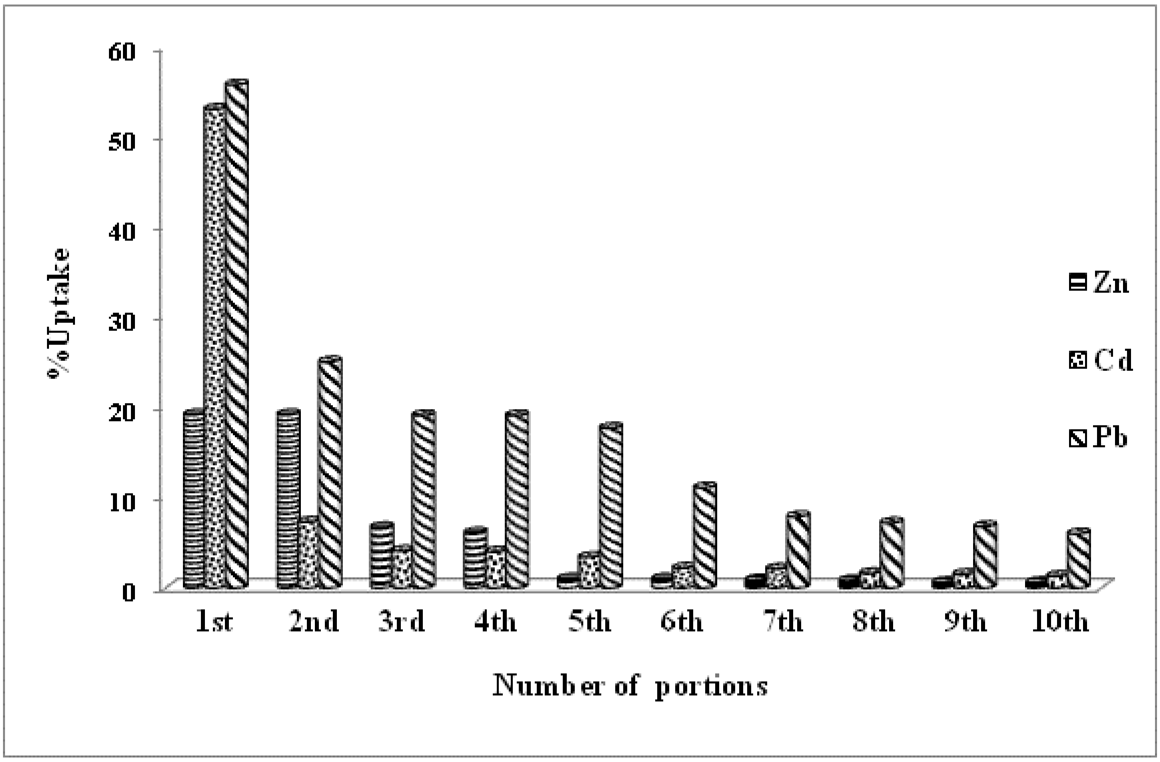
Metal Ions			
10 mL of 1000 ppm (initial conc.) of metal ions(II)	Loaded Conc. (ppm)		
	Zn(II)	Cd(II)	Pb(II)
1st	192	530	557
2nd	192	73	250
3rd	67	41	191
4th	61	40	191
5th	10	34	177
6th	10	22	111
7th	9	21	79
8th	8	16	72
9th	6	15	68
10th	6	13	60
Cumulative load (mg metal ion(II)/2g clay)	56.1	80.5	175.6

Table (3.40): Loaded concentration of metal ions adsorbed by KTD– kaolin clay by column technique.

Metal Ions			
10 mL of 1000 ppm (initial conc.) of metal ions(II)	Loaded Conc. (ppm)		
	Zn(II)	Cd(II)	Pb(II)
1st	58	285	600
2nd	54	10	117
3rd	51	9	104
4th	10	9	99
5th	8	8	95
6th	7	8	77
7th	6	7	47
8th	4	6	38
9th	3	6	34
10th	3	5	8
Cumulative load (mg metal ion(II)/2g clay)	20.4	35.3	121.9

The metal ions showed higher affinity for the modified kaolin clay and displayed a higher adsorption capacity than unmodified clay of the metal ions. The adsorption of the metal ions by both modified kaolin clay followed the order: Pb>Cd>Zn.

This is the same order of the metal ions in the batch experiments, (explained previously in section (3.3.2.4.1.1)).



Figure(3.63): %Uptake of metal ions by FHA– kaolin clay by column technique.

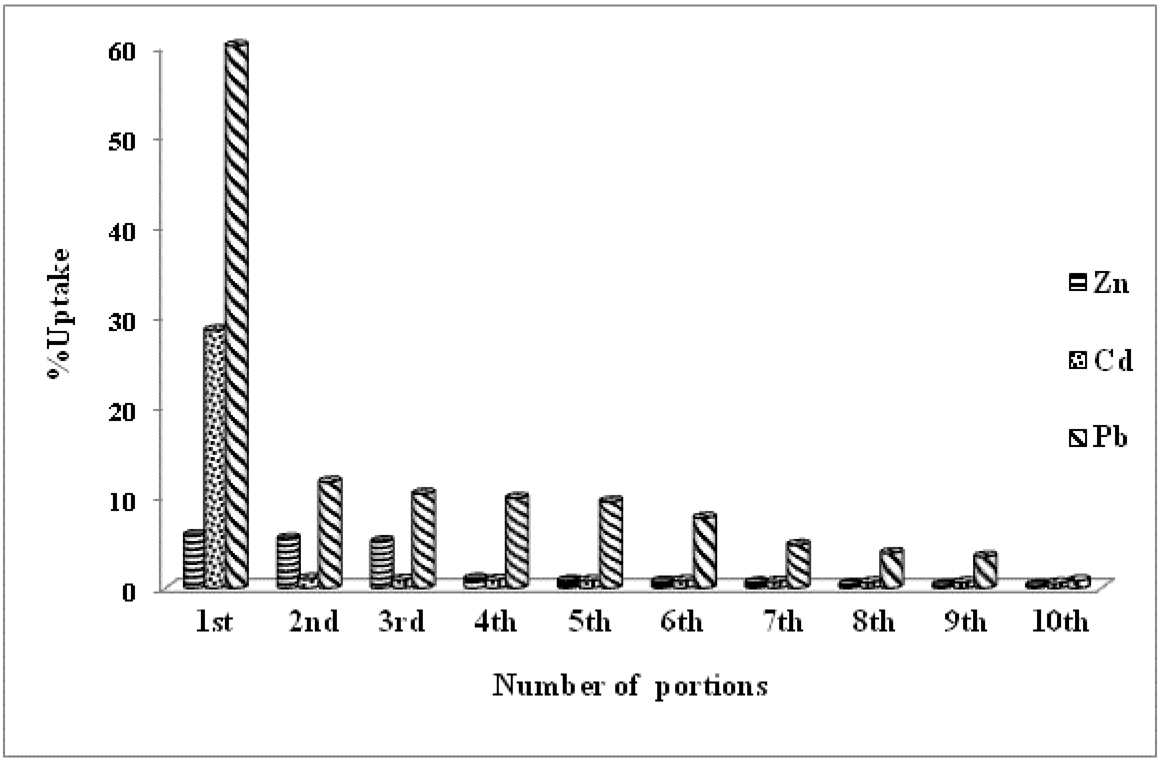
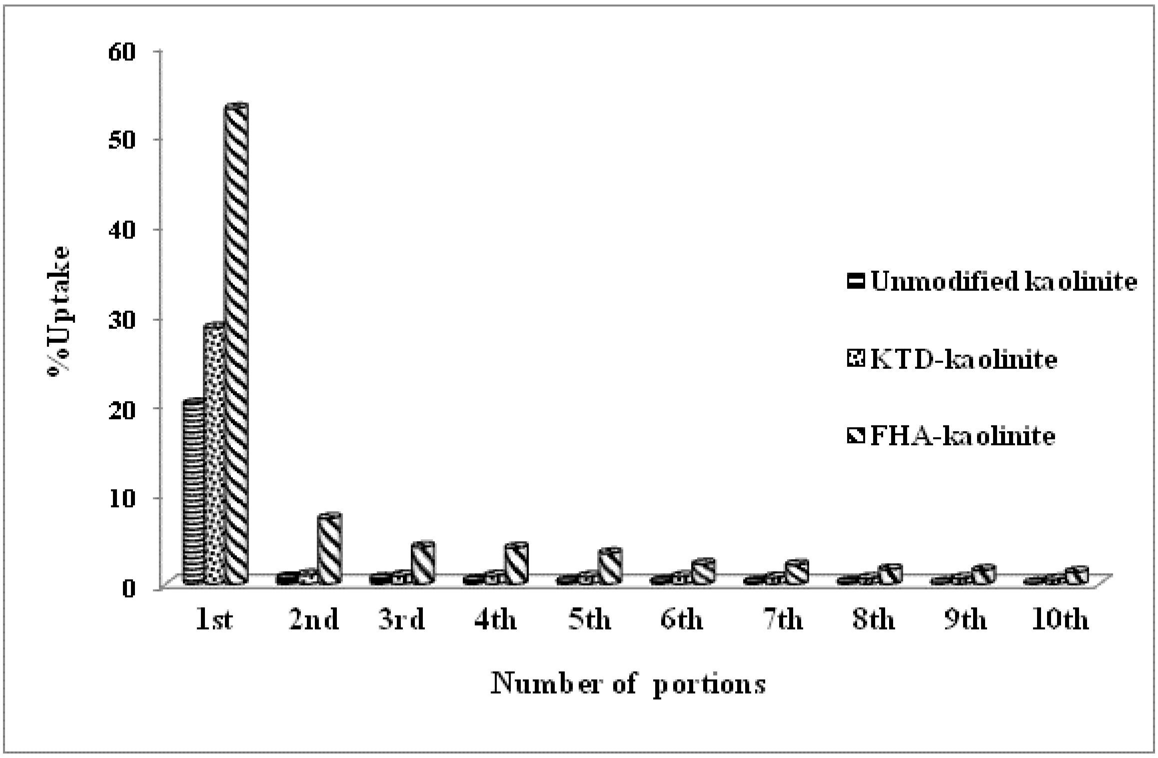


Figure (3.64): %Uptake of metal ions by KTD– kaolin clay by column technique.



Figure(3.65): %Uptake of Cd(II) by unmodified and both modified kaolin clay by column technique.

From Figures (3.64 and 3.65), we can decide that FHA– kaolin clay is better for adsorption of heavy metal ions than KTD– kaolin clay. Therefore, a greater density of adsorption sites e.g. carboxyl and phenolic hydroxyl sites in FHA, enhance the adsorption of metal ions. Similar results were obtained from the values of ΔG, Table (3.37), elemental analysis where % of oxygen in KTD is less than FHA, Table (3.3), EDS analysis, Tables (3.8 and 3.9), surface area and porosity measurements, Table(3.11).

On the other hand, Figure (3.66) shows that modified kaolin clay by humic acid is better for adsorption of heavy metal ions than unmodified kaolin clay. Same result was obtained by batch experiment.

3.5.2. Desorption studies

Desorption of fully adsorbed 1000 ppm of Pb(II), Cd(II) and Zn(II) from the adsorption sites on the surface of the modified kaolin clay sample showed that > 90% of metal ions adsorbed onto modified kaolin clay samples were released, by 0.10M HNO_3 for both Pb(II) and Cd(II) by proton exchange mechanism and 1M EDTA for Zn(II) by forming a complex. Keeping the flow rate of elution of 1 mL/min, the collected elute was analyzed and the results are expressed as percent recovery as shown in Tables (3.41 and 3.42).

Table (3.41): Desorption of metal ions adsorbed onto FHA– kaolin clay.

Eluting agent	%Recovery	%Recovery	%Recovery	%Recovery	% Cumulative recovery
	1st 10mL	2nd 10mL	3rd 10mL	4th 10mL	
0.1M HNO_3	**56.89**	**29.61**	**5.64**	**4.56**	**96.70**
0.1M HNO_3	**48.32**	**39.01**	**11.43**	**0.62**	**99.38**
1M EDTA	**42.06**	**39.75**	**7.31**	**5.70**	**94.83**

Table (3.42): Desorption of metal ions adsorbed onto KTD– kaolin clay.

Eluting agent	%Recovery	%Recovery	%Recovery	%Recovery	% Cumulative recovery
	1st 10mL	2nd 10mL	3rd 10mL	4th 10mL	
0.1M HNO_3	**81.95**	**5.74**	**5.17**	**2.87**	**95.73**
0.1M HNO_3	**88.95**	**6.52**	**3.12**	**0.28**	**98.87**
1M EDTA	**54.90**	**36.27**	**1.96**	**0.49**	**93.63**

Both modified kaolin clay can be desorbed of metal ions completely after 40 mL of eluting agent.

3.5.3. Regeneration Studies

Reusing both adsorbent in repeated cycles of adsorption of metal ions, it was found that metal ions were adsorbed onto both adsorbents. This may be attributed to nitric acid used for desorption, then adsorbents would be protonated so it can adsorb again and still efficient.

Table (3.43): Reloading of metal ions by FHA– kaolin clay after desorption process.

Metal Ion	Initial Conc. (ppm)	Loaded Conc. 1st 10mL (ppm)	Loaded Conc. 2nd 10mL (ppm)	Cumulative load (mg metal ion(II) / 2g clay)
Zn(II)	1000	65	18	1.66
Cd(II)	1000	124	75	3.98
Pb(II)	1000	189	100	5.78

Table (3.44): Reloading of metal ions by KTD– kaolin clay after desorption process.

Metal Ion	Initial Conc. (ppm)	Loaded Conc. 1st 10mL (ppm)	Loaded Conc. 2nd 10mL (ppm)	Cumulative load (mg metal ion(II) / 2g clay)
Zn(II)	1000	123	23	2.92
Cd(II)	1000	298	14	6.24
Pb(II)	1000	559	374	18.66

According to Tables (3.43 and 3.44), same trend of selectivity sequence of metal ions towards modified kaolin clay is shown by reloading process; Pb(II)> Cd(II)> Zn(II). This mean that the desorption process did not affect the modified kaolin clay properties.

KTD– kaolin clay can be reloaded with metal ions more than FHA– kaolin clay for all metal ions.

4. Conclusion

We can modify kaolin clay in order to in enhance its adsorption capacity towards metal ions with humic acid especially it is formed from natural degradation of plant and animal residues.

- Humic acid adsorption by kaolin clay decreases with increasing pH, both the adsorbent surface and the humic acid lose their protons at increasing pH and become negatively charged, and consequently repel each other.
- Clearly, modified kaolin clay by humic acid significantly enhanced the adsorption of metal ions, for example, the Cd(II) adsorbed by natural kaolin clay was 1mg/g, while the amount adsorbed by modified kaolin clay was nearly 22 mg/g, and the later is almost twenty times as much as the natural one. It indicated that the adsorption sites on the clay minerals were largely increased by modification.
- Several characterization methods support the development of modified kaolin clay to adsorb heavy metal ions especially surface area and porosity measurements.
- The metal ions adsorption on modified kaolin clay is highly dependent of pH, that is, the adsorbed metal ions increased with increasing pH. As pH increased, (i.e., as the solution becomes more basic), then more and more protons leave the clay mineral surface (and from adsorbed HA) making the sites available to the metal ion which now increasingly bind to clay surface.
- The best conditions for adsorption metal ions on modified kaolin clay are at pH=6, 45 °C and initial metal concentration of 10 ppm.
- The equilibrium times for the two modified kaolin clay were close to each other, and not that much difference from metal ion to another.
- The arrangement for uptake percent: Pb(II)> Cd(II)> Zn(II) in both modified kaolin clay in batch and column techniques.

- The obtained adsorption data showed fitting for Langmuir, Freundlich and Dubinin–Radushkevich adsorption isotherm models.
- The adsorption was physical process on both homogeneous and heterogeneous surfaces.
- The thermodynamic parameters show that the adsorption process is favorable, but it is in FHA– kaolin clay more favorable than KTD– kaolin clay, and the adsorption of metal ions is an endothermic process.
- A column packed with the modified kaolin clay has good metal ions capacity. And it was found that of metal ions were adsorbed onto both adsorbents while reusing both adsorbent in repeated cycles of adsorption of metal ions.

5. Future Suggestions

- Modify Jordanian kaolin clay by chemical modification.

- Study the effect of ionic strength on the adsorption process.

- Adsorption of organic pollutants by modified Jordanian kaolin clay.

- Adsorption of humic acid from aqueous solutions using other Jordanian clay like zeolite.

References:

Adebowale, K.O. Unuabonah, I. E. Owolabi, B. I. (2005), Adsorption of some heavy metal ions on sulfate– and phosphate–modified kaolin. **Applied Clay Science**. 29 (2), 145– 148.

Adebowale, K. O. Unuabonah, I. E. and Owolabi,B. I. (2006), The effect of some operating variables on the adsorption of lead and cadmium ions on kaolinite clay. **Journal of Hazardous Materials B**, 134 (1–3), 130–139.

Adebowale, K. O. Unuabonah1, E. I. and Owolabi, B. I. (2008), Kinetic and thermodynamic aspects of the adsorption of Pb^{2+} and Cd^{2+} ions on tripolyphosphate–modified kaolinite clay. **Chemical Engineering Journal**, 136 (2–3), 99–107.

Alkan, M. Hopa, C. Yilmaz, Z. G¨uler, H. (2005), The effect of alkali concentration and solid/liquid ratio on the hydrothermal synthesis of zeolite NaA from natural kaolinite. **Microporous Mesoporous Materials**, 86 (1–3), 176–184.

Alkan, M. Kalay, B. Dogan, M. and Demirbas, O. (2008), Removal of copper ions from aqueous solutions by kaolinite and batch design. **Journal of Hazardous Materials**, 153 (1–2), 867–876.

Alkaram, U. Mukhlis, A. and Al–Dujaili, A. (2009), The Removal of Phenol from Aqueous Solutions by Adsorption Using Surfactant–Modified Bentonite and Kaolinite, **Journal of Hazardous Materials**, 169 (1–3), 324–332.

Al–Omari, Hamzeh (2007), Evaluation of the Thermodynamic Parameters for the Adsorption of Cadmium Ion from Aqueous Solutions. **Acta Chimica Slovenica**, 54 (3), 611–616.

Amer, M. Khalili, F and Awwad, A. (2010), Adsorption of lead, zinc and cadmium ions on polyphosphate–modified kaolinite clay. **Journal of Environmental Chemistry and Ecotoxicology**, 2(1), 001–008.

Angove, M. J. Johnson, B. B. and Wells, J. D. (1997), Adsorption of cadmium(II) on kaolinite. **Colloids and Surfaces A: Physicochemical and Engineering Aspects**, 126 (2–3), 137–147.

Anirudhan, T. S. and Suchithra, P. S. (2010), Heavy metals uptake from aqueous solutions and industrial wastewaters by humic acid–immobilized polymer/bentonite composite: Kinetics and equilibrium modeling. **Chemical Engineering Journal**, 156 (1), 146–156.

Araujoa, P. Esteves, M. A. Calvino, D. F. Gandara, D. F. Rio, L. G. Periago, E. L. Mejuto, J. C. and Munoz, J. C. (2007), **Recent Research Developments in Physical Chemistry**, India, Transworld Research Network, vol. 9, 61–83.

Arnarson, T. S. and Keil, R. G. (2000), Mechanisms of pore water organic matter adsorption to montmorillonite. **Marine Chemistry**, 71 (3), 309–320.

Balan E., Delattre S., Guillaumet M., Salje E.K.H. (2010), Low–temperature infrared spectroscopic study of OH stretching modes in kaolinite and dickite. **American Mineralogist**, 95 (8–9), 1257–1266.

Baraka, A. Hall, P. J. and Heslop, M. J. (2007), Preparation and characterization of melamine–formaldehyde–DTPA chelating resin and its use as an adsorbent for heavy metals removal from wastewater. **Reactive and Functional Polymers**, 67 (7), 585–600.

Benefield, L., Judkins, J. & Weand, B. 1982. **Process Chemistry for Water and Wastewater Treatment**. Prentice–Hall, Inc. Englewood Cliffs, New Jersey.

Bhattacharyya, K. and Gupta, S. (2006), Kaolinite, montmorillonite, and their modified derivatives as adsorbents for removal of Cu(II) from aqueous solution. **Separation and Purification Technology**, 50 (3), 388–397.

Bhattacharyya, K. and Gupta, S. (2008), Adsorption of a few heavy metals on natural and modified kaolinite and montmorillonite: A review. **Advances in Colloid and Interface Science**, 140 (2), 114–131.

Bhattacharyya, K. and Gupta, S. (2009), Calcined tetrabutylammonium kaolinite and montmorillonite and adsorption of Fe(II), Co(II) and Ni(II) from solution. **Applied Clay Science**, 46 (2), 216–221.

Bish, D.L. (1993), Rietveld refinement of the kaolinite structure at 1.5 K, **Clays and Clay Minerals**, 41 (6), 738–744.

Burgess, J. (1988), **Ions in solution "Basic principles of chemical interaction"**. second edition, Horwood publishing, England.

Chantawong, V. Harvey, N. W. and Bashkin, V. N. (2003), Comparison of Heavy Metal Adsorptions by Thai Kaolin and Ballclay. **Water, Air, and Soil Pollution**, 148 (1–4), 111–125.

Christl, I. and Kretzschmar, R. (2001), Relating ion binding by fulvic and humic acids to chemical composition and molecular size: 1. Proton binding. **Environmental Science Technology**, 35 (12), 2505–2511.

Cotton, F. A. Wilkinson, G. Murillo, C. A. and Bochmann, M. (1999), **Advanced inorganic chemistry**. Sixth edition, New York, Wiley–Interscience.

Donat, R. Akdogan, A. Erdem, E. and Ceti, H. (2005), Thermodynamics of Pb^{2+} and Ni^{2+} Adsorption onto Natural Bentonite from Aqueous Solutions. **Journal of Colloid and Interface Science**, 286 (1), 43–52.

Davis, J. A. (1982), Adsorption of natural dissolved organic matter at the oxide/water interface. **Geochimica et Cosmochimica Acta**, 46 (11), 2381–2393.

Devidal, J. Dandurand, J. and Gout, R. (1996), Gibbs free energy of formation of kaolinite from solubility measurement in basic solution between 60 and 170^{o}C. **Geochimica et Cosmochimica Acta**, 60 (4), 553–564.

Davies, G. and Ghabbour, E. (1998), **Humic substances (structures, properties and usese)**. United Kingdom, Royal Society of Chemistry, 180.

Dinu, M. V. and Dragan, E. S. (2008), Heavy metals adsorption on some iminodiacetate chelating resins as a function of the adsorption parameters**. Reactive & Functional Polymers**, 68 (9), 1346–1354.

Donat R. Akdogan A. Erdem E. and Ceti H. (2005), Thermodynamics of Pb^{2+} and Ni^{2+} Adsorption onto Natural Bentonite from Aqueous Solutions. **Journal of Colloid and Interface Science**, 286 (1), 43–52.

Dubinin, M. Radushkevich, L. and Dokl, A. (1947), A Theoretical Isotherm for Adsorption on Heterogeneous Surface, **Nauk SSSR**, 55, 331– 333.

Eckenfelder Jr., W. Wesley (1980), **Principles of Water Quality Management**, Boston: CBI Publishing Company, Inc.

El–Eswed, B. and Khalili, F. (2006), Adsorption of Cu(II) and Ni(II) on solid humic acid from the Azraq area, Jordan. **Journal of Colloid and Interface Science**, 299 (2), 497–503.

El– Said, Saad (2010), Selecting kaolinite Clay for Copper Removal in Batch and Fixed Bed Column Systems. **International Journal of Chemical Thechnology**, 2 (3), 88–93.

Farmer V.C, (1998), Differing effects of particle size and shape in the infrared and Raman spectra of kaolinite. **Clay Minerals**, 33 (4), 601 – 604.

Faust, S. D. and Aly, O. M. (1987), **Adsorption Processes for Water Treatment**, First edition, Boston, Butterworth Publishers.

Freundlich, Herbert (1906), Ûber die adsorption in lõsungen. Z. **Physical Chemistry**, 57, 384 – 470.

Freundlich, Herbert (1932), of the adsorption of gases. Section II. Kinetics and Energetic of gas adsorption. Introductory paper to section II, **Transactions of the Faraday Society**, 28, 195–201.

Fu, L. Wang, J. Lu, H. Su, Y. Ren, A. (2008), Comment on “The removal of phenolic compounds from aqueous solutions by organophilic bentonite” **Journal of Hazardous Materials**, 151 (2–3), 851–854.
Giles, C. H. MacEwan, T. H. Nakhwa, S. N. and Smith, D. (1960), Studies in adsorption. Part XI. A system of classification of solution adsorption isotherms, and its use in diagnosis of adsorption mechanisms and in measurement of specific surface areas of solids. **Journal of the Chemical Society**, 3973–3993.

Giles, C. H. and Huitson, A. (1974), A general treatment and classification of the solute adsorption isotherms. **Journal of Colloid and Interface Science**, 47(3), 755–777.

Gu, B. Schmitt, J. Chen, Z. and Liang, L. (1994), Adsorption and desorption of natural organic matter on iron oxide: mechanisms and models. **Environmental Science and Technology**, 28 (1), 38–46.

Guptaa, S. and Bhattacharyya, K. (2008), Immobilization of Pb(II), Cd(II) and Ni(II) ions on kaolinite and montmorillonite surfaces from aqueous medium. **Journal of Environmental Management**, 87 (1), 46–58.

Gupta,V. and Miller, J. D. (2010), Surface force measurements at the basal planes of ordered kaolinite particles. **Journal of Colloid and Interface Science**, 344 (2), 362–371.

Hambidge, M. (2000), Human zinc deficiency. **Journal of Nutrition**, 130, 1344S-1349S.

Heidmann, I. Christl, I. and Kretzschmar, R. (2005), Sorption of Cu and Pb to kaolinite–fulvic acid colloids: Assessment of sorbent interactions. **Geochimica et Cosmochimica Acta**, 69 (7), 1675–1686.

He, J. Hong, S. Zhang, L. Gan, F. and Ho, Y. (2010), equilibrium and thermodynamic parameters of adsorption of methylene blue onto rectorite. **Fresenius Environmental Bulletin**, 19 (11a), 2651 – 2656.

Hizal, J. and Apak, R. (2006a), Modeling of cadmium(II) adsorption on kaolinite–based clays in the absence and presence of humic acid. **Applied Clay Science**, 32 (3–4), 232–244.

Hizal, J. and Apak, R. (2006b), Modeling of copper(II) and lead(II) adsorption on kaolinite–based clay minerals individually and in the presence of humic acid. **Journal of Colloid and Interface Science**, 295 (1), 1–13.

Holm, T. R. and Zhu, X. (1994), Sorption by kaolinite of Cd^{2+}, Pb^{2+} and Cu^{2+} from landfill leachate–contaminated groundwater. **Journal of Contaminant Hydrology**, 16, 271–287.

Ho, Y.S. and McKay, G. (1998), Sorption of Dye from Aqueous Solution by Peat, **Chemical Engineering Journal**, 70 (2), 115–124.

Ho, Y. S. and McKay, G. (1999a), Pseudo–second–order model for the sorption processes, **Process Biochemistry**, 34 (5), 451–465.

Ho, Y. S. and McKay, G. (1999b), Batch lead (II) removal from aqueous solution by Peat: equilibrium and kinetics, **Transactions of the Institution of Chemical Engineers B**, 77 (3),165–173.

http://www.humintech.com/pdf/humicfulvicacids.pdf, 2010.

http://www.quantachrome.com/science/selected_publications.html, 2008.

Huheey, J. Keiter, E. and Keiter, R. (1993), **Inorganic Chemistry of structure and reactivity**, Fourth edition, Harper Collins Collage Puplishernic Matter,USA.

Human Health Fact Sheet, August (2005), **Mixtures of Arsenic, Cadmium, Chromium, and Lead**, http://www.ead.anl.gov/pub/doc/zmixture–as–cd–cr–pb.pdf.

Hunt, J. P. (1965), **Metal Ions in Aqueous Solutions**. Second edition, Benjamin Inc, New York.

Hur, J. and Schlautman, M. A. (2003), Molecular weight fractionation of humic substances by adsorption onto minerals. **Journal of Colloid and Interface Science**, 264 (2), 313–321.

Hur, J. and Schlautman, M. A. (2004), Effects of pH and phosphate on the adsorptive fractionation of purified Aldrich humic acid on kaolinite and hematite. **Journal of Colloid and Interface Science**, 277 (2), 264–270.

Ikeya, K. Hikage, T. Arai, S. and Watanabe, A. (2011), Size distribution of condensed aromatic rings in various soil humic acids. **Organic Geochemistry**, 42, 55–61.

Jiang, M. Q. Jin, X. Y. Lu, X. Q. and Chen, Z. L. (2010), Adsorption of Pb(II), Cd(II), Ni(II) and Cu(II) onto natural kaolinite clay. **Desalination**, 252 (1–3), 33–39.

Jiang, M. Q. Wang, Q. P. Jin, X. Y. and Chen, Z. L. (2009), Removal of Pb(II) from aqueous solution using modified and unmodified kaolinite clay. **Journal of Hazardous Materials**, 170 (1), 332–339.

Jorge C. Trevino1 M. and Coles, C. (2003), Kaolinite properties, structure and influence of metal retention on pH. **Applied Clay Science**, 23 (1–4), 133–139.

Juang, R. Wu, F. and Tseng, R. (1997), Ability of Activated Clay for the Adsorption of Dyes from Aqueous Solutions, **Environmental Technology**, 18 (5), 535.

Kakali, G. Perraki, T. Tsivilis, S. and Badogiannis, E. (2001), Thermal treatment of kaolin: the effect of mineralogy on the pozzolanic activity. **Applied Clay Science**, 20, (1–2), 73–80.

Kaya, A. and Oren, A. H. (2005), Adsorption of zinc from aqueous solutions to bentonite, **Journal of Hazardous Materials B**, 125, (1–3), 183–189.

Katsumata, H. Kaneco, S. Matsuno, R. Itoh, K. Masuyama, K. Tohru Suzuki, T. Funasaka, K. and Ohta, K. (2003), Removal of organic polyelectrolytes and their metal complexes by adsorption onto xonotlite. **Chemosphere**, 52 (5), 909–915.

Khalili, Fawwaz (1987), Humic and Fulvic Acids from Several Locations in Jordan. **Dirasat**, 14 (12), 151–162.

Khalili, Fawwaz (1988), The Nature of Azraq Oasis Humic Acid. Journal **of the Iraqi Chemical Society**, 13 (1), 71–86.

Khalili, F. and Ajjouri, H. (1987), X–ray Diffraction Studies on Jordanian Humic and Fulvic Acids. **Dirasat**, 14 (12), 163–166.

Khoury , H. and El-Sakka, W. (1986), Mineralogical and industrial characterization of the Batn El-Ghoul clay deposits, southern Jordan. **Applied Clay Science** , 1 (4), 321-331.

Lacin, O. Bayrak, B. Korkut, O. and Sayan, E. (2005), Modeling of adsorption and ultrasonic desorption of cadmium(II) and zinc(II) on local bentonite. **Journal of Colloid and Interface Science**, 292 (2), 330–335.

Langmuir, Irving (1918), The Adsorption of Gases on Plane Surfaces of Glass, Mica and Platinum. **Journal of American Chemical Society**, 40 (9), 1361–1403.

Lagergren S. (1898), Zur theorie der sogenannten adsorption gelo¨ ster stoffe. Kungliga Svenska Vetenskapsakademiens Handlingar, 24 (4), 1–39.

Li, A. and Dai, J. (2006). Effects of fulvic fractions on the pH–dependent sorption of Cu (II) to kaolinite. **Water Research**. 40 (10), 1951 – 1956.

Li, H. Sheng, G. Teppen, B. J. Johnston, C. T. and Boyd, S. A. (2003), Sorption and Desorption of Pesticides by Clay Minerals and Humic Acid–Clay Complexes. **Soil Science Society of America Journal**, 67 (1), 122–131.

Limousin, G. Gaudet, J. Charlet, L. Szenknect, S. Barthes, V. and Krimissa, M. (2007), Sorption Isotherms: A Review on Physical Bases, Modeling and Measurement, **Applied Geochemistry**, 22 (2), 249–275.

Manohar, D. Noeline, B. and Anirudhan, T. (2006), Adsorption Performance of Al–Pillared Bentonite Clay for the Removal of Cobalt (II) from Aqueous Phase, **Applied Clay Science**, 31 (3–4), 194–206.

Marzal, P., Seco, A., Gabaldon, C. and Ferrer, J. (1996), Cadmium and zinc adsorption onto activated carbon: Influence of temperature, pH and metal/carbon ratio, **Journal of Chemical Technology & Biotechnology**, 66 (3), 279–285.

Meyer, K. and Klobes, P. (1999), Comparison between different presentations of pore size distribution in porous materials. **Fresenius Journal of Analytical Chemistry**, 363(2), 174–178.

Madejova, J. and Komadel, P. (2001), Baseline studies of the Clay Minerals Society Source Clays: Infrared methods. **Clays and Clay Minerals**, 49 (5), 410‑432.

Manohar, D. Noeline, B. and Anirudhan, T. (2006), Adsorption Performance of Al–Pillared Bentonite Clay for the Removal of Cobalt (II) from Aqueous Phase, **Applied Clay Science**, 31 (3–4), 194–206.

McKnight, D., Bencala, K.E., Zellweger, G.W., Aiken, G.R., Feder, G.L., Thorn, K.A. (1992), Sorption of dissolved organic carbon by hydrous aluminum and iron oxides occurring at the confluence of Deer Creek with the Snake River, Summit County, Colorado. **Environmental Science and Technology**, 26, 1388–1396.

Murray, H. H (1961), Industrial applications of kaolin. **Clays and Clay Minerals**, 10 (1), 291–298.

Orumwense, F. F. O. (1996), Removal of lead from water by adsorption on a kaolinitic clay, **Journal of chemical technology and biotechnology**, 65 (4), 363–369.

Parida, S. K. Dash, S. Patel, S. and Mishra, B. K. (2006), Adsorption of organic molecules on silica surface. **Advances in Colloid and Interface Science**, 121 (1–3), 77–110.

Pauling L. (1930), The structure of the chlorites. **Proceedings of the National Academy of Sciences of the United States of America**, 16 (9), 578–582.

Pearson, Ralph (1968), Hard and soft acids and bases (HASB). I .Fundamental principles, **Journal of Chemical Education**, 45, 581–587.

Plavsic, M. and Cosovic, B. (1999), Voltammetric study of the role of organic acids on the sorption of Cd and Cu ions by alumina particles. **Colloids and Surfaces A: Physicochemical Engineering Aspects**, 151 (1), 189–200.

Polanyi, Michael (1963), The potential Theory of Adsorption, **Science**, 141, 1010 – 1013.

Puls, W.R. and Bohn, H.L. (1988), Sorption of cadmium, nickel, and zinc by kaolinite and montmorillonite suspensions. **Soil Science Society American Journal**, 52, 1289–1292.

Qinyan, Y. Ying, L. and Baoyu, G. (2009), Impact factors and thermodynamic characteristics of aquatic humic acid loaded onto kaolin. **Colloids and Surfaces B: Biointerfaces**. 72, 241–247.

Ramesh, A. Leea, D. J. and Wong, J.W.C. (2005), Thermodynamic parameters for adsorption equilibrium of heavy metals and dyes from wastewater with low–cost adsorbents. **Journal of Colloid and Interface Science**. 291, 588–592.

Reyes, C. A. Williams, C. and Alarcón, O. M. (2010), Synthesis of zeolite LTA from thermally treated kaolinite. **Antioquia**, (53), 30–41.

Rosa, J. M. Knickerb, H. López–Capelc, E.Manningc, D. A. C. González–Perezd, J. A. and González–Vilad, F. J. (2007), Direct Detection of Black Carbon in Soils by Py–GC/MS, Carbon–13 NMR Spectroscopy and Thermogravimetric Techniques. **Soil Science Society of America Journal**, 72 (1), 258–267.

Saada, A. Breeze, D. Crouzet, C. Cornu, S. and Baranger, P. (2003), Adsorption of arsenic(V) on kaolinite and on kaolinite–humic acid complexes Role of humic acid nitrogen groups. **Chemosphere**, 51, 757–763.

Salman, M. El–Eswed, B. Khalili, F. (2007), Adsorption of humic acid on bentonite. **Applied Clay Science**, 38, (1–2), 51–56.

Samal, S. Das R. R. Acharya, S. Mohapatra, P. and Dey, R. K. (2002), A Comparative Study on Metal Ion Uptake Behavior of Chelating Resins Derived From the Formaldehyde–Condensed Phenolic Schiff Bases of 4,4'– Diaminodiphenylsulfone and Hydroxybenzaldehydes. **Polymer–Plastics Technology Engineering**, 41(2), 229–246.

Sa´nchez–Corte´ s, O. Ciavatta, C. and Garc, B. (1998), pH–dependent adsorption of fractionated peat humic substances on different silver colloids studied by surface–enhanced raman spectroscopy. **Journal of Colloid Interface Science**, 198 (2), 308–318.

Santos, A. Botero, W. Bellin, I. Oliveira, L. Rocha, J. Mendonça, A. and Godinhob, A. (2007), Interaction between Humic Substances and Metallic Ions: a Selectivity Study of Humic Substances and their Possible Therapeutic Application. **Journal of the Brazilian Chemical Society**, 18 (4), 824–830.

Scheckel, K. G. and Sparks D. L. (2001), Temperature effects on nickel sorption kinetics at the mineral–water interface. **Soil Science Society America Journal**, 65 (3), 719–728.

Schindler, P. W. Leichti, P. and Westall, J. C. (1987), Adsorption of copper, cadmium and lead from aqueous solution to the kaolinite/water interface. **Netherlands Journal of Agricultural Science**, 35 (3), 219–230.

Schlautman, M. A. and Morgan, J. J. (1994), Adsorption of aquatic humic substances on colloidal–size aluminum oxide particles: influence of solution chemistry. **Geochimica et Cosmochimica Acta**, 58 (20), 4293–4303.

Schnitzer, M. Kodama, H. and Ripmeester, J. (1991), Determination of the Aromaticity of Humic Substances by X–Ray Diffraction Analysis. **Soil Science Society of America Journal**, 55(3), 745–750.

Schwarzenbach, R.P., (1993), **Assessing the behavior and fate of hydrophobic organism compounds in the aquatic environment— general concepts and case studies emphasizing volatile halogenated hydrocarbons**. Swiss Federal Institute of Technology, EAWAG, CH–8600 Dubendor.

Sing, K. S. W. Everett, D. H. Haul, R. A. W. Moscou, L. Pierotti, R. A. Rouquerol, J. and Siemieniewska, T., (1985), Reporting physisorption data for gas/solid systems with special reference to the determination of surface area and porosity. **Pure and applied chemistry**, 57(4), 603–619.

Singh, V. K. and Tiwari, P. N. (1997), Removal and recovery of chromium (VI) from industrial wastewater, **Journal of Chemical Technology & Biotechnology**, 69 (3), 376–382.

Sparks, D. L. (1995), **Environmental Soil Chemistry**, Second edition, Academic Press, Inc., California, U.S.A.

Srivastava, P. Singh, B. and Angove, M. (2005), Competitive adsorption behavior of heavy metals on kaolinite. **Journal of Colloid and Interface Science**, 290 (1), 28–38.

Srivastava, P. and Singh, B. (2010), Effect of ionic strength on cadmium adsorption onto kaolinite in single– and multi–element systems. **19th World Congress of Soil Science, Soil Solutions for a Changing World**, Brisbane, Australia, 55–57.

Stevenson, F. J. (1982), **Humus Chemistry. Genesis, Composition, Reactions**. First edition, New York, John Wiley and Sons, P:443.

Sudibandriyo, M. (2010), A simple technique for surface area determination through supercritical CO_2 adsorption. **Journal of Makara Technology**, 14(1), 1–6.

Summers, R. S. and Roberts, P. V. (1988), Activated carbon adsorption of humic substances. **Journal of Colloid and Interface Science**, 122 (2), 367–381.

Takahashi, Y. Minai, Y. Ambe, S. Makide, Y. and Ambe, F. (1999), Comparison of adsorption behavior of multiple inorganic ions on kaolinite and silica in the presence of humic acid using the multitracer technique. **Geochimica et Cosmochimica Acta**, 63 (6), 815–836.

Tan, K.H. (1998), **Principles of Soil Chemistry**, Third edition, New York, Marcel Dekker, Inc., p: 267.

Tan, K. H. Hajek, B. F. and Barshad, I. (1986), **Methods of Soil Analysis**, Part 1. Second edition, Agron. Monogr. 9. ASA and SSSA, Madison, WI, p: 151–183.

Tashauoei, H. R. Attar, H. M. Amin, M. M. Kamali, M. Nikaeen, M. and Dastjerdi, V. (2010), Removal of cadmium and humic acid from aqueous solutions using surface modified nanozeolite A. **International Journal of Environmental Science and Technology**, 7 (3), 497–508.

Taylor, M. D. and Theng, B. K. G. (1995), Sorption of cadmium by complexes of kaolinite with humic acid. **Communications in soil science and plant analysis**, 26, (5 and 6), 765–776.

Trevino J and Coles C. (2003), Kaolinite properties, structure and influence of metal retention on pH. **Applied Clay Science**, 23 (1–4), 133–139.

Unlu N, Ersoz M. (2006), Adsorption characteristics of heavy metal ions onto a low cost biopolymeric sorbent from aqueous solutions. **Journal of Hazardous Materials**, 136 (2), 272–280.

Unuabonah, E. I. Adebowale, K. O. Owolabi, B. I. Yang, L. Z. and Kong, L. X. (2008), Adsorption of Pb(II) and Cd(II) from aqueous solutions onto sodium tetraborate–modified Kaolinite clay: Equilibrium and thermodynamic studies. **Hydrometallurgy**, 93 (1–2), 1–9.

Unuabonaha, E. I. Owolabi, B. I. Adebowale, K. O. and Ofomaja, A. E. (2007), Adsorption of lead and cadmium ions from aqueous solutions by tripolyphosphate–

impregnated Kaolinite clay. **Colloids and Surfaces A: Physicochemical Engineering Aspects**, 292 (2–3), 202–211.

Varga, Gabriel (2007), **The structure of kaolinite and metakaolinite**. Constantine the Philosopher University, Építoanyag 59. 1. Szám, 6–9.

Wanga, S. Hub, J. Li, J. and Yunhui Dong, Y. (2009), Influence of pH, soil humic/fulvic acid, ionic strength, foreign ions and addition sequences on adsorption of Pb(II) onto GMZ bentonite. **Journal of Hazardous Materials**, 167, 44–51.

Wang, G. Wang, X. Chai, X. Liu, J. and Deng, N. (2010), Adsorption of uranium (VI) from aqueous solution on calcined and acid – activated kaolin. **Applied Clay Science**, 47, 448–451.

Wang, K. and Xing, B. (2005), Chemical Extraction Affect the Structure and Phenanthrene Sorption of Soil Humin, **Environmental Science and Technology**, 39 (21), 8333–8340.

Wan, Y. and Liu, C. (2006), The effect of humic acid on the adsorption of REEs on kaolin. **Colloids and Surfaces A: Physicochemical Engineering Aspects**, 290 (1–3), 112–117.

Webb, P. A. (2001), An Introduction To The Physical Characterization of Materials by Mercury Intrusion Porosimetry with Emphasis On Reduction And Presentation of Experimental Data. **Micromeritics Instrument Corporation**. Norcross, Georgia, 1–23.

Wen, D. Ho, Y.S. and Tang X. (2006), Comparative sorption kinetic studies of ammonium onto zeolite, **Journal of Hazardous Materials**, B, 133, 252–256.

Wendlandt, W. W. (1974), **Thermal Methods of Analysis**, Part 1, Second edition, New York, Intersci. Publ., John Wiley & Sons.

Westall, J. C. (1982), **The FITEQL: a program for the determination of chemical equilibrium constants from experimental data. Technical Report**, vol. 82–01. Chemistry Department, Oregon State University, Corvallis, OR.

Wilson, M. A. T. Verheyen, V. Vassallo, A. M. Hill, R. S. and Perry, G. (1987), Selective loss of carbohydrates from plant remains during coalification. **Organic Geochemistry**, 11 (4), 265–271.

Xu, D. Tan, X. Chen, C and Wang, X. (2007), Adsorption of Pb(II) from Aqueous Solution to MX–80 Bentonite: Effect of pH, Ionic Strength, Foreign Ions and Temperature, **Applied Clay Science**, 41(1–2), 37–46.

ادمصاص أيونات المعادن الثقيلة على الكاولين الأردني المطور بحمض الهيوميك

إعداد :–

خنساء محمد سلامه العيسى

المشرف :–

الأستاذ الدكتور فواز عزت الخليلي

ملخص

تم تطوير الكاولين الأردني المأخوذ من منطقة الأزرق بواسطة حمض الهيوميك (HA)، وتمت دراسة عملية ادمصاص حمض الهيوميك من قبل الكاولين، بتغيير عاملي درجة الحموضة (3.00 ، 4.00 ، 5.00 و 6.00) ودرجات الحرارة (25، 35 و 45 درجة مئوية) وكا نت النسبة المئوية القصوى لادمصاص حمض الهيومك على الكاولين عند pH=3.00 ودرجة حرارة 45 درجة مئوية وعلى تركيز منخفض منHA .
تمت دراسة الخواص الإدمصاصية للأيونات ثنائية التكافؤ لمعادن الرصاص و الكادميوم والزنك على سطح الكاولين المطور باستخدام تقنية الدفعات ، و بتغيير عاملي الحرارة (25، 35 و 45 درجة مئوية) ودرجة الحموضة(4.00 ، 5.00 و 6.00) . وتمت دراسة أثروقت التفاعل و كتلة االمادة الماصة و تركيز المعادن الأولية.
و تم دراسة حركية الادمصاص، و قد وجد أن مقدار الادمصاص يتناسب طرديا مع الزمن حتى يصل للاتزان في أقل من ساعتين. و أن هذه النتائج تتطابق مع نموذج الرتبة الثنائية الزائف.
كما تم بحث الخواص الإدمصاصية لامتصاص أيونات المعادن على سطح الكاولين المعدل، ووجدنا أن شكل منحنى الادمصاص للرصاص على الكاولين المعدل هوالمنحنى L ، في حين أن شكل منحنى الادمصاص للكادميوم والزنك على الكاولين المعدل هوالمنحنى C.
ووجد أن الخواص الإدمصاصية لامتصاص أيونات المعادن على سطح الكاولين المعدل تطابق نماذج لانجمير وفريندليش و دوبنين رادوشكيفتش.ولكن أفضل نموذج يمثل النتائج هو لانجمير، وكانت عملية الادمصاص على السطوح المتجانسة وغيرالمتجانسة على حد سواء.
وكان أعلى ادمصاص على كل نوع من الكاولين المطور لأيون الرصاص. و قد وصلت قيمة الادمصاص للتراكيز القليلة من بعض أيونات المعادن كالرصاص الى أكثر من 90% . ولقد وجد أن ترتيب ادمصاص الأيونات عليهما كالتالي(Pb(II)> Cd(II)> Zn(II. و أظهرت النتائج أيضا أن الادمصاص على الكاولين المطوربحمض الهيوميك من شركة(Fluka) أعلى من الادمصاص على الكاولين المطوربحمض الهيوميك من منطقة سد الملك طلال لجميع الأيونات.
و وجد أن عملية الادمصاص عملية مفضلة وذلك لأن R_L بين (0 – 1) و(n>1) ، و حسبت الطاقة المصاحبة لعملية الإدمصاص وبناء عليه وجد أن عملية الادمصاص فيزيائية.
قيم ΔG السالبة تشير إلى درجة التفضيل لعملية الادمصاص، في حين أن قيم ΔH الموجبة تشير الى ان هذه العملية ماصة للحرارة ، ومن ناحية أخرى ، فإن قيم ΔS الموجبة تعني أن عملية الادمصاص تزيد من عشوائية النظام.

تم استخدام تجربة العمود لتحديد سعة تحميل الكاولين المطوربحمض الهيوميك لأيونات المعادن، ولقد وجد أن ترتيب ادمصاص الأيونات عليهما كالتالي: (Pb(II)> Cd(II) > Zn(II. وتم دراسة قدرة الكاولين المطور على الانفكاك عن المعادن المدمصة بواسطة حمض النتريك HNO_3 (0.1M) و EDTA (1M) و قد اظهر كفاءة عالية في إزالة أيونات المعادن المدمصة و امكانية إعادة استخدامه.